INDEX

ABSTRACT

DNA methylation is one of several epigenetic mechanisms that cells use to control gene expression and could be a possible mechanism involved in modulating drug response. In this thesis we evaluated the role of DNA methylation in relation: to glucocorticoid (GC) response in idiopathic nephrotic syndrome (INS) patients, to azathioprine (AZA) pharmacokinetics in early onset pediatric patients with inflammatory bowel disease (IBD) and to methotrexate (MTX) response in pediatric patients with juvenile idiopathic arthritis (JIA). In particular:

1) NLRP3, a member of the NALP3 inflammasome, can activate CASP1 which can cut the glucocorticoid receptor, leading to its inactivation and GC resistance. We found a lower level of NLRP3 promoter methylation in the adult population compared to the pediatric one (p-value: 0.012). Moreover, INS patients presented a lower NLRP3 methylation compared to controls especially in the adult population (2.2×10^{-7}). The effect of NLRP3 on GC resistance was assessed by setting up an in vitro model using U937 immortalized monocytes. The activation of the inflammasome pathway produced a reduction in GC sensitivity in U937 cells (p-value: 0.027) due to a lower GC receptor amount inside the cells (p-value < 0.05), evaluated by western blot.

2) AZA is a prodrug used to maintain disease remission in IBD. A higher AZA inactivation metabolism was reported in literature in early onset pediatric patients with IBD, probably due to an age-related higher TPMT activity. Thirty early onset (age < 6) and 90 non-early onset (age between 12 and 18) pediatric patients with IBD have been enrolled and analyzed in terms of cg22736354 methylation, TPMT promoter methylation, AZA active metabolites (TGN), TPMT expression and TPMT activity. AZA dose (mg/kg/day), TGN levels and the ratio between TGN and AZA dose resulted lower in early onset compared to non-early onset patients in a statistically significant way (p-value: 0.0003, 0.01, 0.0005 respectively). A higher TPMT activity was also present in early onset patients (p-value: 0.02). Interestingly, results show a statistically significant difference in the methylation of cg22736354, located in TPMT upstream neighborhood, between early-onset and non-early onset IDB patients (p-value: 4.6×10^{-5}) while no differences were seen in TPMT promoter methylation.

3) MTX is an immunosuppressive drug and is the first line therapy for JIA with a high variability in response. The methylation of the CDH4 gene in 71 JIA patients (Italy 24 patients, Kansas City 28 patients and Cincinnati 19 patients) was measured with Illumina methylation EPIC BeadChip array; each cohort was analyzed independently and then data have been pooled together with a meta-analysis. From the analysis between CDHs methylation and ACR Pedi (disease improvement index) measured at last follow up visit, 3 differentially methylated positions on the CDH4 gene resulted significant. Moreover, CDH4 gene expression has been analyzed in a cohort of 47 JIA patients available on GEO, in 20 JIA patients' blood and in different immortalized cellular lines. CDH4 expression resulted very low in all patients. U937 resulted the only immortalized line that expresses the CDH4 gene.

In conclusion, this thesis demonstrated the role of DNA methylation as possible biomarker of drug response in 3 different diseases. Our findings suggest that: an epigenetic NLRP3 regulation, mediated by age and disease status, can play a role in GC resistance in INS. Early onset pediatric patients with IBD have a lower cg22736354 methylation that could contribute to the increased AZA inactivation metabolism. The methylation of 3 CpG sites in the CDH4 gene might be a possible biomarker of MTX response in JIA patients.

RIASSUNTO

La metilazione del DNA è uno dei numerosi meccanismi epigenetici che le cellule utilizzano per controllare l'espressione genica ed è un possibile meccanismo implicato nella modulazione della risposta ai farmaci. In questa tesi è stato esaminato il ruolo della metilazione del DNA in relazione: alla risposta ai glucocorticoidi (GC) in pazienti con sindrome nefrosica idiopatica (SNI), alla farmacocinetica dell'azatioprina (AZA) in pazienti pediatrici con malattia infiammatoria cronica intestinale (MICI) ad esordio precoce, ed alla risposta al metotressato (MTX) in pazienti pediatrici affetti da artrite idiopatica giovanile (AIG).

1) NLRP3, una proteina chiave dell'inflammosoma NALP3, è in grado di attivare la caspasi CASP1 che è in grado a sua volta di tagliare il recettore dei glucocorticoidi, portando alla sua inattivazione e di conseguenza a resistenza ai GC. In questa tesi è stato individuato un livello inferiore di metilazione del promotore NLRP3 nella popolazione adulta rispetto a quella pediatrica (p-value: 0.012). Inoltre, i pazienti con SNI presentavano una metilazione di NLRP3 inferiore rispetto ai controlli soprattutto nella popolazione adulta (2.2×10^{-7}). L'effetto di NLRP3 sulla resistenza ai GC è stato confermato mettendo a punto un modello in vitro utilizzando la linea monocitaria immortalizzata U937. L'attivazione della pathway dell'inflammosoma ha prodotto una riduzione della sensibilità ai GC nelle cellule U937 (p-value: 0.027) a causa di una minore quantità di recettore dei GC all'interno delle cellule (p-value <0.05), valutata mediante western-blot.

2) L'AZA è un profarmaco utilizzato nelle MICI per mantenere la malattia in stato di remissione. In letteratura è stato riportato un aumentato metabolismo di inattivazione dell'AZA in pazienti pediatrici affetti da MICI ad esordio precoce, probabilmente a causa di una maggiore attività età-dipendente dell'enzima TPMT. In questa tesi sono stati arruolati 30 pazienti pediatrici con MICI ad esordio precoce (età < 6) e 90 pazienti ad esordio non precoce (età compresa tra 12 e 18 anni), dei quali sono stati analizzati: metilazione del sito cg22736354, metilazione del promotore TPMT, metaboliti attivi dell'AZA (TGN), espressione di TPMT e attività di TPMT. La dose di AZA (mg/ kg/die), i TGN ed il rapporto tra TGN e dose di

farmaco sono risultati inferiori nei pazienti ad esordio precoce rispetto ai pazienti adolescenti, in maniera statisticamente significativa (p-value: 0.0003, 0.01, 0.0005 rispettivamente). Inoltre, è stata riscontrata una aumentata attività di TPMT nei pazienti ad esordio precoce (p-value 0.02). Inoltre, i nostri risultati mostrano dei livelli significativamente inferiori di metilazione di cg22736354 (p- valore: 4.6 x 10^{-5}), un sito CpG facente parte dell'orologio epigenetico, nei pazienti pediatrici ad esordio precoce. Non sono invece emerse differenze nella metilazione del promotore di TPMT.

3) Il MTX è un farmaco immunosoppressivo utilizzato come terapia di prima linea per il trattamento dell'AIG anche se caratterizzato un'elevata variabilità nella risposta. In questa tesi è stata analizzata la metilazione del gene CDH4 in 71 pazienti con JIA (Italia 24 pazienti, Kansas City 28 pazienti e Cincinnati 19 pazienti) tramite array Illumina methylation EPIC BeadChip; ogni coorte è stata analizzata da un punto di vista statistico in maniera indipendente ed in seguito i dati sono stati uniti tramite metanalisi. Dall'analisi tra metilazione del gene CDH4 e ACR Ped (indice di miglioramento della malattia) calcolato all'ultima visita di controllo, 3 posizioni differenzialmente metilate sul gene CDH4 sono risultate statisticamente significative dopo la metanalisi. Inoltre, l'espressione del gene CDH4 è stata analizzata in una coorte composta da 47 pazienti disponibile sulla piattaforma GEO, successivamente nel sangue di 20 pazienti affetti da AIG e in diverse linee cellulari immortalizzate disponibili nel nostro laboratorio. L'espressione di CDH4 è risultata molto bassa in tutti i pazienti mentre la linea U937 è risultata l'unica in grado di esprimere il gene CDH4.

In conclusione, questa tesi ha dimostrato il ruolo della metilazione del DNA come possibile biomarcatore della risposta ai farmaci in tre diverse patologie. I nostri risultati mostrano che: la regolazione epigenetica di NLRP3, mediata dall'età e dallo stato di malattia, può giocare un ruolo importante nella resistenza agli steroidi in pazienti con SNI. I pazienti pediatrici affetti da MICI ad esordio precoce hanno una ridotta percentuale di metilazione del sito cg22736354 che potrebbe contribuire all'aumentato metabolismo di inattivazione dell'AZA; la metilazione di 3 siti CpG nel gene CDH4 potrebbe essere un possibile biomarcatore della risposta al MTX nei pazienti pediatrici affetti da AIG.

1. INTRODUCTION

1.1 Epigenetics and its molecular mediators

The term “epigenetics” was originally used to denote poorly understood processes by which a fertilized zygote developed into a mature, complex organism. Subsequently Conrad Waddington (1905–1975) defined it as the complex of developmental processes between the genotype and phenotype (1). The modern and generally accepted definition of epigenetics is the study of heritable changes in gene activity or function that is not associated with any change of the DNA sequence (2). With the exception of some particular spontaneous or environmentally induced mutations in the genome, all the cells in a multicellular organism contain the same genetic information while they differ from one another because they express different sets of RNAs and proteins (3,4). The most important physiological role of this different expression patterns among cells is to guarantee phenotypic tissue differentiation (5). As representative examples, many studies have been conducted on the role of epigenetics for the differentiation and maturation of the central nervous system in mammals (6,7), stem cells differentiation into different tissue subtypes (8,9), osteogenic differentiation (10) and immune system maturation (11,12).

Several molecular mechanisms are responsible of epigenetic regulation including DNA methylation, histone modification, chromatin remodeling and non-coding RNAs including miRNAs (13). Interestingly, all those mechanisms are highly influenced and affected by the organism’s environment and they collaborate to create a cell-specific gene expression patterns that could also contribute to the development of certain type of disease (14–16).

1.2 DNA methylation

DNA methylation is an epigenetic mechanism involving the transfer of a methyl group onto the C5 position of cytosine residues to form 5-methylcytosine (5meC). DNA methylation was firstly noticed in 1948 by Rollin Hotchkiss who first discovered modified cytosine in a preparation of calf thymus using a paper chromatography technique (17). It was only late in the 1980s that scientists started to understand the role of DNA methylation in regulating gene expression and cell differentiation (18). As representative example, in 1986 the paper by Adrian P. Bird was one of the first underlying the importance of the “CpG doublet” repetition in gene promoters both for its rarity across the genome and because of the possible presence of a methyl group on the cytosine base that was associated with the expression of the gene itself (19).

In mammalian organisms, DNA methylation mostly occurs on CpG sites (cytosine followed by a guanine) (20) even though it has also been found at sites other than CpG sequences (non-CpG methylation) and includes methylation at cytosines followed by any of the other nucleotides (21). Non-CpG methylation is estimated to be only the 0.02% and its biological mechanisms is yet poorly understood (21).

On the other hand, CpG dinucleotides, the major carrier of DNA methylation, frequently occur in CpG islands, regions with a high frequency of CpG sites, that are mostly located in proximity of gene promoter regions (20). Most CpG dinucleotides around the genome are methylated on cytosine residues, whereas CpG dinucleotides within promoters of genes constitutively expressed in a specific tissue tend to be protected from methylation as previously mentioned (figure 1).

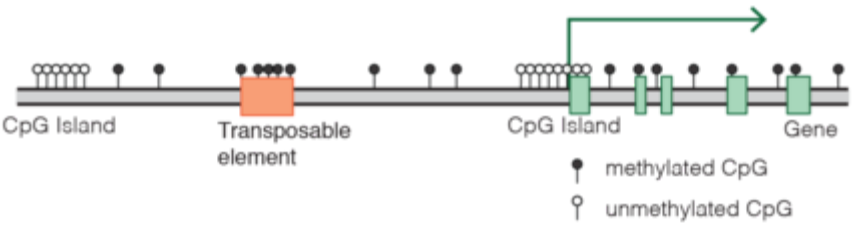

Figure 1 Typical mammalian DNA methylation landscape (22)

DNA methylation is regulated by a family of enzymes called DNA methyltransferases (DNMTs) which in mammals consist in 3 structurally and functionally distinct proteins: DNMT1, DNMT3a and DNMT3b (23). DNA methylation processes can be divided into:

- *Maintenance methylation* performed by DNMT1, which maintains methylation patterns during chromosome replication and repair. A hemimethylated DNA strand is needed in order for the DNAMT1 to be recruited and to methylate the adequate cytosine on the newly synthetized DNA strand.
- *De novo methylation* performed by DNMT3a and DNMT3b, that establish the methylation at certain CpG pairs without the need of a hemimethylated DNA strand.

Interestingly, it is also well documented in the literature that in primordial germ cell and in early embryogenesis DNA methylation is completely erased (24), leading scientists to investigate on the mechanisms involved in DNA methylation removal. In recent years, DNA de-methylation was discovered to be a mechanism that might occur by a passive or an

active process. Active DNA demethylation refers to an enzymatic process that results in the removal of the methyl group from the 5meCs by an enzymatic cascade that mainly encompasses the involvement of the ten-eleven translocation (TET) enzymes (25). In contrast, passive DNA demethylation refers to the lack of maintenance methylation during consequent DNA replication processes (24).

In particular, active DNA demethylation is a process that comprises 3 steps mediated by TET enzymes and one final reaction of decarboxylation performed by thymine DNA glycosylase (an enzyme involved in the correction of G/T mismatches during DNA repair), as reported in figure 2.

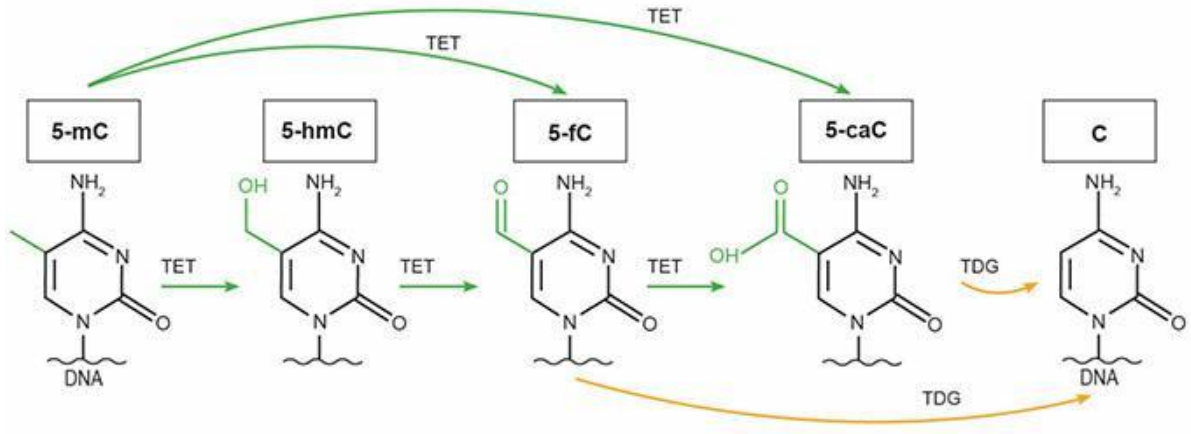

Figure 2. DNA demethylation pathway (26). 5-mC, 5 methyl cytosine; 5-hmC, 5-hydroxymethylcytosine; 5-fC, 5-formylcytosine; 5-caC, 5-carboxylcytosine; C, cytosine; TET, ten-eleven-translocation; TDG, thymine DNA glycosylase.

Apart from 5meC, the aforementioned cascade of enzymatic reactions produces 5-hydroxymethylcytosine, 5-formylcytosine and 5-carboxylcytosine. Besides being intermediates in the demethylation process, these bases might play their own role in regulating epigenetic processes even though their precise function has not yet been clarified. In order to investigate on the role of the above mentioned intermediates in influencing biological processes, big advances have been achieved in recent years thanks to the introduction of modern technologies and implementation of next generation sequencing for the identification of 5-hydroxymethylated cytosines and the other intermediates (27–29).

1.2.1 DNA methylation and drug response

The DNA methylation status has emerged as a promising epigenetic biomarker for several types of cancer, and diseases (30). Several publications have suggested that measurement of genome DNA methylation along with gene promoters' methylation can be used to identify

different type of cancer or determine disease prognosis (30–32). The same approach has started to be used also in pharmacogenomics, with the aim of identifying differentially methylated genes or regions, potentially associated with pharmacological phenotypes such as drug response, pharmacokinetics or drug toxicity.

Downregulation of specific genes by hypermethylation of their promoters has already been associated with drug resistance and in particular with resistance to antitumoral therapy in several types of cancer. For example, Liping Ye and collaborators reported a hypermethylation of SALL2 promoter in tamoxifen-resistant breast cancer cells (33). SALL2 was discovered to be a key upstream factor of estrogen-receptor-α in breast cancer patients. Moreover, a reduced expression of SALL2 due to its promoter hypermethylation could abrogate serum deprivation‐induced cell cycle arrest. After restoring the expression of SALL2 with a DNMT inhibitor, the authors re-sensitized resistant cells to tamoxifen therapy.

Another recently published paper from Sònia Palomeras and colleagues identified a hypermethylation and consequent mRNA downregulation of TGFBI, CXCL2, and SLC38A1 genes in trastuzumab resistant HER2 positive breast cancer cell model (34) using a genome wide DNA methylation array. Even though the transforming growth factor beta induced (TGFBI) gene has been reported to be involved in tumorigenesis, its role is yet not clear. To better understand TGFBI's function, the authors validated the role of DNA methylation and mRNA expression of the TGFBI gene in a small cohort of breast cancer patients, suggesting TGFBI promoter hypermethylation could be a potential epigenetic biomarker for trastuzumab response.

Recently, DNA hypermethylation at 11 and 4 specific loci have been associated with future glycemic response and intolerance to metformin respectively in 2 cohorts (discovery and validation) of type 2 diabetes subjects. In particular, patients with higher degrees of methylation at these sites were up to 2.5 times and up to 3 times more likely to not respond to and to not tolerate metformin respectively (35).

Finally, Paugh and collaborators, have reported a hypomethylation of NLRP3 promoter, and a consequent upregulation of the gene, in glucocorticoid resistant acute lymphoblastic leukemia pediatric patients. In the same work the authors identified a hypomethylation and upregulation of the CASP1 gene, that encodes for the caspase 1 protein which, together with NLRP3, are fundamental components of the NALP3 inflammasome. NLRP3 acts by activating caspase 1 which has been demonstrated to be able to cleave the glucocorticoid

receptor at different sites leading it into an inactive form and increasing the risk of developing steroid resistance due to the lack of glucocorticoid receptor (36).

1.2.2 DNA methylation and ageing

Several pharmacological changes occur with increasing age (37). Pharmacokinetics age-related changes are well documented in the literature especially for pediatric patients due to physiologic changes, especially during the first year of life (38). In particular, neonates and infants represent an unstable pharmacokinetic condition and big modifications of drug absorption, distribution, and clearance occur in the first few months of life (38). Nowadays little is known about the molecular mechanisms able to explain age related pharmacological differences, even though great expectations rely on the study of DNA methylation. In particular, at the end of the 80s the need of identifying age-associated biomarkers in model organisms (mice and rats) pushed the US National Institute on Ageing to start a program which required both the introduction of innovative technologies for genomic analysis and availability of results data sets in freely available repositories, such as the Gene Expression Omnibus (GEO). Many biological features were analyzed in order to find the best biological age estimator such as telomere length, transcriptomic profiles, metabolome, proteome and of course methylome (39). Thanks to the effort of this project, DNA methylation was discovered to be the first accurate multi tissue biomarker of ageing even though the molecular mechanisms that regulates age related DNA methylation changes are still not clear and further studies are needed (40).

Several papers demonstrating how chronological age induces remarkable changes on genome-wide DNA methylation levels have been published to date (41–44). In particular, thanks to the advent of genome wide DNA methylation array, initially developed as a technique to map the methylation changes in thousands of CpG sites obtained from DNA of cancer cells, it was possible to look at the DNA methylation state of all the almost 30.000 CpG islands of the human genome. Remarkably, among the estimated number of 28 million CpG sites across the genome that compose the above mentioned CpG islands, the methylation of millions of CpG sites was identified to change with age (44–46).

The increasing effort in studying DNA methylation as ageing biomarker then led to the development of the so called “epigenetic clock theory of ageing”. An epigenetic clock is a set of CpG sites (known as clock CpGs) statistically associated with chronological age of multiple DNA sample sources (40).

Several DNA-methylation based epigenetic clocks have been identified so far with a specificity that varies between different tissues. In particular, Gregory Hannum built a model that measures the rate at which an individual's methylome ages (with a strong impact of gender and genetic variants). In particular, the “Hannum epigenetic clock” comprises 71 CpG sites selected from the Illumina 450k array whom methylation, analyzed in white blood cells, strongly correlates with chronological age (47).

Furthermore, one of the most relevant epigenetic clocks is the Age-Acceleration-Residual clock identified by Steve Horvath in 2013 and defined as the residual resulting from regressing the epigenetic age on the chronological age. This clock is a universal and multi-tissue measure of age acceleration (defined as the difference between age estimated on the base of DNA methylation and chronological age) based on the methylation of 353 CpGs identified by analyzing the methylation of DNA samples obtained on more than 50 tissues of healthy subjects and several cancer samples (40,48).

In a meta-analysis published by Gibson and collaborators in 2019, a genome wide association study has been conducted on both the Hannum and Horvath epigenetic clocks. Interestingly, the cytosine cg22736354 (located in the downstream neighboring region of TPMT within the NHLRC1 gene), emerged as the only CpG site in cis-acting methylation quantitative trait loci with rs76244256 and rs7744541 that intersects with both the Hannum and Horvath clocks (49).

1.2.3 DNA methylation for therapy personalization in autoimmune diseases

As previously described, DNA methylation has emerged as promising biomarker for disease prognosis and diagnosis but also as predictor of pharmacological response and age-related biological differences. In this study we will evaluate the role of DNA methylation in relation to drug response in 3 different immunological diseases affecting children, in particular: idiopathic nephrotic syndrome, inflammatory bowel disease and juvenile idiopathic arthritis.

1.3 Idiopathic nephrotic syndrome

Idiopathic Nephrotic Syndrome (INS) is a disease characterized by the symptoms triad of proteinuria, hypoalbuminemia and edema resulting from abnormalities in glomerular permeability. INS can affect both the pediatric and adult populations, with an annual incidence rate of approximately 1.5-16.9 per 100,000 each year (50,51). For the pediatric population the peak of incidence of the disease is at 3-4 years of age and one third of

children affected have previously suffered of atopy, that occurs with asthma, eczema and rhinitis. An unexplained male preponderance is observed, with male to female ratio's ranging from 1.5 to 3.1 (52).

The clinical features that typically characterize INS are the following:

- urinary protein excretion greater than 50 mg/kg per day;
- hypoalbuminemia − less than 3 g/dL of serum albumin;
- edema;
- hyperlipidemia.

INS pathophysiology is complex and still not completely defined. Especially in children, complete effacement of the foot processes of podocytes (figure 3) with the loss of normal architecture and loss of the negative charge of the glomerular filtration barrier are the main causes of proteinuria (53), leading to the excretion of albumin, transferrin and other plasma proteins with a molecular weight ranging from 70 to 80 kDa, and accumulation of larger molecules such as immunoglobulins in plasma.

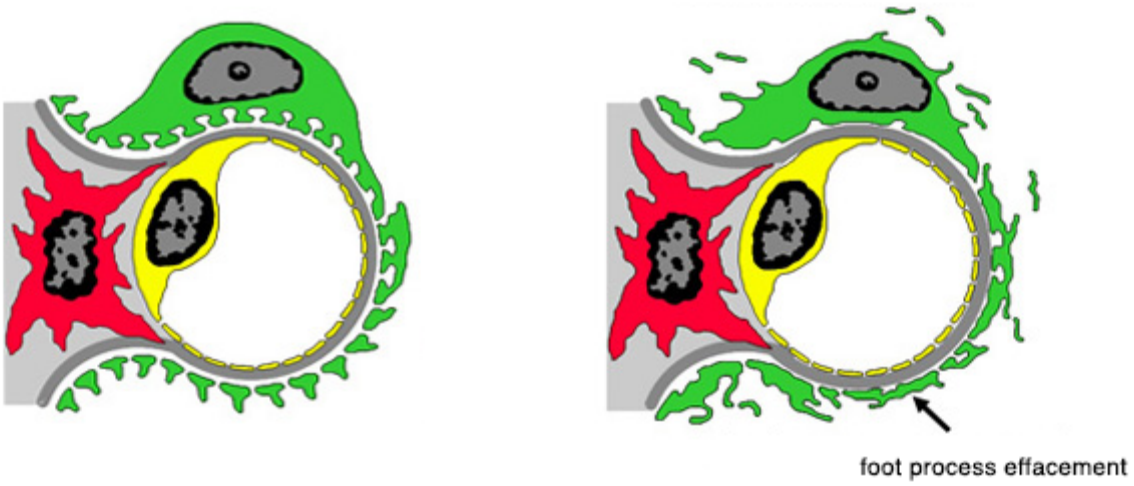

Figure 3. Podocytes foot process effacement in idiopathic nephrotic syndrome (right). Normal glomerular capillary (left) (54).

High proteinuria level induces a series of consequences that causes renal tubule-interstitial inflammation, with resulting increased sodium retention that overwhelms the physiologic mechanisms for removing edema (55). Besides edema, anorexia, irritability, fatigue, abdominal pain and diarrhea are other symptoms commonly present during the acute phase of the disease (56).

Although many INS disease subtypes are reported in the literature, minimal change disease (MCD) and focal segmental glomerulosclerosis (FSGS) are the most frequent manifestation

of INS, especially in children (57). MCD is characterized by no obvious glomerular changes detectable by light microscopy, no staining on immunofluorescence microscopy, and foot process effacement (53), whereas FSGS is a histological lesion characterized by segmental areas of glomerular sclerosis (58). However, there are cases where pathological features between the two diseases are less clear and renal lesions evolve from initial minimal lesions to FSGS (59).

The pathogenesis of INS is still not completely understood even though in all INS forms an alteration of the structure of podocytes is always present. What is certain about INS is the multifactorial nature of the disease. In particular, immunological abnormalities, primary glomerulus defects, the presence of circulating factors (such as heparinase, hemopexin, angiopoietin-like 4, cardiotrophin-like cytokine-1 and the soluble urokinase plasminogen activator receptor) and epigenetic factors such as changes in patients' T-helper DNA methylation, have been demonstrated to be related to the insurgence of INS (60–62).

1.3.1 Pharmacological therapy

Several pharmacological strategies can be undertaken to treat INS. In the acute phases, salt and fluid intake restriction is mandatory in order to reduce edema (63). Glucocorticoid (GC) treatment with prednisone or its active metabolite prednisolone at the dose of 60 mg/m^2 together with the antibiotic therapy are the primary drugs used worldwide at disease onset both for pediatric and adult populations.

Other immunomodulatory agents such as cyclophosphamide, cyclosporine, mycophenolate mofetil, levamisole or rituximab could be also used in order to reduce the use of GCs and consequently their side effects. Eventually antiproteinuric drugs such as angiotensin converting enzyme inhibitors can be used in order to manage high blood pressure resulting from kidney malfunctioning (64).

1.3.2 Glucocorticoids

GCs are steroid hormones widely used in a wide variety of disorders that act by regulating several physiological processes involved in inflammation, immunity and metabolism (65). The pharmacological function of GCs is obtained when they bind the GC receptors (GR), a member of the nuclear receptor superfamily (66). When not bound to GC, the GR is in an inactive form in the cytoplasm, stabilized by a multimeric complex composed of various chaperones and co-chaperones, such as Hsp90, FKBP51, FKBP52, p23, Hsp70 and Hop, from which it dissociates upon ligand binding (67,68). When bound to GC, the GR forms a

homodimer that migrates to the nucleus where it operates as transcription factor binding to GC response elements (GRE), specific DNA sequences recognized by the GR (figure 4). This mechanism leads to transcriptional changes responsible for diminished proliferative capacity and apoptosis of immune cells (69). As representative example, the glucocorticoid-induced leucine zipper (GILZ) is a gene that is transactivated by the GR and is responsible of regulating T cell activities, such as activation and differentiation, and controls the regulation of pro-inflammatory target genes (70).

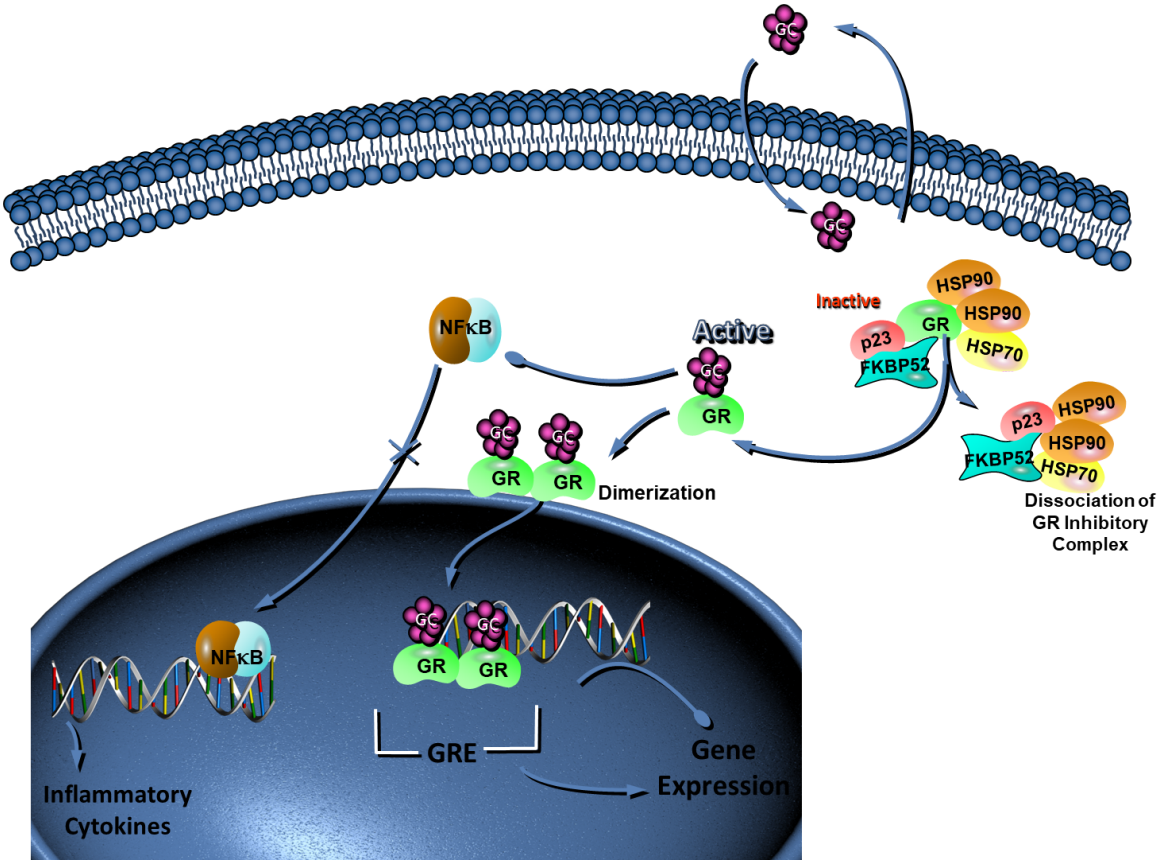

Figure 4. Glucocorticoid mechanism of action (71)

GCs can also act by nongenomic mechanisms that are responsible for effects characterized by a rapid onset and medium-short duration. In particular, in the cytoplasm the GC/GR complex triggers internal signaling events within the cell such as the release of annexin-A1, a protein that has anti-inflammatory properties because it is able to suppress both the activity of phospholipase A2 and the leukocytes activity (72).

It is well known that patients differ in their clinical response to GCs and many factors have been associated with treatment response and side-effects.

1.3.4 Glucocorticoid response in INS

Most of the time GC therapy for INS starts with 4–6 weeks of steroids each day (prednisone or prednisolone given at 60 mg/m^2), followed by a minimum of 6 weeks of alternate day therapy. Based on the clinical response to glucocorticoid therapy, approximately 85% of patients with INS are classified as steroid-sensitive (SS) if responding to high-dose prednisone within the first 8 weeks of treatment. The remaining 15% do not achieve a complete remission after 8 weeks of corticosteroid therapy and are classified as steroid resistant (SR) (73). Two consecutive relapses during steroid therapy or within 2 weeks from therapy completion define the patient as steroid dependent (SD). Although, there are several conditions due to chronic use of steroids and related to their side effects, less than 5% of children with steroid sensitive nephrotic syndrome (SSNS) progress to end-stage renal disease (ESRD) while steroid resistant nephrotic syndrome (SRNS), that usually presents resistance to the vast majority of immunosuppressants used to treat INS, is reported to be the major determinant for future ESRD which is characterized by a lowered life expectancy after dialysis initiation (61).

The underlying mechanisms of both resistance and dependence remain largely unknown and the therapeutic approach of SD and SR patients must be carefully chosen according to potentially severe side effects for long-term steroid therapy (73). At present, many biological factors are concerned in SRNS and various molecular pathways are reported to be deregulated (74,75).

Even though GCs have been first choice treatment for INS for decades, at present a biomarker usable as clinical tool to predict GC response is still not available.

1.3.5 NLRP3

The NOD-like receptor pyrin domain containing 3 (NLRP3) inflammasome is a multiprotein complex, composed of apoptosis-associated speck-like protein containing a CARD domain (ASC) and procaspase-1 (pro-CASP1), which is an important constituent of innate immunity (76). After its activation, the NLRP3 inflammasome catalyzes the conversion of pro-CASP1 into CASP1 which promotes secretion of pro-inflammatory cytokines such as interleukin 1β and interleukin-18 (76). Different signals such as viruses, bacteria, ATP release, environmental origin irritants, etc, are able to activate NLRP3 inflammasome both in vivo and in vitro (77,78). Several studies have demonstrated that inflammation plays a critical role in the development and prognosis of chronic kidney

disease (CKD) (79). In particular, the expression of NLRP3 in the kidney and the activity of NLRP3 inflammasome are significantly increased in different types of CKDs in both classical immune cells, such as infiltrating macrophages and resident dendritic cells as well as in renal tubular epithelial cells, and even in podocytes (figure 5) (80,81).

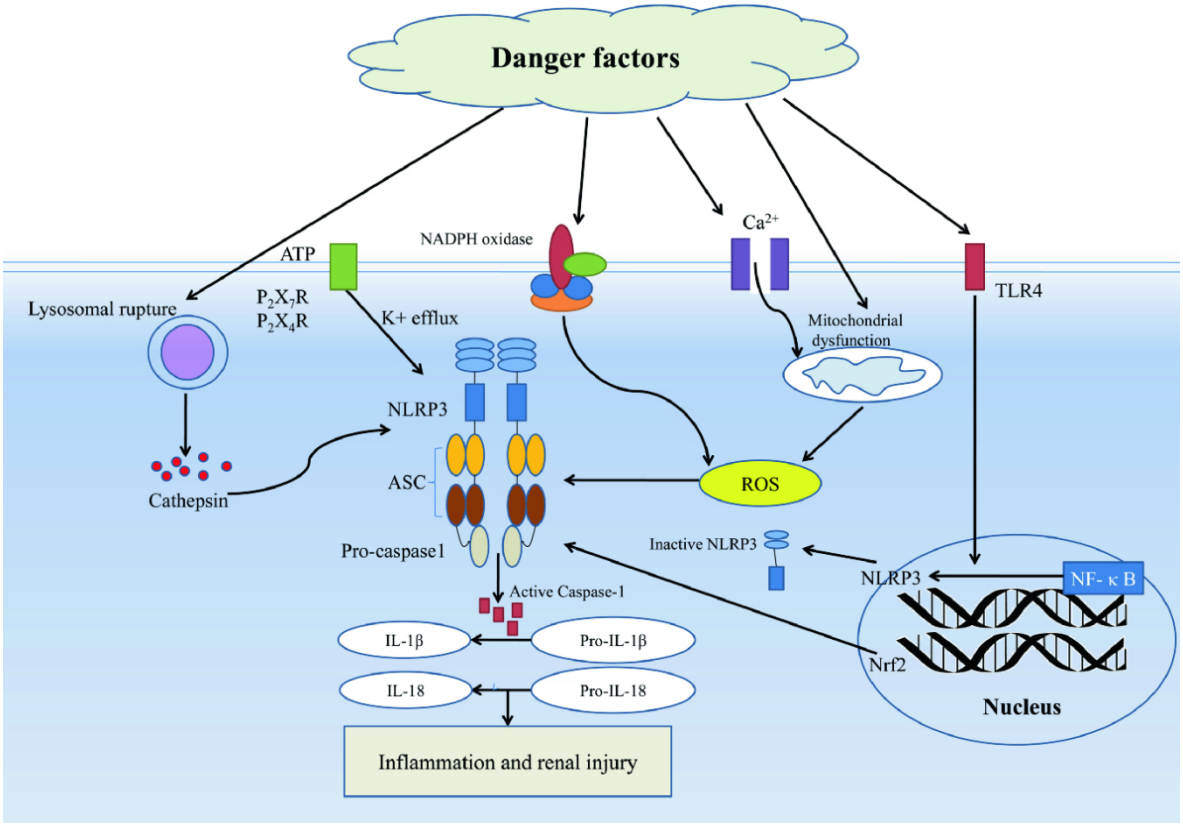

Figure 5. NLRP3 inflammasome involvement in renal injury (82).

NLRP3 was also found over-activated in white blood cells of hemodialyzed patients with kidney disease (83). Furthermore, inhibition of the NLRP3 inflammasome with different molecules ameliorates renal injury in animal models (84,85).

Interestingly, the DNA methylation of NLRP3 gene promoter together with the other proteins forming the inflammasome complex, was discovered to be reduced in patients with high inflammation levels (86,87). Lastly, it was recently discovered that the DNA methylation of NLRP3 plays a role in regulating GCs response in a cohort of patients with acute lymphoblastic leukemia. Paugh and collaborators have documented that increased expression of NLRP3, due to hypomethylation of its promoter, causes glucocorticoid resistant acute lymphoblastic leukemia due to the ability of CASP1 to cleave the GR,

leading it into an inactive form and unable to translocate inside the nucleus and act by binding to the GREs (figure 6) (36).

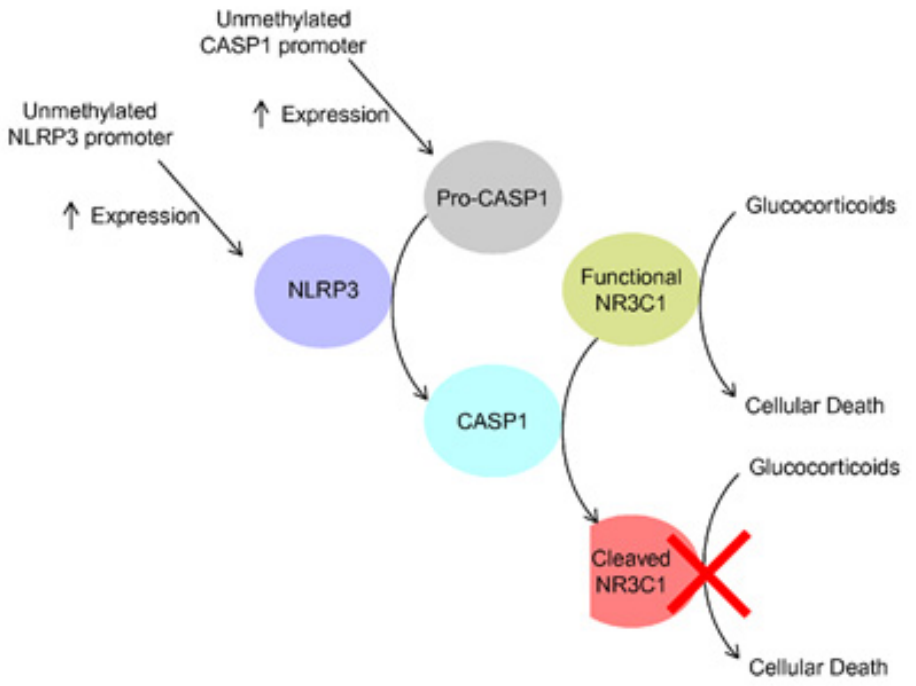

Figure 6. Epigenetic regulation of the NLRP3 inflammasome and glucocorticoid receptor inactivation (36). NLRP3, The NOD-like receptor pyrin domain containing 3; pro-CASP1, pro-caspase-1; CASP1, caspase-1; NR3C1, glucocorticoid receptor.

1.4 Inflammatory bowel disease

Inflammatory bowel diseases (IBDs) are a group of chronic inflammatory disorders, characterized by repetitive episodes of inflammation that involve the gastrointestinal tract, especially the colon and the small intestine. The two most representative IBDs are Crohn's disease (CD) and ulcerative colitis (UC). These two disorders differ in location of the chronic phlogosis, histology and progression of the disease while many other features are in common (88). IBDs can be associated with extraintestinal manifestations such as ankylosing spondylitis, coeliac disease, psoriasis, systemic lupus erythematosus, rheumatoid arthritis and multiple sclerosis (89). Recent studies show that the incidence of IBD in the world population is increasing, with an estimated value of 84.3 cases/100,000 people in 2017 (90). Usually 25% of IBD cases have an onset in childhood, while the incidence of patients under 16 years old is between 8 and 11 cases/100.000 inhabitants/year (91). Pediatric IBD has important differences if compared with adult IBD due to its

dependence with growth, development, pubertal maturation and bone health (92). The more precocious these symptoms are, the more aggressive they are both in terms of the extent of the disease and its progression (93). Patients who develop these IBD symptoms before the age of 6 are defined as early onset IBD (EO-IBD) and this growing sub-cohort of patients represents 15% of pediatric IBD patients (93–95).

1.4.1 Pharmacological therapy

The chronic nature of IBD results in a long-term therapy that cannot predict a complete recovery of the patient. Nowadays CD and UC are not curable diseases both in pediatric and adult populations and the therapy aims to achieve three main objectives, which follow one another as the therapy progresses for both conditions:

- remission induction
- remission maintenance
- ensuring a good quality of life for the patient

The therapeutic strategy for the treatment of IBD can vary considerably both for the drugs used and for their dosages. This is due to the great variability of the parameters that are considered for this type of therapy, such as disease subtype, patient age, severity, location, course of the disease and the presence of complications (96,97). Moreover, growth delay due to inflammation and in particular delayed skeletal maturation and a delayed onset of puberty are a factor of relevance in defining the therapeutic strategy in pediatric patients with CD (97,98). So far, corticosteroids in adults and enteral nutrition in children have been considered the standard treatment to induce the remission in CD while thiopurines are the first-line therapy for preventing disease relapse in patients who achieved remission (99). Generally, IBD treatment is the same in adults and pediatric patients for maintaining remission while is different for inducing remission.

Aminosalicylates are one of the oldest therapies currently used both to induce and maintain remission in UC even though their exact mechanism of action is still not completely understood (100). Salazopyrin is the prototype drug in this category, but mesalazine is the active moiety of this parent compound and is the main aminosalicylate used in IBD treatment today (101).

The most commonly used drugs to induce remission in pediatric patients are GCs, in moderate to severe active CD and UC, and anti-TNFα agents for most serious cases (96).

The importance of limiting steroids use increases when considering the treatment of a pediatric patient because of the inhibiting activity of prolonged steroid treatment on linear growth and bone density and their additional side effects that can physically compromise a young age patient. Anti-TNFα biological drugs, such as infliximab or adalimumab, have a rapid onset of effect, usually within 2 weeks after initiation of therapy and are usually effective in patients with IBD who do not adequately respond to GCs and immunosuppressants. Anti TNFα drugs could also lead to serious adverse effects, such as opportunistic infections (102).

Despite this multitude of drugs, the primary therapy for the induction of the remission in pediatric patients is the exclusive enteral nutrition. This strategy aims to optimize the patient's nutritional status through a diet composed of only polymeric formulas (103).

Mercaptopurine (MP) and its pro-drug azathioprine (AZA) are the drugs used to maintain remission of the disease due to their slow time of action, between 8 and 12 weeks (100). More recently, these immunosuppressants are also employed with biological therapies, as they can reduce the immunogenicity of biologics (100).

1.4.2 Azathioprine

Azathioprine, being a pro-drug, is not active itself and needs to be activated into thioguanine nucleotides (TGNs) that are considered the active metabolites, directly causing immunosuppression. After reaction with the glutathione transferases (GST) or by spontaneous hydrolysis, azathioprine is almost totally converted into mercaptopurine and then transported inside the cells by multiple trans membrane transporters (100). Once in the cytoplasm mercaptopurine is converted into TGNs by a cascade of enzymes of the purine salvage pathway, as shown in figure 7.

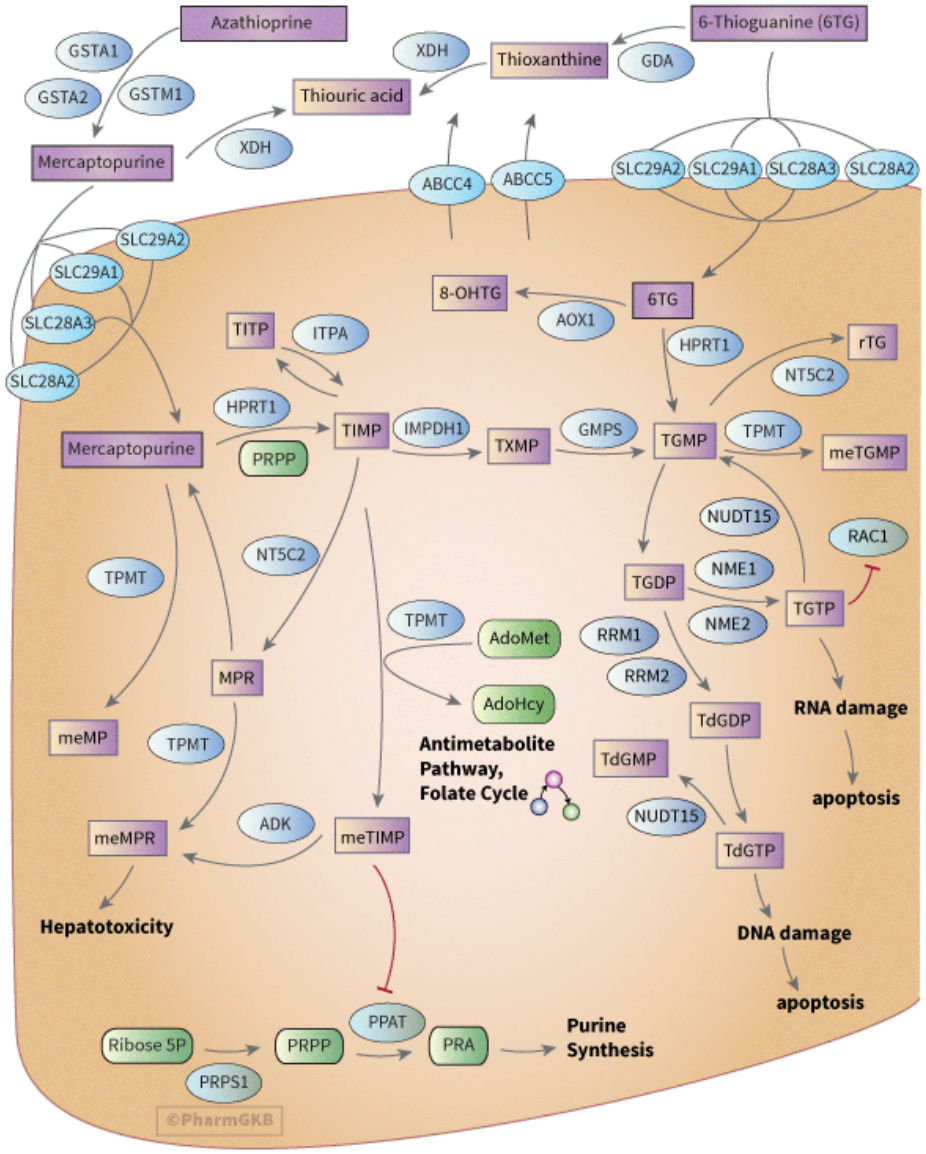

Figure 7. Thiopurine pathway (104).

To date, the cytotoxic effects of thiopurines can be explained through 4 principal pathways:

1. Incorporation of thiopurine active metabolites into DNA and RNA leading to an inhibition of several enzymes involved in DNA replication and repair. It also induces DNA damage such as single strand-breaks, DNA-protein cross-links and chromatid exchanges (105,106).
2. Inhibition of de novo purine synthesis mediated by methylmercaptopurine nucleotides (MMPN) (107).

3. Inhibition of the small signaling GTPase Rac1. TGNs, as all GTP analogues, suppress the activation of Rac1 target genes leading to a mitochondrial pathway of apoptosis in activated T lymphocytes (108).
4. Reduction of intracellular glutathione levels used as substrate of GSTs in azathioprine transformation to mercaptopurine (109).

1.4.3 TPMT

Thiopurine-S-methyltransferase (TPMT) is an enzyme that plays an important role in the metabolism of AZA because it catalyzes the S-methylation of thiopurine drugs leading them into an inactive form.

TPMT gene is highly polymorphic and the most relevant of these variant alleles are nonsynonymous single-nucleotide polymorphisms (SNPs) (110). In particular, the TPMT wild-type allele (TPMT*1) presents a normal, high activity while the most characterized variant alleles (*2, *3A, *3B, *3C, *4, *8) present low or deficient activity (111). Since different alleles produce TPMT enzymes with different inactivation efficiency, the knowledge of a patient's genotype is essential in order to avoid adverse effects like myelosuppression (112). Clinical guidelines recommend decreasing AZA dosage by 10 folds and to administer the adjusted dose thrice weekly instead of daily for homozygous patients for TPMT variant alleles (111). A homozygous TPMT-deficient patient treated with normal thiopurine dosage usually experience severe myelosuppression (111).

Recently, age has been demonstrated to affect the activity of TPMT and the efficacy of thiopurines in pediatric IBD patients, with effects particularly strong in EO patients (age < 6 years), which had increased TPMT activity and need a higher pro-kg dose of AZA in order to let the TGNs reach the therapeutic window compared to adolescent patients (91). Moreover, a meta-analysis published in 2019 by Gibson and collaborators demonstrated that TPMT is an epigenetic-age associated gene and, in particular, SNPs located on the TPMT gene strongly associate with the epigenetic age calculated with the Horvath epigenetic clock (49).

Considering the abovementioned evidences, the hypothesis of an age-dependent epigenetic regulation of the TPMT gene is highly possible. In particular, the analysis of TPMT promoter and neighboring regions methylation could give interesting insights on the pharmacokinetic differences between VEO and adolescent patients.

1.5 Juvenile idiopathic arthritis

Juvenile idiopathic arthritis (JIA) is a chronic disease characterized by persistent joint inflammation; characteristics signs of joint inflammation are pain, swelling and limitation of movement. JIA is the most common chronic rheumatic disease of childhood and is an important cause of disability (113). For this reason, a rapid pharmacological control of inflammation allows avoiding structural damage and growth impairment. JIA has an estimated global incidence between 1.6 and 23 cases per 100,000 children (114) while the incidence in the Caucasian population is reported to be 8.3 per 100,000 children (115). JIA can be divided in 7 categories each one with its distinct phenotype and genetic background according to the consensus conference of the International League of Associations for Rheumatology (ILAR) in 2001 (116), in particular the categories are defined according to the number of painful joints and the presence of other symptoms, such as enthesitis, psoriasis or the rheumatoid factors.

The causes and triggers of all the JIA subtypes have not yet been clearly identified even though the abnormal immune responses activation in JIA patients has been associated with both environmental and genetic factors (117,118). In particular, also thanks to studies conducted on monozygotic twins (119), genetic factors play a significant role and several genetic mutations on the HLA genes have been associated with the onset of all the previously mentioned JIA subtypes (117,120).

Arthritis is the common feature presented by patients of all subtypes of JIA. Inflammation of the joints results in pain, morning stiffness, and loss of function. Cutaneous rash, loss of appetite and high body temperature are also usually present, especially in the acute phases of the disease even though skin findings occur mostly in systemic, polyarticular and psoriatic arthritis (121).

Moreover, some JIA patients develop uveitis, a condition characterized by inflammation of the uveal components of the eye that may lead to partial or complete vision loss (122).
From an immunological prospective, laboratory analysis show an important role of innate immunity in JIA. In particular, the cytokines interleukine-1, interleukine-6 and interleukine-18 have been demonstrated to be highly expressed in patients' blood as well as other specific proteins such as S100A8, S100A9 and S100A12 that are secreted consequently to the aberrant activation of T cells and phagocytic macrophages (123,124).

Histologically, the synovia of JIA patients shows a high degree of infiltrating inflammatory cells, especially T and B lymphocytes, plasma cells and macrophages. Moreover, villous

hypertrophy, hyperplasia of synoviocytes, endothelial hyperplasia and activation and increased vascularization with hyperemia is also evident in JIA patients' joints (125).

A better understanding of the pathophysiological mechanisms of JIA has led to great improvement in disease management and pharmacological treatment, with the recent introduction of biologic drugs able to selectively attack the abovementioned cytokines and proteins (126). Treatment aims at reducing symptoms and at normalizing the biochemical alterations characterizing JIA patients.

1.5.1 Pharmacological treatment

Pharmacological treatment of JIA requires anti-inflammatory and immunomodulatory drugs and depends on the disease subtypes, disease severity and damage, associated disease, and family acceptance.

Nonsteroidal anti-inflammatory drugs (NSAIDs) are the first line treatment for all subtypes in order to immediately reduce the severity of symptoms. NSAIDs inhibit cyclooxygenases, enzymes that regulates the synthesis of prostaglandins and are frequently associated with serious side effects such as gastric ulcer. Due to their frequent side effects and their only symptomatic activity, NSAID use in JIA has decreased over time with the introduction of modern aggressive treatment, including methotrexate (MTX), biologics such as etanercept and adalimumab and the IL-1 blocker Anakinra.

Intra-articular corticosteroid injections are also widely used in the management of children with oligoarthritic-JIA, in order to induce rapid relief of inflammatory symptoms and improve articular mobility without systemic corticosteroids side effects (127).

1.5.2 Methotrexate

MTX is the first choice disease-modifying anti-rheumatic drug (DMARD) in JIA, however, 35-45% of patients fail to respond (128,129), and the delay in identifying the optimal treatment at an early stage of disease can influence the long-term joint damage. The pharmacodynamic profile of MTX can to a large extent be explained by its interactions with enzymes in the folate pathway (figure 8).

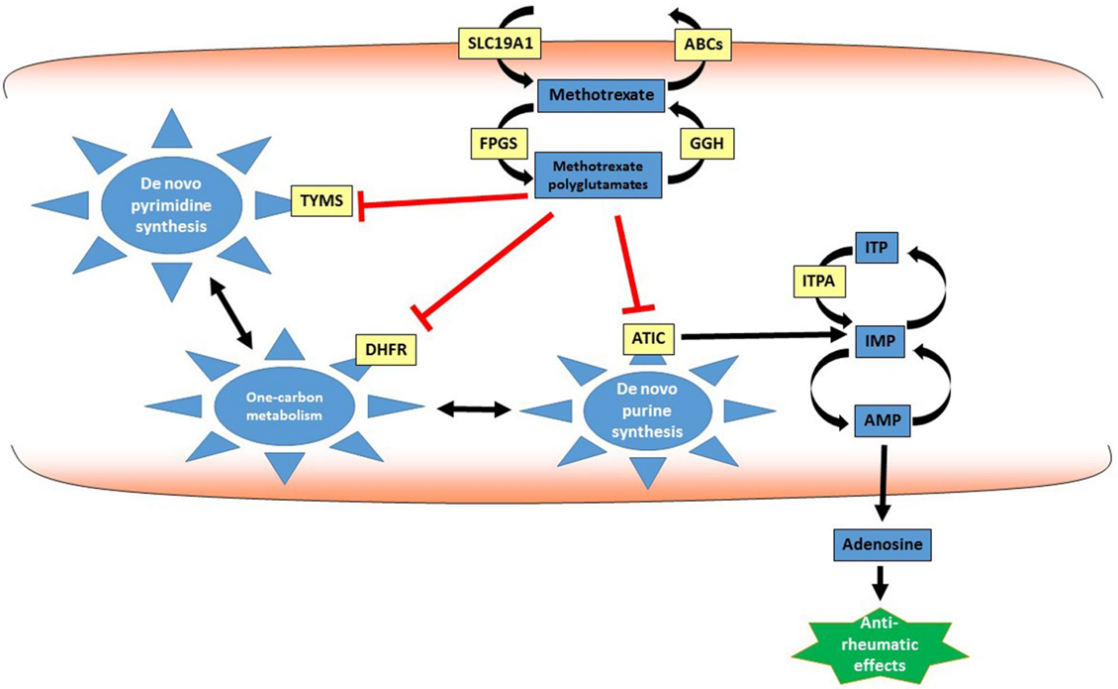

Figure 8. Methotrexate pathway (130). AMP, adenosine monophosphate; ATIC, adenosine ribonucleotide transformylase; DHFR, dihydrofolate reductase; FPGS, folylpolyglutamate synthase; GGH, gamma-glutamyl hydrolase; IMP, inosine monophosphate; ITP: inosine triphosphate; ITPA, inosine triphosphate-pyrophosphatase; SLC19A1, solute carrier family 19 member 1; TYMS, thymidylate synthetase.

MTX inhibits the enzyme dihydrofolate reductase (DHFR), an enzyme able to convert dihydrofolate to tetrahydrofolate which is essential both for de novo purine synthesis and one-carbon metabolism (131). MTX enters cells actively mainly through the reduced folate carrier SLC19A1 whereas efflux across the cell membrane is mediated by ATP-binding-cassette (ABC) transporters (130). Inside the cells, MTX is converted to the more active methotrexate polyglutamates (MTXPGs) by folylpolyglutamate synthetase (FPGS), which adds glutamate residues to MTX (132).

MTX for JIA is given weekly at low doses around 10-15 mg/m^2. At this dosage MTX action mostly occurs via the release of adenosine thanks to the inhibition of ATIC by MTX. Adenosine, considered one of the principal mediators of the anti-rheumatic effect of MTX, binds to its receptors (adenosine receptors ADOR1A, ADOR2A, ADOR2B and ADOR3) all of which have potent inhibitory effects on several inflammatory cell types, leading to the reduction of joint inflammation in JIA patients. MTXPGs have been investigated in relation to the clinical outcomes in JIA and higher concentrations of long chain MTXPGs have been associated with risk of gastrointestinal and hepatic toxicity in JIA (133).

Considering the high variability in response in JIA patients, there is the need to identify determinants, such as genetic and immunological biomarkers, influencing response to MTX in order to individualize treatment strategies. Recent studies have evaluated the effects of candidate genetic variants in the complex pathway of genes involved in MTX pharmacokinetics and pharmacodynamics on the response to the medication in children with JIA. These studies demonstrate that genetic variants in the MTX pathway, such as ATIC, ITPA, and SLCO1B1 are associated with MTX response in JIA (133–135). However, results are still contrasting and no definitive genetic marker of MTX response useful for the clinician to tailor therapy of children with JIA has been identified. This may be due to the lack of studies considering fine mapping of genetic variants in relevant candidate genes in a sufficiently powered and prospectively followed-up patients' population.

Recently, MTX has been demonstrated to modify global DNA methylation during therapy of patients with arthritis (136,137). Clinical studies considering the association between MTX response in JIA and DNA methylation in whole blood are presently missing. It is also becoming clear that JIA patients display a differentially methylated genome when compared to healthy individuals (138) but, to our knowledge, studies about the influence of epigenetic variations, and the related alteration in gene expression, on response to MTX in pediatric patients with JIA are not available in the literature.

1.5.3 CDH4 gene and MTX response

The CDH4 gene encodes retinal cadherin (R-cadherin), a calcium-dependent cell-cell adhesion glycoprotein composed of five extracellular cadherin repeats, a transmembrane region, and a highly conserved cytoplasmic tail (139). Deregulation of CDH4 has previously been associated with several human cancers including colorectal, gastric, and nasopharyngeal carcinomas (140,141).

Moreover, as occurs for most cadherins, the region at the 5′ end of the first exon of the CDH4 gene presents a dense CpG island spanning about 2 kb around the first exon (140,142). This CpG island functions as a promoter element and actively regulates CDH4 gene expression.

Surprisingly, two studies available in the literature have found interesting correlations between the CDH4 gene and methotrexate response. In particular, Haupl T. and collaborators reported an overexpression of the CDH4 gene in synovial cells of rheumatoid

arthritis patients compared to healthy donors that became comparable after MTX treatment (143). Moreover, a genome wide study from Cobb J. and colleagues identified 10 intronic SNPs on the CDH4 gene that correlate with the visual analog scale (VAS), ACR ped index and limited joints count (144).

To our knowledge, a study that correlates the methylation of the CDH4 gene to MTX response in JIA patients is still not available and might give interesting insights on the mechanisms of MTX resistance.

2. AIM OF THE THESIS

DNA methylation involves the transfer of a methyl group onto the C5 position of the cytosine to form 5-methylcytosine and it is one of several epigenetic mechanisms that cells use to control gene expression. Differentially methylated genes or DNA regions can be associated with pharmacological phenotypes such as drug response, pharmacokinetics or drug toxicity and could potentially explain the interindividual variability in drug response. In this thesis the role of DNA methylation in relation to the response of different drugs used to treat specific autoimmune diseases was evaluated.

In particular the aims of this thesis are to investigate:

1) Whether NLRP3 methylation could be associated with age and gender in idiopathic nephrotic syndrome patients. Moreover an in vitro model potentially explaining the role of NLRP3 in GC resistance in INS has been set up.

2) The role of DNA methylation in relation to azathioprine pharmacokinetics in EO pediatric patients with IBD. In particular, we assessed azathioprine active metabolites, TPMT activity TPMT, DNA methylation and TPMT expression in early onset and non-early onset pediatric IBD patients presenting age-related pharmacological differences.

3) The role of CDH4 methylation in relation to MTX response in pediatric patients with JIA. In particular, in this thesis we assessed the association between the ACR Pedi index and the DNA methylation of the CDH4 gene, and its neighboring regions, in 3 different cohorts of pediatric patients with JIA.

The results of this research could give interesting insights on the role of DNA methylation as epigenetic biomarker for the prediction of drug response of immunosuppressive therapies in different autoimmune diseases. These results could be a step forward for therapy personalization, giving the clinicians the possibility to adjust or modify a pharmacological therapy according to the DNA methylation status of specific CpG sites or genomic regions, avoiding drug side effects and disease progression due to inadequate therapies.

3. MATERIAL AND METHODS

3.1 NLRP3 METHYLATION AND GLUCOCORTICOID RESPONSE IN IDIOPATHIC NEPHROTIC SYNDROME PATIENTS

3.1.1 INS Patients

A total of 28 adult patients with a history of INS in clinical follow-up at the Renal Unit of Hospital/University of Verona were enrolled in the study. Eighteen of them (13 with MCD and 5 with FSFS) were classified as INS glucocorticoid-sensitive patients (all of them were in clinical remission and out of corticosteroids/immunosuppressive treatment for more than 6 months). Remission was defined as the disappearance of proteinuria for at least 3 consecutive days. All the 10 glucocorticoid-resistant patients were in hemodialysis (out of any immunosuppressive therapy for more than 6 months). These patients received a kidney histological diagnosis of FSGS. At diagnosis, INS was defined according to KDIGO 2012 guidelines (145). To avoid confounding factors, all adult patients with secondary glomerulonephritis, concomitant infectious diseases, diabetes, chronic lung diseases, neoplasm and patients receiving antibiotics or non-steroidal anti-inflammatory agents were excluded. Patients with less than 12 months of follow-up were also excluded.

To exclude potential confounding effects on NLRP3 promoter methylation due to previous immunosuppressive treatments and/or hemodialysis, a control group of children with a first episode of INS, presenting at 49 Pediatric and Pediatric Nephrology Units in 10 Italian regions, were enrolled. At the time of diagnosis and before treatment, in all pediatric patients' whole blood was obtained. Subsequently, they were treated with prednisone at a dose of 60 mg/m2/day for either 4 or 6 weeks, depending on whether time to remission was $<$ or $\geq$ 10 days. Remission was defined as the disappearance of proteinuria for at least 3 consecutive days, as in the adult patients. Prednisone was then tapered over a 16-weeks period. As previously described (73), patients were then classified into the two study groups: glucocorticoid-resistant if they did not achieve remission after therapy with daily prednisolone at a dose of 60 mg/m2/day for 4-6 weeks, whereas those patients achieving remission were considered glucocorticoid-sensitive.

Seven patients resulted glucocorticoid-resistant, while 14 children were glucocorticoid-sensitive (age 4-18 years). The study was carried out according to the Declaration of Helsinki. The patients or parents of all participating children gave written informed consent before being enrolled in the study. Ethics Committee approval was obtained from all the participating centers.

Finally, a cohort of 52 healthy subjects (41 adults, 11 women, mean age 44.5 ± 11.8 years, and 11 children, 5 girls, age 10.2 ± 5.5 years) was also enrolled.

3.1.2 NLRP3 promoter methylation analysis

NLRP3 promoter methylation was measured by SNuPE assay after DNA bisulfite conversion and bisulfite-specific PCR of genomic DNA obtained from peripheral blood of both adult and pediatric INS patients. This assay evaluated NLRP3 promoter methylation at a CpG site previously linked to glucocorticoid resistance in acute lymphoblastic leukemia cells, in particular cg21991396 for NLRP3. Episcope Methylated and Unmethylated HCT116 gDNA were utilized as controls. To amplify regions containing CpG sites of interest in the NLRP3 gene, Episcope MSP kit was used and the PCR cycling conditions were as follows: 95°C-30 seconds, 98°C-5 seconds, 52°C-30 seconds, 7 °C-60 seconds (repeat steps 2-4, 39 times), 72°C-5 minutes, hold at 4°C. The PCR samples along with a 1 kb DNA ladder for molecular weight determination were then loaded onto a 2% agarose gel containing SYBR safe DNA gel stain and electrophoresed at 100 to 150 Volts. Subsequently, using an UV illuminator, the DNA bands were excised, and the DNA extracted using Qiagen QIAquick gel extraction kit, following the supplied protocol. To determine whether the fragment of interest was methylated or not, a single-nucleotide primer extension reaction was performed: this reaction uses a primer specific for a promoter region that, in presence of Cy3-marked nucleotides, is extended either with dUTP or dCTP, complementarily to the amplified bisulfite-converted products. Control oligos are prepared using NLRP3-Methylated/Unmethylated oligo duplexes for 0%, 25%, 50%, 75%, 100% methylation control. Purified PCR products were added in duplicate to a PCR 96 well plate, and to each sample a mix containing either dUTP or dCTP was added. The mix contains the SNuPE oligos (that will undergo the primer extension) and Taq DNA polymerase (ThermoFisher, Waltham, MA, USA). Cycling conditions were as follows: 94°C-1 minute, 50°C-30 seconds, 68°C-30 seconds, 4°C-indefinitely. Each sample was loaded in 15% TBE-urea gels, pre-run for an hour, loading dCTP and dUTP reaction products in adjacent wells. After electrophoresis, the gels were imaged at 600 nm to acquire Cy3 fluorescent signal. Once this signal was acquired, gels were stained with SYBR Gold and imaged again at 600 nm to acquire the total nucleic acid signals to confirm that equal amounts of DNA were present in the dCTP and dUTP lanes. Methylation levels for each sample were calculated as follows:

$$\text{methylation} = (\text{dCTP signal}) / (\text{dCTP signal} + \text{dUTP signal}).$$

3.1.3 Cell culture

Human monocytic U937 cell lines were purchased from ATCC (Manassas, VA, USA). Cells were cultured in suspension in RPMI 1640 medium (Lonza, Basel, Switzerland) supplemented with 10% FBS (fetal bovine serum) and 2 mM L-glutamine. Where indicated, U937 cells were stimulated with LPS (10 ng/ml) (Sigma-Aldrich, St. Louis, MO, USA) for 4 h followed by ATP (Sigma-Aldrich, St. Louis, MO, USA) 1 mM for 15 min, in RPMI 1640 without FBS, to induce the activation of the NLRP3 inflammasome pathway.

3.1.4 In vitro proliferation assay

The effect of prednisone on the proliferation of the U937 cells was determined by labeling metabolically active cells with [methyl-3H] thymidine (PerkinElmer, Milan, Italy) as previously reported. Cells were seeded into 96-well plates (10.000 cells/well) and treated with or without LPS/ATP and then exposed to prednisone (range from 0.5 μM to 100 μM) for 24 hours. After 19 hours of incubation, cells were pulsed with [methyl-3H] thymidine (final concentration of 2.5 μCi/ml) and the incubation was continued for additional 5 hours. The radioactivity of the cells was determined by a liquid scintillation analyzer (Wallac 1450 Microbetaliquid scintillation counter, PerkinElmer). Raw count per minute (cpm) data were converted and normalized to percent of maximal survival for each experimental condition (cpm prednisone /cpm control*100).

3.1.5 Total RNA isolation

Total RNA from U937 monocytes was extracted using the TRIzol® reagent (Thermo Scientific). TRIzol® reagent maintains the integrity of RNA due to the highly effective inhibition of RNase activity while completely dissociating the nucleoprotein complex homogenizing cells. The samples were incubated with 1 mL of TRIzol® for 5 minutes at room temperature to dissociate the nucleoprotein complex. Chloroform (0,2 mL; Sigma-Aldrich) was added and after 3 minutes of incubation at room temperature, a centrifugation at 12,000 × g for 15 minutes at 4°C was performed. After centrifugation, the mixture separates into a lower red phenol-chloroform phase containing protein, an interphase containing DNA and a colorless upper aqueous phase containing RNA. The upper phase was then transferred into a new RNase-free tube to proceed with the RNA isolation procedure. After precipitation with 500 μL of 100% isopropanol (Sigma-Aldrich) and a wash step with 1 mL of 75% ethanol (Sigma-Aldrich), the RNA pellet was resuspended in 20 μL RNase-free water (Gibco-Life Technologies) and incubated in a water

bath at 55–60 °C for 15 minutes. Then, the RNA concentration and purity were evaluated by a NanoDrop instrument (NanoDrop 2000, EuroClone®). Quantity of initial TRIzol® and following reagents were halved if the number of cells was < 1 x 10^6.

3.1.6 Reverse transcription

Reverse transcription is a process that converts RNA to single-stranded complementary DNA (cDNA) using a primer to the 3' end of the RNA template and serves as a starting point for the polymerase chain reaction (PCR). The reverse transcription was performed using the High Capacity RNA to-cDNA Kit (Applied Biosystem) with up to 1 μg of total RNA per 20 μL of reaction containing 10 μL of 2 x RT Buffer, 1 μL of 20x RT Enzyme Mix.

Reverse transcription was performed in a thermal cycler (Applied Biosystems 2720 Thermo Fisher Scientific). The thermal protocol provides a first incubation of samples to start the reaction at 37°C for 60 minutes and a stop of the reaction by heating to 95°C for 5 minutes and a final hold step at 4°C. The cDNA obtained is ready for use in real-time PCR applications or long-term storage in freezer.

3.1.7 Quantitative real-time PCR (TaqMan®)

Expression levels of GILZ and 18S were evaluated by real-time RT-PCR TaqMan® analysis using the CFX96 real-time system-C1000 Thermal Cycler (Bio-Rad Laboratories, Hercules, CA, United States).

The real-time PCR is a development of the PCR techniques that enables reliable detection and measurement of products generated during each cycle of the PCR process. The amplification of the RNA sequence of interest can be obtained by a process consisting of 30-40 thermal cycles of heating and cooling. The real-time PCR process can be generally divided into three steps:

1. Initial denaturation. At the start of real-time PCR, the temperature is raised to ensure that all complex double stranded cDNA molecules are separated into single strands for amplification.
2. Cycling: denaturation, annealing and extension. During denaturation the temperature is increased to 95°C and all double stranded cDNA are converted into single stranded cDNA. During the annealing phase, the temperature is lowered to approximately 5°C below the melting temperature (TM) of the primers (often

45–60°C) to promote primer binding to the template. The primers are designed to bind the sequence of interest and the region of sequence that lies between them is referred to as the amplicon. In general, the annealing temperature may be estimated to be 5 °C lower than the melting temperature of the primer template DNA duplex. In the extension step, the temperature is increased to 72°C, which is optimum for DNA polymerase activity to allow the extension from the 3' of each primer to the end of the amplicon.

3. Repeat cycling. The denaturation, annealing and extension steps are repeated cyclically resulting in exponential amplification of the amplicon.

Expression levels of the target gene have to be normalized using an endogenous reference gene, the housekeeping gene. The expression of GILZ was evaluated using the TaqMan® Gene Expression Assay (according to the manufacturer's instructions) and the 18S housekeeping gene was used as normalizer and expression levels were reported as $2^{-\Delta Ct}$ (146). The results are provided as the mean and standard error of up to three replicates for the immortalized cellular line. A list of the TaqMan® assay probes' IDs is reported in table 1.

Gene name	TaqMan® assay ID
18S	Hs03003631_g1
GILZ	Hs00608272_m1

Table 1. Real-time PCR probe sequences for 18S and GILZ.

3.1.8 Western blot analysis

Western blot is an analytical technique used to detect and quantify specific proteins in a biological sample. Samples are prepared as follows: 20 µg of proteins are added with 5 µL of LDS Loading buffer 1x (Thermo Fisher) to a final volume of 20 µL with protein lysis buffer under non-reducing conditions. Each sample is then loaded on Sodium Dodecyl Sulphate – Polyacrylamide Gel Electrophoresis (SDS-PAGE) 10% (precast Bolt 10%, Bis-Tris Plus Gels, Thermo Fisher) which permits to separate proteins based on their molecular weight since it breaks tertiary and secondary protein structures and charges amino acids negatively. Gel is also loaded with 5 µL of protein marker (Thermo Fisher) that separates in colored bands depending on the molecular weight in order to follow protein run. The gel is inserted in an electrophoretic chamber filled with Running Buffer 1x (Thermo Fisher) that is connected to electrodes on which a voltage of 200 V is applied for

about 40 minutes. Gel is then put in a Power Blotter (Thermo Fisher) placed on a nitrocellulose membrane (Thermo Fisher) previously wetted with Transfer Buffer 1x (Thermo Fisher). A constant electric current of 1.3 A (25 V) is applied for 7 minutes. To verify if the gel is completely transferred on the membrane, Ponceau red is used. This solution binds proteins unselectively and imparts them a bright red color. It is washed away using distilled water. After transfer on nitrocellulose, the membrane is cut using markers as a guide to separate proteins of interest from the others. Afterwards, each sample is incubated with 5% milk solution in T-TBS (0.012 % p/V Trizma (Sigma); 0.009 % p/V NaCl (Sigma); 0.001% Tween 20 (Sigma)) for 1 hours at 4 °C on a rocking platform. This phase is needed to bind all non-specific binding sites on the membrane.

After blocking, incubation with the following primary antibodies at 4 °C was performed overnight: anti-glucocorticoid receptor 1:500 (Santa Cruz Biotechnologies, Dallas, TX USA and anti-Actin 1:3000 (Abcam, Cambridge UK, Cat. N. ab8227). An anti-mouse (Cell Signalling, Danvers, MA USA, Cat. N. 7076S) diluted 1:40000 secondary antibody and an anti-rabbit HRP conjugated (OriGene technologies, Rockville, MD USA, Cat. N. TA13002) diluted 1:1000 secondary antibody were incubated for 1 hour at 4 °C. After each step of antibody incubation, membranes are washed with T-TBS, four times for 5 minutes and are ready to be developed. In order to develop the membranes, LiteABLOT Turbo Chemiluminescent Substrate (Euroclone) is used. The kit is composed of Peroxidase Buffer and Luminol: HRP enzyme in presence of hydrogen peroxide catalyses the oxidation of luminol, resulting in a fluorescent emission. The solution is spread on the membrane and incubated for 5 minutes. The fluorescence produced by luminol is impressed on the photographic plate (Sigma) placed on the membrane for 3 minutes in a cassette. The plate is then developed with Developer solution (1:5 in water, Thermo Fisher), washed with water and stained with Fixer solution (1:5 in water, Thermo Fisher). Images were analyzed with ImageJ program and data were normalized on β-actin.

3.1.9 Statistical analysis

The association between methylation at the NLRP3 CpG site and demographic and clinical covariates was evaluated by generalized linear models considering methylation as the dependent variable and the demographic and clinical covariates as the independent variables. Normality of methylation level was assessed by Shapiro test. Statistical analyses were performed using the software R.

For NLRP3 the in vitro studies, statistical analyses were performed using GraphPad Prism version 4.00. Two‐way ANOVA with Bonferroni post‐test and t‐test were used for the analysis of inhibition of proliferation and gene expression. All p-values <0.05 were considered statistically significant.

3.2 TPMT METHYLATION AND AZATHIOPRINE PHARMACOKINETICS AND RESPONSE IN PEDIATRIC PATIENTS WITH INFLAMMATORY BOWEL DISEASE

3.2.1 IBD Patients

In this study, 120 patients with IBD were enrolled by the participating centers between May 2005 and June 2021. The inclusion criteria were age up to 6 years for cases and older than 12 years and younger than 18 years for controls, a previous diagnosis of IBD and treatment with azathioprine for at least 90 days. The exclusion criteria were concomitant therapy with anti–tumor necrosis factor biological agents (infliximab or adalimumab) and TGN levels under 50 pmol/[(8 × 108) erythrocytes] as signal of bad patients' therapy compliance. Other cotreatments, such as aminosalicylates, GCs, or enteral therapy, were allowed. Blood samples, collected for measuring AZA metabolites, TPMT activity, TPMT gene expression, TPMT DNA methylation and for genotyping, were taken at the first clinic visit occurring after at least 3 months of therapy and 1 month on stable AZA dose. The patients enrolled were all the eligible consecutive cases taking azathioprine at the participating centers in the timeframe of the study.

3.2.2 DNA extraction and genotypes

Genomic DNA was extracted from IBD patients peripheral blood using a commercial kit (SIGMA, Milan, Italy), to characterize the most relevant genetic polymorphisms in the candidate gene TPMT (rs1800462, rs1800460, and rs1142345), using TaqMan assays (Thermoscientific, Milan, Italy). The TaqMan® technique requires the use of an oligonucleotide probe containing a fluorescent reporter dye on the 5' end and a quencher dye on the 3' end and a pair of unlabeled primers. The 6-carboxyfluorescein (FAM) was used as fluorescent dye on 5' end for mutant allele while the 2′-chloro-7′phenyl-1,4-dichloro-6-carboxy-fluorescein dye (VIC) for the wild type allele. Samples genotyping was repeated twice.

3.2.3 DNA bisulfite conversion

DNA bisulfite conversion involves treating methylated DNA with bisulfite, which converts unmethylated cytosines into uracil. Methylated cytosines remain unchanged during the treatment. Once converted, the methylation profile of the DNA can be determined by PCR amplification followed by DNA sequencing. The EZ DNA Methylation™ Kit is based on the three-step reaction that takes place between cytosine and sodium bisulfite where cytosine is converted into uracil.

In a 0.2mL PCR Eppendorf, 5 µl of M-Dilution Buffer was added to 200ng-500ng of whole blood DNA extracted from patients' peripheral blood and the total volume was adjusted to 50 µl with water. The solution was mixed by flicking or pipetting up and down and incubated at 37°C for 15-20 minutes. 100 µl of the CT Conversion Reagent were then added to each sample and the solution was mixed by pipetting up and down. The sample was then placed in thermal cycler (Applied Biosystems 2720 Thermofischer Scientific) at (95°C for 30 sec., 50°C for 60 min.) x 16 cycles and a final hold step at 4°C. After the incubation, 400 µl of M-Binding Buffer were added to a Zymo-Spin IC™ column which was placed into the collection tube provided in the kit. The sample was then loaded into the Zymo-Spin IC Column containing the M-Binding Buffer and mixed by inversion several times. The column was centrifuged at full speed (≥10,000 x g) for 30 seconds and the flow-through was discarded. Then, 100 µl of M-Wash Buffer was added to the column and centrifuged at full speed for 30 seconds. 200 µl of M-Desulphonation Buffer was added to the column and let stand at room temperature (20–30°C) for 15–20 minutes. Following incubation, the sample was centrifuged at full speed for 30 seconds. 200 µl of M-Wash Buffer was then added to the column and the sample was centrifuged at full speed for 30 seconds. This step was repeated twice. The column was placed in a 1.5 ml microcentrifuge tube. 10 µl of M-Elution Buffer was added directly to the column matrix and the sample was centrifuged at full speed to elute the DNA. At this point, the DNA was stored at temperatures at temperatures ≤ - 80°C for further analyses. The CT Conversion Reagent and the M-Wash Buffer were prepared according to the manufacturer's protocol.

3.2.4 Illumina methylation EPIC bead-chip array

Genome wide DNA methylation profiles were obtained using an Illumina Methylation EPIC BeadChip array kit. All experimental methods were performed strictly according to the manufacturer's protocols (Illumina). The IDAT file, a raw data file containing the

intensities of the probes in the array, was analyzed using the ChAMP package of R/Bioconductor (147). The probes for which detection P values were < 0.01 across all samples were used. Average beta values were used for comparison.

3.2.5 Pyrosequencing analysis for DNA methylation

In order to analyze the methylation of cg22736354 located on TPMT downstream neighboring region and 2 CpG sites, chr6:18,154,513 chr6:18154820, located on TPMT promoter, pyrosequencing assay was performed using the PyroMark Q96 MD (Qiagen, Inc.; Germantown, MD). Custom primer sets were designed for both cg22736354 located in the neighboring region of TPMT (on NLHRC1 gene) and TPMT promoter. Methylation was then quantitated with Pyro Q-CpG (version 1.0.9; Biotage, Inc.). Regarding the cg22736354 assay, other 3 CpG sites have been analyzed (2 upstream CpGs (chr6:18,122,713 and chr6:18,122,715) and 1 downstream CpG (chr6:18,122,722) of cg22736354) due to the assay design. Table 2 provides a list of the primers and sequencing probes, specific for the bisulfite converted DNA sequence, used to quantitate these sites.
The average beta (essentially the ratio of the methylated to unmethylated signal) for each site was used to test for differences.

CpG site	**Genomic location**	**Oligos**	**Sequence 5' – 3'**
cg22736354	chr6:18,122,719 (GR38)	P.F.	GAATGGGTATTAGAGGGTTAGAGT
		P.R.	[BIO]ATCAACCTACTCCAATACAAAATATACTTT
		S.P.	GATTAAGTGGTAGTAGGATAGGTT
TPMT promoter	chr6:18,154,589 (GR38)	P.F.	AGGGATTATTTATTATTTGGTAGTATT
		P.R.	[BIO]CCCAACCTCCTCCATAACTAAAACTACA
		S.P.	ATATATTAGGTTGGGGAA

Table 2. *List of primers and sequencing probes for pyrosequencing analysis. P.F., primer forward; P.R., primer reverse; S.P., sequencing probe, [BIO], 5'-biotinilated primer; GR38, genome reference 38.*

3.2.6 Measurement of Azathioprine Metabolites

Azathioprine metabolites (TGN and methylmercaptopurine nucleotides, MMPN) were measured at the Department of Life Sciences, University of Trieste in IBD patients' erythrocytes using a high-performance liquid chromatography (HPLC) assay by Dervieux et al (148). Blood samples were centrifuged for collection of erythrocytes; erythrocytes were stored at −20°C until analysis. Metabolites concentration is expressed as pmol/ (8×10^8) erythrocytes. The ratio between TGN and the dose of azathioprine was calculated considering for each individual measurement the dose the patients were taking the day the blood sample for the metabolite's assessment was collected.

3.2.7 Measurement of TPMT Activity

TPMT activity was measured in IBD patients' erythrocytes at the Department of Life Sciences, University of Trieste using an HPLC assay based on in vitro conversion of mercaptopurine to methylmercaptopurine, using S-adenosyl-methionine as the methyl donor (149). TPMT activity is expressed as pmol of methylmercaptopurine produced by 10^9 patients' erythrocytes, during 1 hour of incubation at 37°C in the presence of mercaptopurine.

3.2.8 TPMT RNA expression in total blood

Whole blood of IBD patients was collected into PAXgene blood RNA tubes for immediate stabilization of intracellular RNA and stored at -80°C until the RNA extraction. PreAnalytix RNA isolation kit was used to extract total RNA according to manufacturing protocol. Then, the RNA concentration and purity were evaluated by a NanoDrop instrument (NanoDrop 2000, EuroClone®). The reverse transcription was performed using the High Capacity RNA to-cDNA Kit (Applied Biosystem) with up to 1 µg of total RNA per 20 µL of reaction containing 10 µL of 2 x RT Buffer, 1 µL of 20x RT Enzyme Mix as described above.

Expression levels of the TPMT gene have been normalized using the GAPDH housekeeping gene and expression levels were reported as $2^{-\Delta Ct}$ (146). The thermal cycler used was the CFX96 real-time system-C1000 (Bio-Rad Laboratories). A list of the TaqMan® probes' IDs is reported in table 3.

Gene name	TaqMan® assay ID
GAPDH	Hs02786624_g1

TPMT	Hs00909010_g1

Table 3. Real-time PCR probe sequences for GAPDH and TPMT.

3.2.9 Statistical analysis

The association between pharmacological phenotypes of interest (i.e., dose of azathioprine, TGN metabolites concentrations, MMPN metabolites concentrations, ratio TGN/dose, TPMT activity and TPMT expression) and the considered covariates (i.e., demographic variables including age-group classification, IBD type, and TPMT genotypes) was evaluated in a univariate analysis using generalized linear models of appropriate family (Gaussian/analysis of variance [ANOVA] for continuous and logistic regression for categorical variables). In these univariate analyses, the dependent variable was the pharmacological phenotype of interest and the independent variable the demographic, clinical, or pharmacogenetic covariate. For all parametric analyses (i.e., linear models used in the univariate analysis), normality of the phenotype was tested by the Shapiro test and log10, square root or BoxCox transformation were applied if needed, to adjust the normality of the distribution. For DNA methylation and AZA duration, due to their not normal distribution and the impossibility to normalize them, Wilcoxon test and Spearman correlation were used to test the association with age category and pharmacological variables.

For the DNA methylation pilot study, data available on GEO of 3 different cohorts (GSE112611, GSE112611, GSE62219) have been analyzed independently using Wilcoxon test and then data have been pooled together with a meta-analysis using the weighted inverse Z method accounting for direction of effect but without weighing for sample size (150).

Multivariate analysis was performed to test the independence of the significant effects identified in univariate analyses on the phenotypes considered; for this multivariate analysis, generalized linear models of the appropriate family were used combining covariates significant in the univariate analysis as the independent variables. False discovery rate (FDR) was used to adjust for multiple comparisons All p-values <0.05 were considered statistically significant.

3.3 CDH4 METHYLATION AND METHOTREXATE RESPONSE IN PATIENTS WITH JUVENILE IDIOPATHIC ARTHRITIS

3.3.1 JIA Patients

In this study, 71 patients who fulfilled International League of Associations for Rheumatology (ILAR) criteria for JIA and who received MTX for active arthritis were enrolled by the participating centers between November 2014 and December 2020. In particular, 24 patients have been enrolled at Burlo Garofolo Children's hospital in Trieste (Italy), 19 at Cincinnati Children Hospital Medical Center (CCHMC) in Cincinnati (OH) and the last 28 at the Children Mercy Hospital in Kansas City (MO). The inclusion criteria were age up to 18 years and previous diagnosis of JIA treated exclusively with MTX. The exclusion criteria were concomitant therapy with anti–tumor necrosis factor biological agents (infliximab or etanercept) and presence of uveitis or systemic JIA. Other cotreatments, such as NSAIDs, glucocorticoids or folate, were allowed. Fully informed parental consent and child assent when appropriate was obtained. Demographic and clinical data were collected at baseline (up to 4 weeks before starting methotrexate), after 3, 6 and 12 months of MTX therapy. MTX treatment lasted a minimum of 6 months. Weekly MTX was given by either oral or subcutaneous route at 10–15 mg/m2. Clinical response has been evaluated using the ACR Pediatric index (ACR Pedi). This core set is composed of the following 6 measures: physician global assessment of disease activity, parent/patient global assessment of well‑being, active joint count, restricted joint count, functional assessment, and a laboratory measure of inflammation (151). Venous blood samples were taken when the child required blood sampling for routine clinical care.

3.3.2 Illumina methylation EPIC bead-chip array

CDH4 DNA methylation profiles were obtained using an Illumina Methylation EPIC BeadChip array kit (Illumina) from DNA extracted from peripheral blood of 71 JIA patients. In particular, all the 513 probes located on the CDH4 gene, including also the neighboring regions (± 50kb) have been selected for further analyses. All experimental methods were performed strictly according to the manufacturer's protocols (Illumina). The IDAT file, a raw data file containing the intensities of the probes in the array, was analyzed using the ChAMP package of R/Bioconductor (147). The probes for which detection P values were < 0.01 across all samples were used. Average beta values were used for comparison.

3.3.3 CDH4 RNA expression in total blood and immortalized cellular lines

Whole blood of 20 JIA patients was collected into PAXgene blood RNA tubes for immediate stabilization of intracellular RNA and stored at -80°C until the RNA extraction. PreAnalytix RNA isolation kit was used to extract total RNA according to manufacture protocol. Then, the RNA concentration and purity were evaluated by a Nano Drop instrument (NanoDrop 2000, EuroClone®). The reverse transcription was performed using the High Capacity RNA to-cDNA Kit (Applied Biosystem) with up to 1 µg of total RNA per 20 µL of reaction containing 10 µL of 2 x RT Buffer, 1 µL of 20x RT Enzyme Mix as described above.

Expression levels of the CDH4 gene have been normalized using the GAPDH housekeeping gene and expression levels were reported as $2^{-\Delta Ct}$ (146). The thermal cycler used was the CFX96 real-time system-C1000 (Bio-Rad Laboratories). A list of the TaqMan® probes' IDs is reported in table 4.

Gene name	TaqMan® assay ID
GAPDH	Hs02786624_g1
CDH4	Hs00899698_m1

Table 4. Real-time PCR probe sequences for GAPDH and CDH4.

3.3.3 Statistical analysis

The association between CDH4 methylation and ACR Pedi has been evaluated independently for each of the 3 cohorts with a Spearman correlation test while for the association between DNA methylation at baseline and at last follow up visit Wilcoxon test was used.

Data obtained for each cohort have been pooled together statistically with a meta-analysis using the weighted inverse Z method (150), weighting by sample size and accounting for direction of effect. Fisher test was used to assess whether CDH4 gene body has a higher concentration of statistically significant CpGs then the neighboring regions. For the RNA-seq analysis, data of 47 JIA patients and 14 age matched controls available on GEO (GSE81259) has been downloaded and analyzed using Wilcoxon test for comparisons. For the RNA expression using TaqMan probes in 20 JIA patients and 5 immortalized cellular lines no statistical analysis was conducted due to the extremely low expression of the samples. All statistical analyses have been conducted using software R, version 3.6.1. All p-values <0.05 were considered statistically significant.

4. RESULTS

4.1 NLRP3 METHYLATION AND GLUCOCORTICOID RESPONSE IN IDIOPATHIC NEPHROTIC SYNDROME PATIENTS

4.1.1 Adults and pediatric INS patients

Out of the 28 adult patients with INS enrolled, 10 were glucocorticoid resistant while the other 18 were glucocorticoid sensitive. Age was not different between the two groups with a mean (years) of 54.1 ± 15.5 for resistant patients and 53.8 ± 17.9 for the sensitive ones (p-value: 0.96). No statistically significant differences emerged also for gender, plasmatic creatinine levels, total cholesterol and proteinuria levels (table 5) between the two groups of patients. All resistant patients presented FSGS while, in the sensitive group, 13 patients presented MCD and 5 FSGS.

As a validation cohort, 21 pediatric patients with INS have also been enrolled and properly divided in glucocorticoid resistant (n = 7) and glucocorticoid sensitive (n = 14) patients. As for the adult cohort, glucocorticoid sensitive and glucocorticoid resistant pediatric patients with INS did not present any differences in plasmatic creatinine levels, total cholesterol, proteinuria levels, gender and age (mean (years) 10.5 ± 2.8 and 7.3 ± 3.9 respectively, p-value: 0.08, table 5). In the pediatric group, 2 steroid resistant patients presented FSGS while all the remaining patients presented MCD.

Finally, a cohort of 52 healthy subjects (41 adults, 11 women, mean age 44.5 ± 11.8 years, and 11 children, 5 girls, age 10.2 ± 5.5 years) was also enrolled.

	Discovery cohort (adults)			Validation cohort (children)		
	Glucocorticoid sensitive	**Glucocorticoid resistant**	**p-value**	**Glucocorticoid sensitive**	**Glucocorticoid resistant**	**p-value**
Number	10	18	/	7	14	/
Age, y	54.1 ± 15.5	53.8 ± 17.9	0.96	7.3 ± 3.9	10.5 ± 2.8	0.08
Creatinine, mg/dl	/	1.0 ± 0.4	/	0.6 ± 0.2	0.4 ± 0.1	0.21
Total cholesterol, mg/dl	207.8 ± 26.2	215.8 ± 23.4	0.37	365 ± 83.1	404.2 ± 117.2	0.49
Proteinuria, g/24 h	/	0.1 ± 0.2	/	4.7 ± 2.5	4.4 ± 5.9	0.90
Systolic BP, mmHg	130.4 ± 10.3	124.4 ± 16.8	0.25	124 ± 19.0	107.6 ± 13.1	0.07
Diastolic BP, mmHg	81.4 ± 8.6	76.4 ± 8.0	0.09	61.0 ± 6.4	64.6 ± 7.6	0.30
Disease: FSGS, MCD	10. 0	5, 13	/	2, 5	0, 14	/

Table 5. Demographic and clinical characteristics of INS patients enrolled. Values are expressed as mean ± standard deviation (SD). The p values calculated by t-test. Abbreviations: BP, blood pressure; FSGS, focal segmental glomerulosclerosis; MCD, minimal change disease.

4.1.2 NLRP3 methylation and age or gender

The extent of NLRP3 promoter methylation was significantly higher in pediatric patients compared to adult patients, with an inverse correlation between NLRP3 methylation and age in the combined pediatric and adult cohort (generalized linear model p-value = 0.012, r = -0.80). No significant effect of gender could be identified (figure 9).

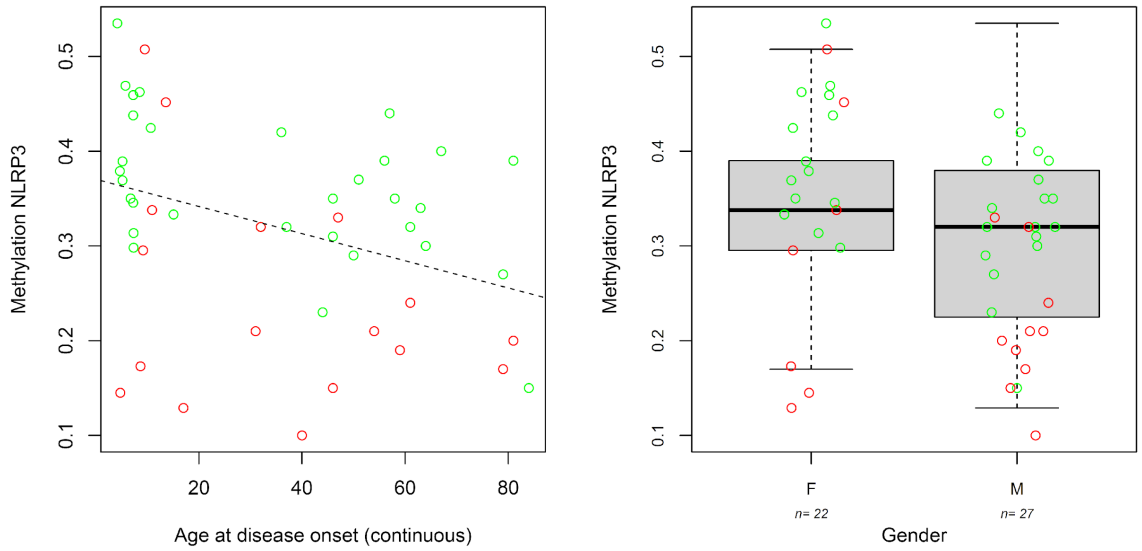

Figure 9. NLRP3 methylation and age (left) or gender (right) in the grouped pediatric and adult population. Red circles represent resistant patients and green circles sensitive patients.

4.1.3 NLRP3 methylation and age group in patients with INS and healthy controls.

NLRP3 methylation was significantly reduced in INS patients (generalized linear model p-value = 2.2 x 10^{-7}) compared to age-matched controls and a significant interaction between age and disease status was observed (generalized linear model p-value = 0.019) (figure 10).

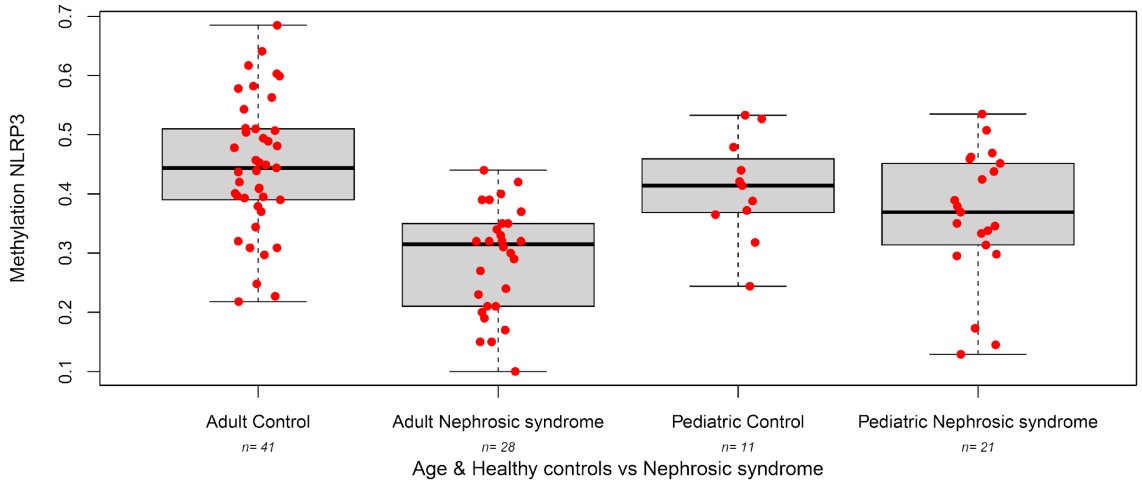

Figure 10. NLRP3 methylation and age groups in patients and healthy controls.

4.1.4 NLRP3 inflammasome activation contributes to glucocorticoid resistance in U937 monocytes

In order to evaluate whether the activation of the NLPR3 inflammasome could induce steroid resistance in U937 monocytes, the cell line was treated with or without LPS (10 ng/mL)/ATP (1 mM) for 4 hours to activate the inflammasome, then incubated with increasing concentrations of prednisone (PRED) for 24 h. By measuring the proliferation rate of U937 cells with the [methyl-3H] thymidine assay we demonstrated that NLRP3 inflammasome activation increased significantly the resistance to glucocorticoids (GCs) (178 µM vs. 275 µM, p-value: 0.027) as reported in figure 11 confirming the involvement of NLRP3 inflammasome in the mechanism of resistance to GCs.

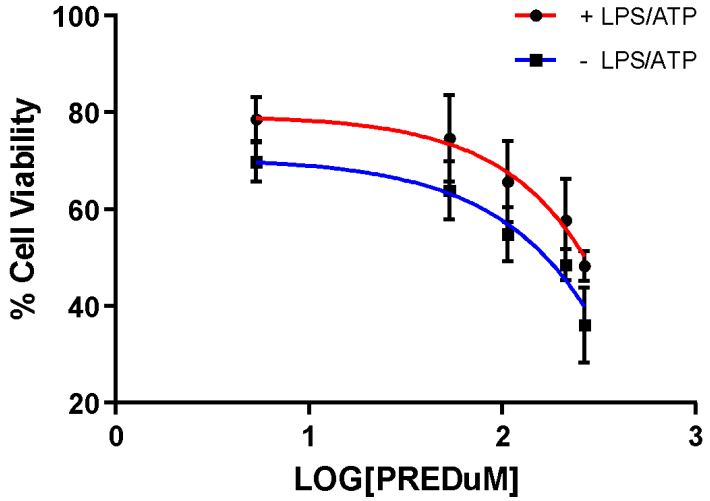

Figure 11. Dose response curve showing a reduction in PRED sensitivity after NLRP3 inflammasome activation (+LPS/ATP, red line) compared with the U937 cells without NLRP3 inflammasome activation (-LPS/ATP, blue line). Two-way analysis of variance (ANOVA), inflammasome activation p-value: 0.023, dose-response p-value: < 0.05. Results are mean values ± SD from four independent experiments. ATP, adenosine triphosphate; LPS, lipopolysaccharides, PRED, prednisone.

Subsequently we show by western blot analysis a statistically significant reduction in the levels of the GC receptor (GR) after the activation of the inflammasome both with or without the treatment with a fixed dose of PRED (p-value < 0.05) as reported in Figure 12.

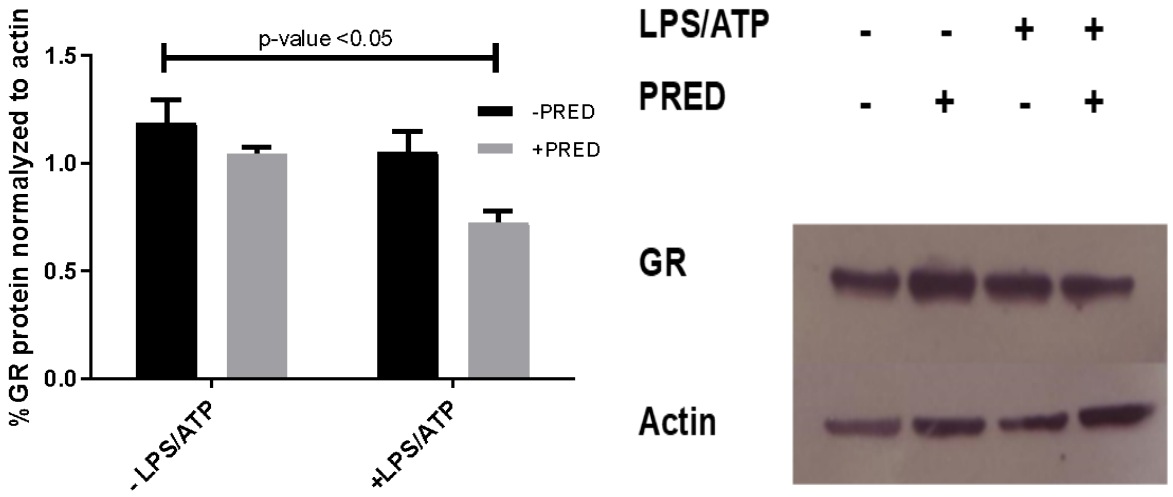

Figure 12. Levels of glucocorticoid receptor (GR) diminished significantly after the activation of the NLRP3 inflammasome and the treatment with PRED ($p < 0.05$). ATP, adenosine triphosphate; LPS, lipopolysaccharides, PRED prednisone.

Finally, we evaluated the ability of the GR to increase the expression of GILZ after incubation with PRED with or without activating the inflammasome in U937 cell line. GILZ expression resulted notably reduced after NLRP3 inflammasome activation compared to the monocytes not activated (p-value: 0.0045), results consistent with reduced GC transcriptional effect after NLRP3 activation (Figure 13).

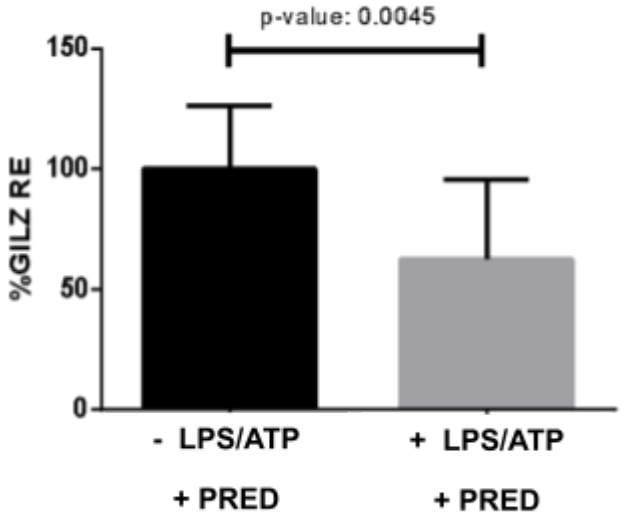

Figure 13. Relative expression (RE) of GILZ after treatment with or without LPS/ATP and exposure to PRED (2 μg/mL) for 3 h. For the t-test analyses ($p = 0.0045$), the data are reported as means ± SD of four independent experiments performed in triplicate. ATP, adenosine triphosphate; GILZ, glucocorticoid-induced leucine zipper; LPS, lipopolysaccharides, PRED, prednisone.

4.2 TPMT METHYLATION AND AZATHIOPRINE PHARMACOKINETICS IN EARLY ONSET PEDIATRIC IBD PATIENTS

4.2.1 Patients

This multicentric (1:3) case-control study recruited 30 early-onset (EO) patients with IBD, considered as cases, matched to 90 patients with later-onset (non-EO) IBD, considered as controls. From May 2005 to June 2021, peripheral blood samples have been collected to measure DNA methylation, azathioprine metabolites, TPMT activity and TPMT expression. Demographic and clinical characteristics of the patients are reported in table 6.

	All patients	**Early onset**	**Non early onset**	**p-value**
		Age < 6 year	Age > 12 to < 18	
	n = 120	n = 30	n = 90	
Age (years)	12.0 ± 4.8	4.4 ± 1.4	14.6 ± 1.9	2.2×10^{-16}
Sex				
Female (%)	54 (45.0%)	14 (46.7%)	40 (44.4%)	0.19
Male (%)	66 (55.0%)	16 (53.3%)	50 (55.6%)	
IBD type				
CD (%)	35 (29.1%)	6 (20.0 %)	29 (32.2 %)	0.78
UC (%)	85 (70,9%)	24 (80.0 %)	61 (67.8 %)	

Table 6. Demographic and clinical characteristic of patients enrolled. Age is expressed as mean ± standard deviation. p-values are from generalized linear models.

Age was different between EO (mean 4.4 ± 1.4) and non-EO (mean 14.6 ± 1.9) (p-value: 2.2×10^{-16}) while no differences in gender (14 and 40 females in EO and non-EO respectively) and IBD type (24 and 61 UC in EO and non-EO respectively) were evident.

4.2.2 Genotyping

TPMT genotyping was available for 30 cases and 88 controls. All polymorphisms considered were in accordance with Hardy–Weinberg equilibrium, and their distribution is comparable with what has been reported in the literature for patients of white ethnicity. Frequency of TPMT variant genotypes was similar among cases and controls (p-value =1). In particular, 1 EO patient (3.3%) and 6 non-EO patients (6.6%) presented the variant heterozygous genotype of rs1142345 (A719G) while for 2 nonearly-onset patients genotype was not available due to technical problems. Among these, the early-onset patient and 3 non-EO patients presented also the rs1800460 (G460A) variant in heterozygous form. No

patient presented the rs1800462 (G238C) variant. Therefore, in terms of variant alleles, 4 patients (1 case and 3 controls) were heterozygous for TPMT*3A, whereas 2 controls were heterozygous for TPMT*3C. All other patients with available DNA for genotyping were considered homozygous for the TPMT*1 allele.

4.2.3 Azathioprine doses and metabolites in patients with early-onset IBD in comparison with non-early onset patients

EO patients required higher doses of AZA with a median dose of 2.5 mg/kg/day (interquartile range 2.0 - 2.8) compared to non-early onset patients, with a median dose of 1.9 (interquartile range 1.7 - 2.3) (p-value ANOVA: 0.0003, figure 14).

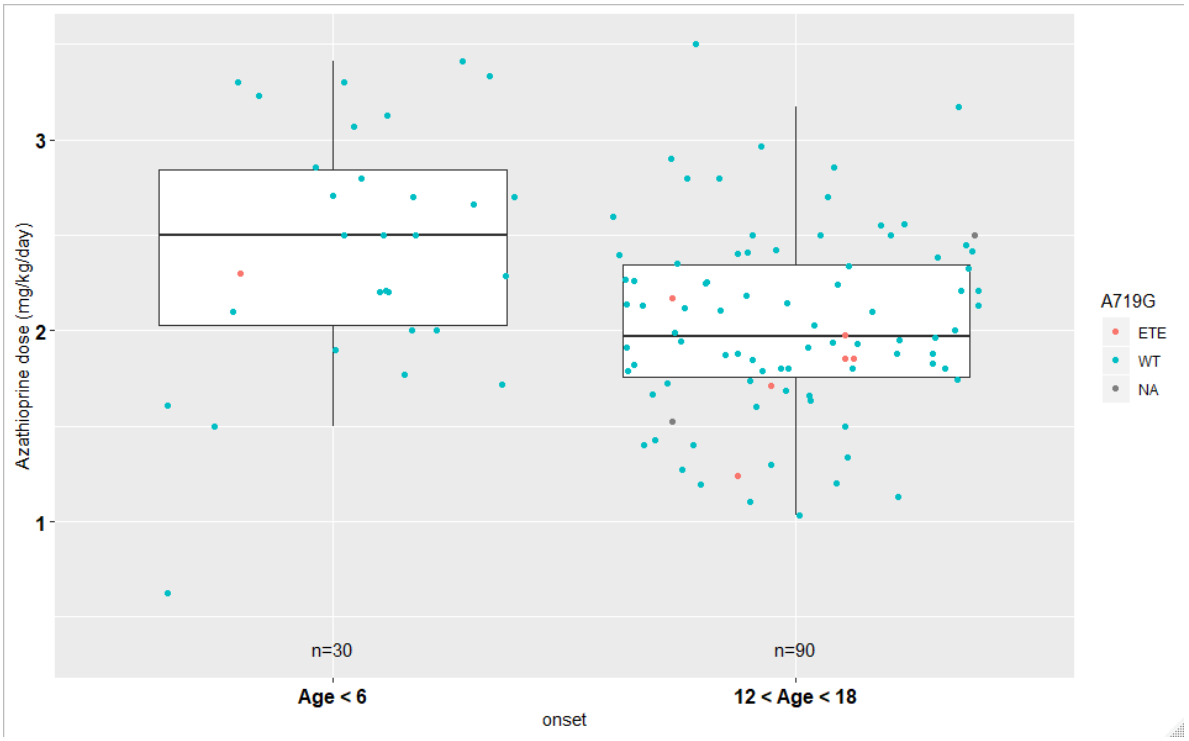

Figure 14. The boxplots show azathioprine doses ($mg \cdot kg^{-1} \cdot d^{-1}$) in patients with early-onset IBD (aged < 6 years) than in non-early–onset IBD (aged > 12 and <18 years) obtained after at least 3 months of therapy; blue and red points display azathioprine dose values for patients with wild-type and variant TPMT for A719G respectively while black points refer to patients for whom genotyping was not possible due to technical problems.

Azathioprine active metabolites (TGNs) concentrations were lower in early onset patients presenting a median of 256.50 pmol/8 × 10^8 erythrocytes (interquartile range 153.25 - 345.39) versus 357.5 pmol/8 × 10^8 erythrocytes (interquartile range 268.6 - 459.0) of non-early onset patients (p-value ANOVA = 0.01, figure 15). Also, the multivariate

generalized linear model showed that EO (p-value: 0.008, estimate: 0.19) and variant TPMT genotype (p-value: 0.0005, estimate: -0.51) are independent determinants of TGN plasma concentrations. Furthermore, MMPN levels were comparable between the two groups (median 1385.1 pmol/8 × 10^8 erythrocytes, interquartile range 657.5 - 2078.0, versus 1429.5 pmol/8 × 10^8 erythrocytes, interquartile range 522.2 - 4096.0, p-value ANOVA = 0.71, figure 16). Moreover, MMPN concentration showed a statistically significant association with TPMT genotype (p-value ANOVA: 0.0003).

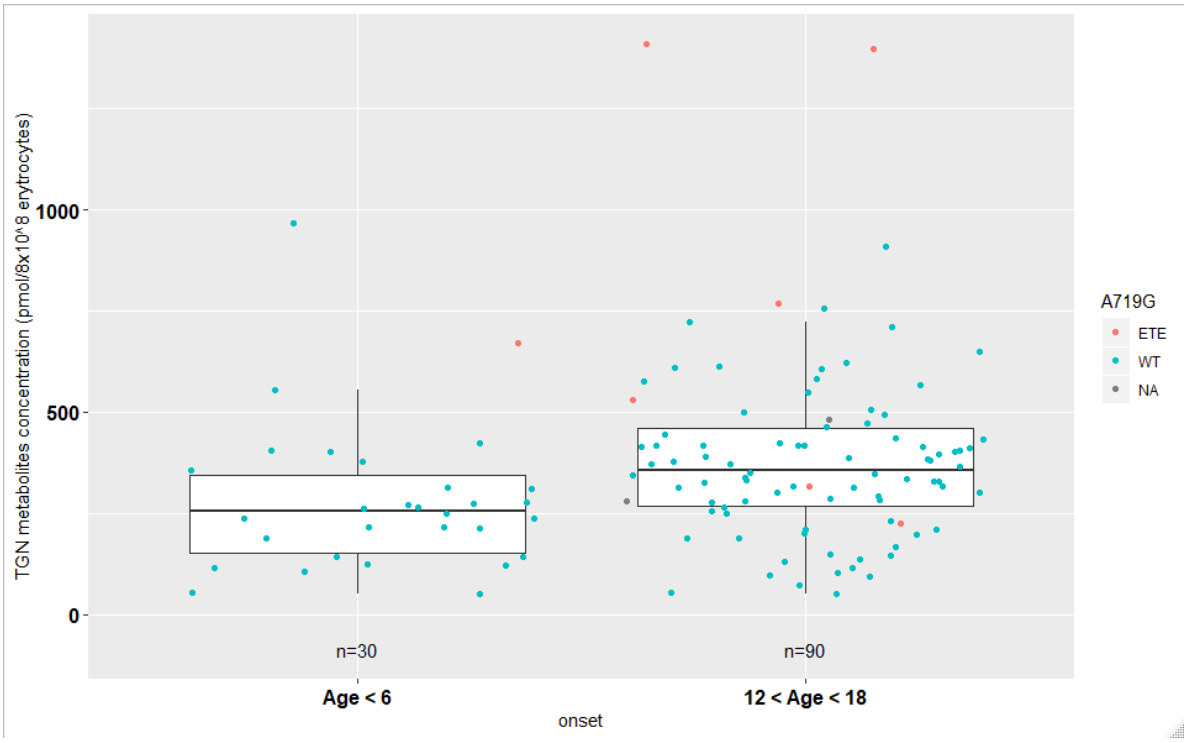

Figure 15. The boxplots show TGN concentrations (pmol/8 × 10^8 erythrocytes) in patients with early-onset IBD (aged < 6 years) or nonearly–onset IBD (aged > 12 and <18 years); blue and red points display TGN concentration values for patients with wild-type and variant TPMT for A719G respectively while black points refer to patients for whom genotyping was not possible due to technical problems.

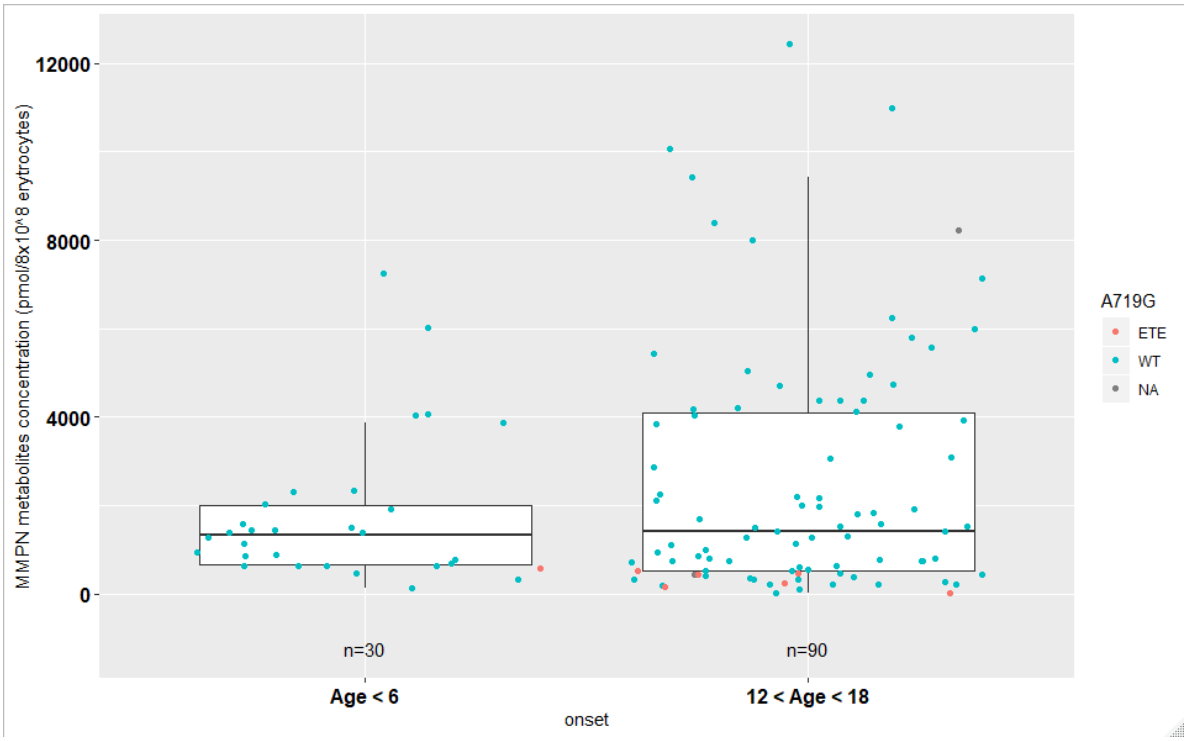

Figure 16. The boxplots show MMPN concentrations (pmol/8 × 10^8 erythrocytes) in patients with early-onset IBD (aged < 6 years) or nonearly–onset IBD (aged > 12 and <18 years); blue and red points display MMPN concentration values for patients with wild-type and variant TPMT for A719G respectively while black points refer to patients for whom genotyping was not possible due to technical problems.

Lower TGN metabolites/azathioprine dose ratios were found in EO patients median 96.66 [(pmol/8 × 10^8 erythrocytes)/(mg/kg/d)], interquartile range 66.27 - 154.16 versus non-EO patients, median 179.6 [(pmol/8 × 10^8 erythrocytes)/(mg/kg/d)], interquartile range 134.6 - 234.4 (p-value ANOVA = 0.0005, figure 17). Moreover, the multivariate generalized linear model showed that EO (p-value: 0.0003, estimate: 0.08) and variant TPMT genotype (p-value: 0.0006, estimate: -0.14) are independent determinants of TGN metabolites concentration per unit of azathioprine administered.

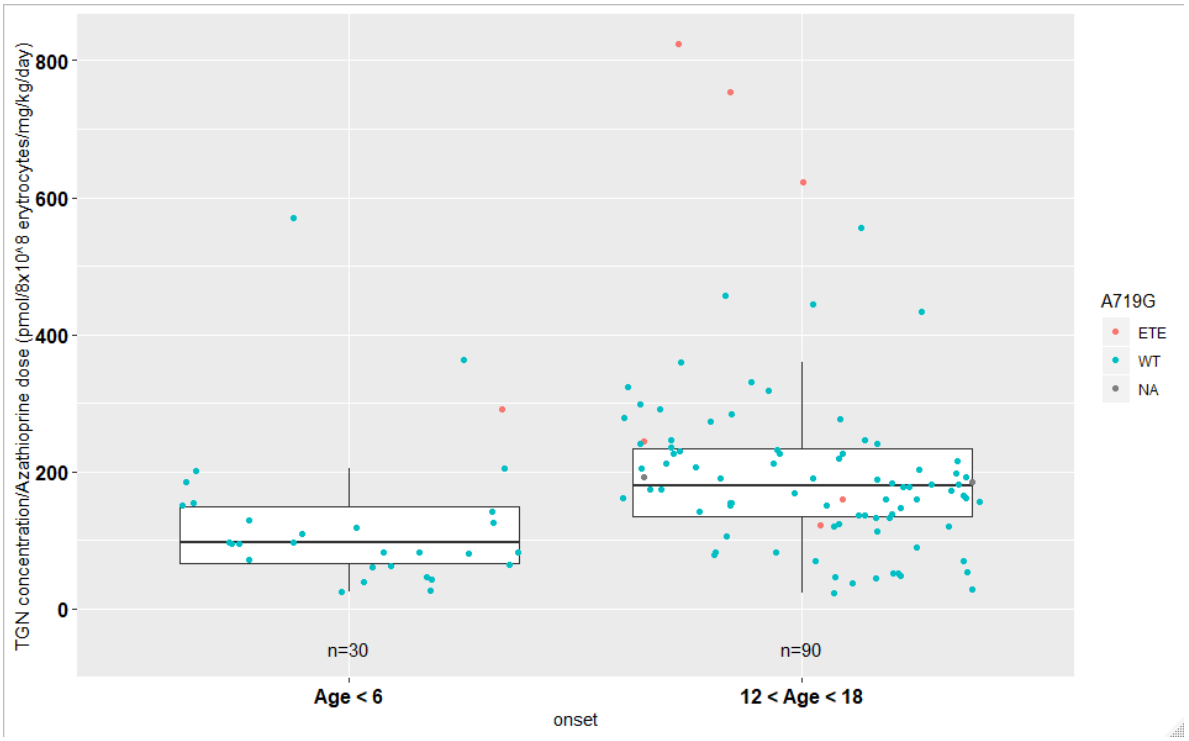

Figure 17. The boxplots show the ratio between TGN concentrations and azathioprine doses (pmol/8 × 10^8 erythrocytes mg−1·kg·d−1) in patients with early-onset IBD (aged < 6 years) or nonearly–onset IBD (aged > 12 and <18 years. Blue and red points display TGN/azathioprine dose ratios concentration values for patients with wild-type and variant TPMT for A719G respectively while black points refer to patients for whom genotyping was not possible due to technical problems.

AZA treatment duration was not different between cases and controls (median 388.5, interquartile range 238.8 – 661.2 versus 413.0, interquartile range 149.5 – 1045.5, p-value Wilcoxon test = 0.51, data not shown). Moreover, no differences in AZA duration emerged between cases and controls also after adjusting for IBD subtype (p-value: 0.21).

4.2.4 TPMT activity in a subset of patients with early-onset IBD in comparison with non-early onset IBD Patients

TPMT activity could be measured in a subset of patients for which sufficient blood sample was available after the quantification of thiopurine metabolites. This population was representative of the whole group because no demographic variable was different between this subgroup of patients and the whole study population in terms of the demographic, clinical, and pharmacological variables, as reported in table 7.

	Case-control cohort	TPMT activity cohort	TPMT Methylation pilot study cohort	Methylation validation cohort	TPMT expression cohort
Patients (EO number)	120 (30)	73 (17)	18 (10)	68 (20)	38 (14)
Female	54	32	10	31	19
IBD type	84 UC - 36 CD	50 UC - 22 CD	13 UC - 5 CD	46 UC - 22 CD	27 UC - 11 CD
Median TGN **IQR**	328.5 223.5 - 422.5	313.8 193.8 - 414.5	216.0 122.3 - 343.5	327.0 207.6 - 426.0	311.3 203.9 - 377.8
Median AZA dose **IQR**	2.1 1.8 - 2.5	2.2 1.9 - 2.5	2.2 1.8 - 2.7	2.0 1.8 - 2.5	2.0 1.8 - 2.5
Median AZA duration IQR	391.0 170.0 - 848.2	477.5 172.0 - 1116.5	716.5 478.75 - 1347.75	375.0 131.0 - 807.0	307.0 162.0 - 609.0
Age (mean ± SD)	12.0 ± 4.8	12.1 ± 4.7	10.1 ± 5.7	11.7 ± 5.1	10.9 ± 5.4

Table 7. Demographic and clinical characteristics of all patients enrolled divided by subgroups. Pharmacological variables are expressed as median and interquartile range (IQR). Age is expressed as mean ± standard deviation (SD).

In particular this cohort is composed of 17 EO and 55 non-EO. Interestingly, EO patients presented higher activity of TPMT than non EO patients (median 253.0, interquartile range 178.2 - 309.9 versus 207.66, interquartile range 175.71 - 244.56 pmol of methylmercaptopurine/10^9 erythrocytes /h, p-value ANOVA = 0.046, figure 18). Moreover, the multivariate generalized linear model showed that EO (p-value: 0.035, estimate: -37.9) and variant TPMT genotype (p-value: 0.003, estimate: 109.5) are independent determinants of TPMT activity.

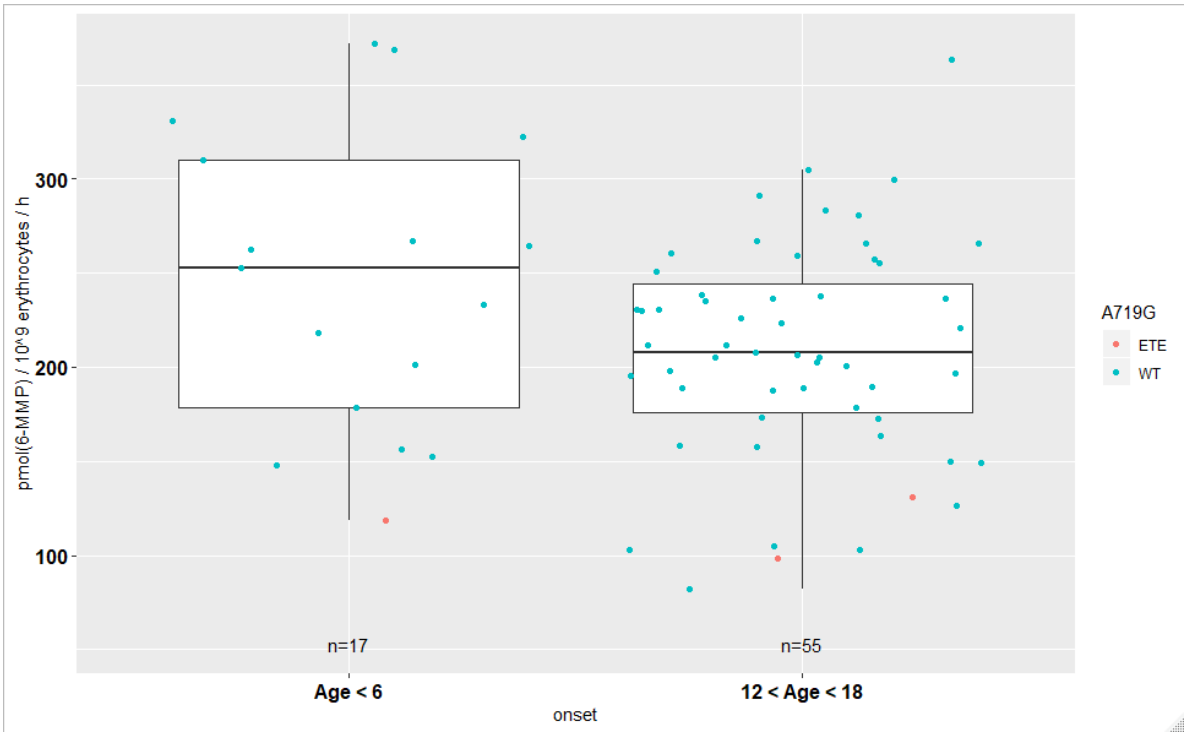

Figure 18. The boxplots show TPMT activity (pmol/10^9 erythrocytes/hour) in patients with early-onset IBD (aged < 6 years) or nonearly–onset IBD (aged > 12 and <18 years); blue and red points display TPMT activity values for patients with wild-type and variant TPMT for A719G respectively.

4.2.5 Illumina methylation EPIC BeadChip array pilot analysis in 10 early-onset and 8 non early–onset pediatric patients with IBD

TPMT methylation was initially analyzed using Infinium Methylation EPIC BeadChip Array in whole blood of a subgroup of patients composed of 10 EO and 8 non-EO IBD patients (patients' demographic, clinical, and pharmacological variables are reported in table 7). Thirty-two CpG sites, available on the EPIC array, on TPMT gene (chr6:18128545-18155374 according to human genome assembly 19) and its neighboring regions (± 50000 base pair of the TPMT gene), have been analyzed.

In this small group of patients analyzed, age was different between EO and non-EO (p-value: 0.0004) while no differences in gender and IBD type were evidenced. AZA duration was different between EO and NEO patients (p-value = 0.003, Wilcoxon test), while AZA active metabolites levels (TGN), AZA doses and TPMT activity showed no difference (data not shown). As reported in table 8, five CpG sites resulted differentially methylated between EO and NEO ($p < 0.05$, Wilcoxon test). One CpG is located on the TPMT gene body (cg0670276) while the other 4 are located on the upstream or downstream neighboring regions.

Probe ID	*Gene name*	*Position on Chr6*	*% of methylation in EO*	*% of methylation in non-EO*	*p-value Wilcoxon*
cg22736354	NHLRC1	18122719	0.088 ± 0.02	0.124 ± 0.03	0.0266
cg18068140	NHLRC1	18123164	0.69 ± 0.04	0.65 ± 0.04	0.0434
cg01869138	NHLRC1	18123241	0.83 ± 0.03	0.78 ± 0.05	0.0205
cg06702726	TPMT	18152154	0.98 ± 0.00	0.96 ± 0.01	0.0342
cg04231636	KDM1B	18186411	0.36 ± 0.02	0.33 ± 0.03	0.0342

Table 8. Statistically significant CpG sites in the pilot study cohort. Abbreviations: Chr6, chromosome 6; EO, early onset.

4.2.6 Meta-analysis between our cohort and 3 other cohorts available on the GEO platform

In order to reduce the bias of the different AZA duration and its impact on DNA methylation and select the candidate CpG sites for which the methylation is influenced only by age in IBD patients, a meta-analysis to compare DNA methylation and patients' age, between our cohort (study 1) and 3 other cohorts available on the GEO platform, was performed. In particular a CD cohort, GSE112611 (study 2), of 145 patients (12 EO and 113 non-EO) and two healthy subjects' cohorts: GSE112611 (study 3) of 52 individuals (6 EO and 46 non-EO) and GSE62219 (study 4) composed of 10 EO have been analyzed. All DNA samples from GSE112611 were taken before starting AZA therapy.

The meta-analysis performed between our cohort and the 3 GEO cohorts, showed 7 significant CpGs. Four of them were significant also after false discovery rate (FDR) adjustment (table 9). Two of the identified CpGs were significant also in our IBD cohort (cg22736354 and cg04231636). The direction of the methylation was the same in each cohort for all the CpGs identified. In particular cg22736354 resulted the only CpG whose

methylation increases with age and was selected for further validation in a larger cohort of pediatric IBD patients.

ProbeID	*cg22736354*	*cg16879574*	*cg00772000*	*cg18068140*	*cg01869138*	*cg08448780*	*cg04231636*
Gene Name	NHLRC1	NHLRC1	NHLRC1	NHLRC1	NHLRC1	TPMT	KDM1B
Position on Chr6	18122719	18123047	18123049	18123164	18123241	18148790	18186411
% of methylation in EO	0.096 ± 0.01	0.17 ± 0.03	0.10 ± 0.02	0.68 ± 0.06	0.83 ± 0.03	0.83 ± 0.05	0.38 ± 0.05
% of methylation in non-EO	0.12 ± 0.02	0.13 ± 0.01	0.07 ± 0.02	0.63 ± 0.06	0.78 ± 0.04	0.80 ± 0.05	0.33 ± 0.06
Study 1	2.66E-02	5.45E-02	1.46E-01	4.34E-02	2.05E-02	3.60E-01	3.43E-02
Study 2	7.13E-01	5.51E-01	1.00E+00	4.43E-01	8.87E-01	7.55E-01	4.43E-01
Study 3	1.80E-01	1.32E-01	1.32E-01	3.94E-01	3.10E-01	6.49E-02	6.49E-02
Study 4	2.60E-01	5.35E-07	1.79E-03	4.21E-02	NA	NA	4.25E-02
Meta	3.70E-03	1.10E-06	1.90E-03	1.10E-02	3.40E-02	1.05E-02	1.00E-04
FDR	2.90E-02	3.13E-05	1.96E-02	5.60E-02	1.53E-01	5.60E-02	2.00E-03

Table 9. Meta-analysis results. Only statistically significant CpG sites are reported. For each of the 4 cohorts, study-specific p-values are reported (study 1, study 2 , study 3 and study 4). Percentages of methylation are calculated as mean methylation between EO and non-EO across all the 4 studies. Abbreviations: Chr6, chromosome 6; EO, early onset; Meta, meta-analysis p-value; FDR, false discovery rate p-value.

4.2.7 Analysis of the methylation of cg22736354 using pyrosequencing in a validation cohort composed of 20 early onset and 48 non-early onset pediatric IBD patients

The DNAs for the methylation validation analysis with pyrosequencing was available in a subset of patients composed of 20 EO and 48 non-EO. This population was representative of the whole group because no demographic variable was different between this subgroup of patients and the whole study population in terms of the demographic, clinical, and pharmacological variables, as reported in table 7.

The DNAs extracted from blood have been processed and analyzed by pyrosequencing in order to quantify the methylation amount of cg22736354 (chr6:18,122,719, human genome 19). Interestingly, the methylation of cg22726354 resulted lower in EO patients (median methylation 4.00% (3.75 - 4.25)) compared to non-EO (median methylation 6.0% (5.0 - 8.0)) (p-value Wilcoxon: 4.6×10^{-5}, figure 19).

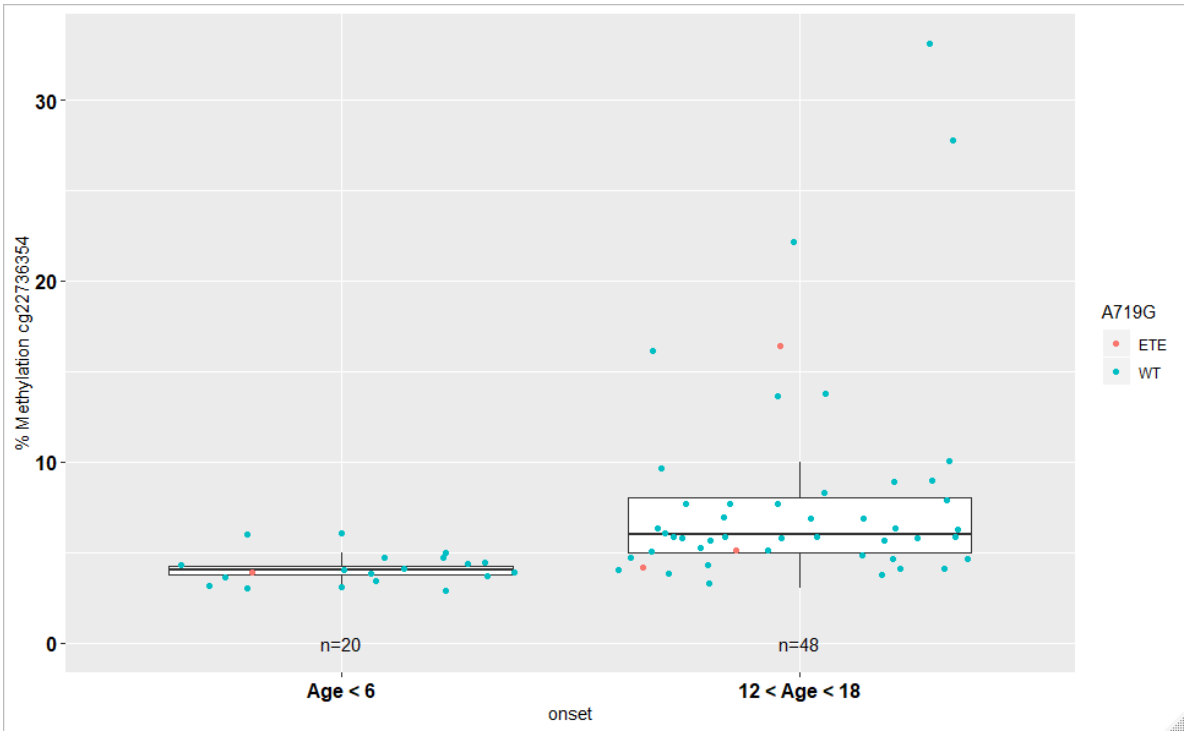

Figure 19. The boxplots show cg22736354 methylation (%) in patients with early-onset IBD (aged < 6 years) than in non-early–onset IBD (aged > 12 and <18 years); blue and red points display methylation values for patients with wild-type and variant TPMT for A719G respectively.

Other 3 CpG sites adjacent to cg22736354 have also been analyzed in the same assay, due to its technical design (i.e., pyrosequencing that allows the sequencing of 10 to 20 bp in a targeted region). In particular the methylation of 2 CpG sites upstream (chr6:18,122,713 and chr6:18,122,715, human genome 19) and 1 CpG site downstream (chr6:18,122,722, human genome 19) of cg22736354 have been analyzed. The methylation of all the 3 CpG resulted significantly lower in EO patients compared to non-early onset patients, as reported in table 10 and figure 20.

Position	Early onset (median - IQR)	Non early onset (median - IQR)	p-value Wilcoxon
chr6:18,122,713	3.80 (3.75 - 4.00)	5.00 (4.00 - 8.00)	2.3×10^{-5}
chr6:18,122,715	2.50 (2.00 - 3.00)	4.00 (3.00 - 6.00)	7.4×10^{-6}
chr6:18,122,722	4.50 (4.00 - 5.00)	7.50 (6.00 - 11.25)	1.7×10^{-8}

Table 10. Methylation (%) of chr6:18,122,713, chr6:18,122,715 and chr6:18,122,722 expressed as median and inter-quartile-range (IQR) in early onset and non-early onset patients.

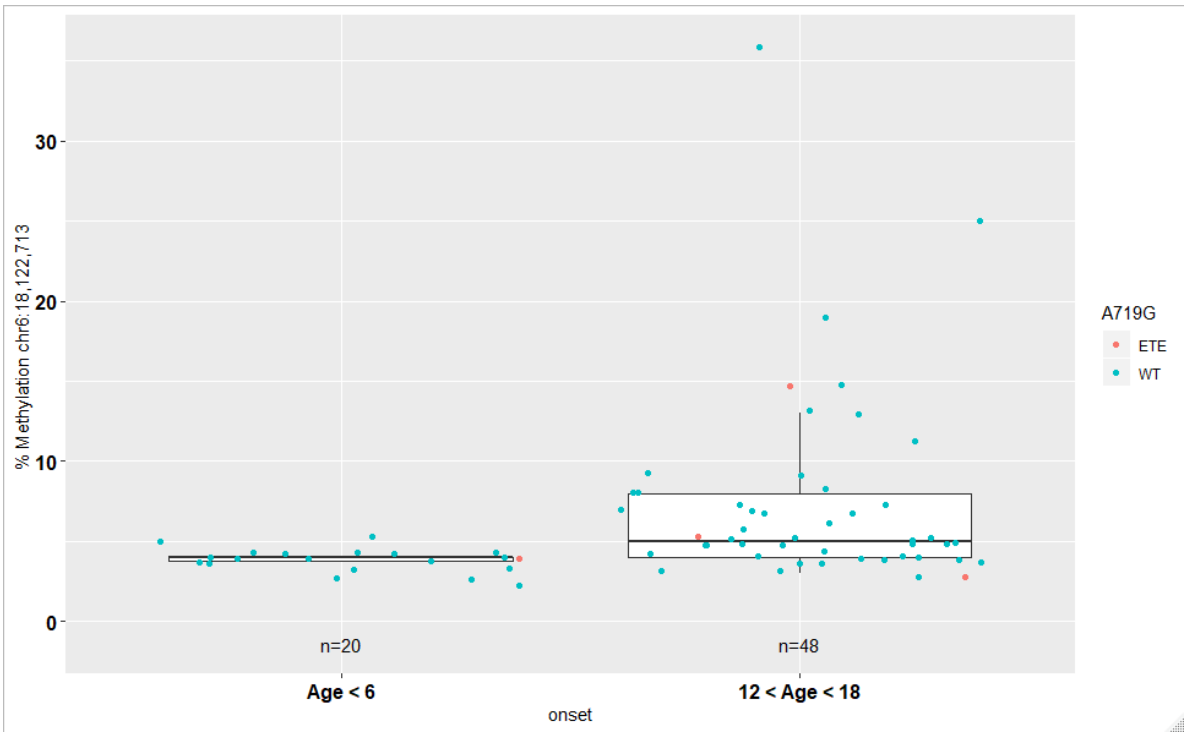
% Methylation chr6:18,122,713
30
20
10
0
n=20
n=48
Age < 6
12 < Age < 18
onset
A719G
ETE
WT

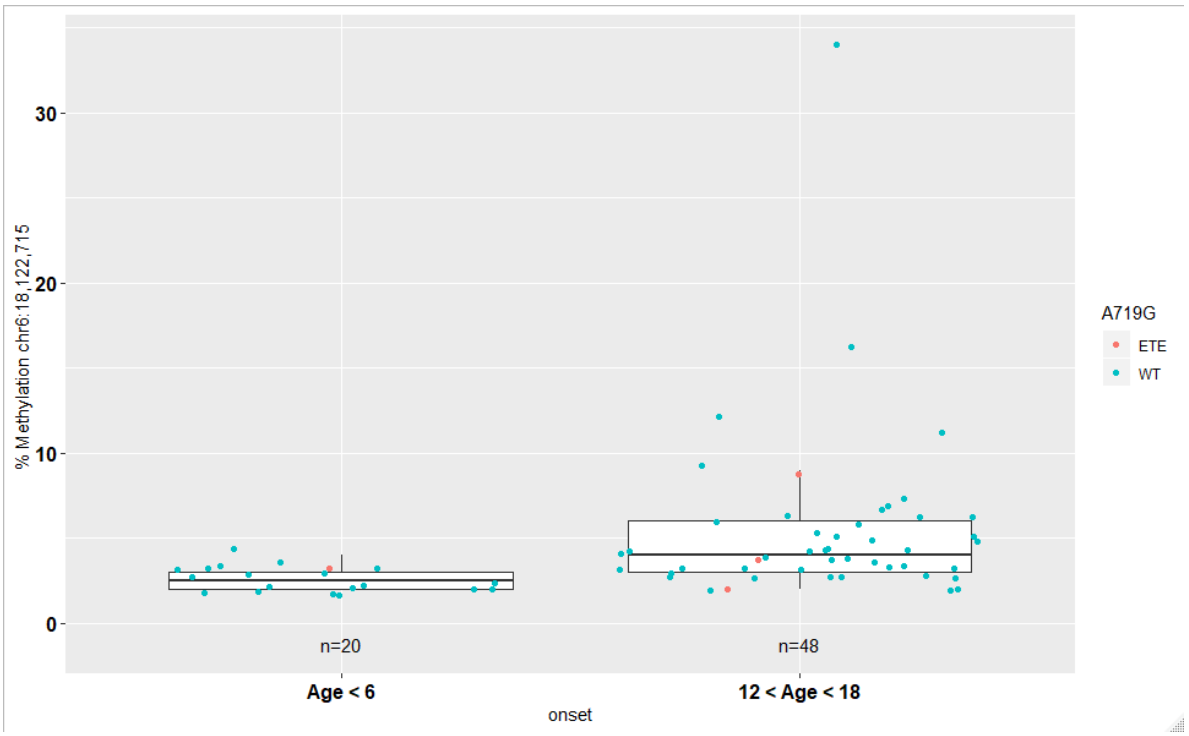
% Methylation chr6:18,122,715
30
20
10
0
n=20
n=48
Age < 6
12 < Age < 18
onset
A719G
ETE
WT

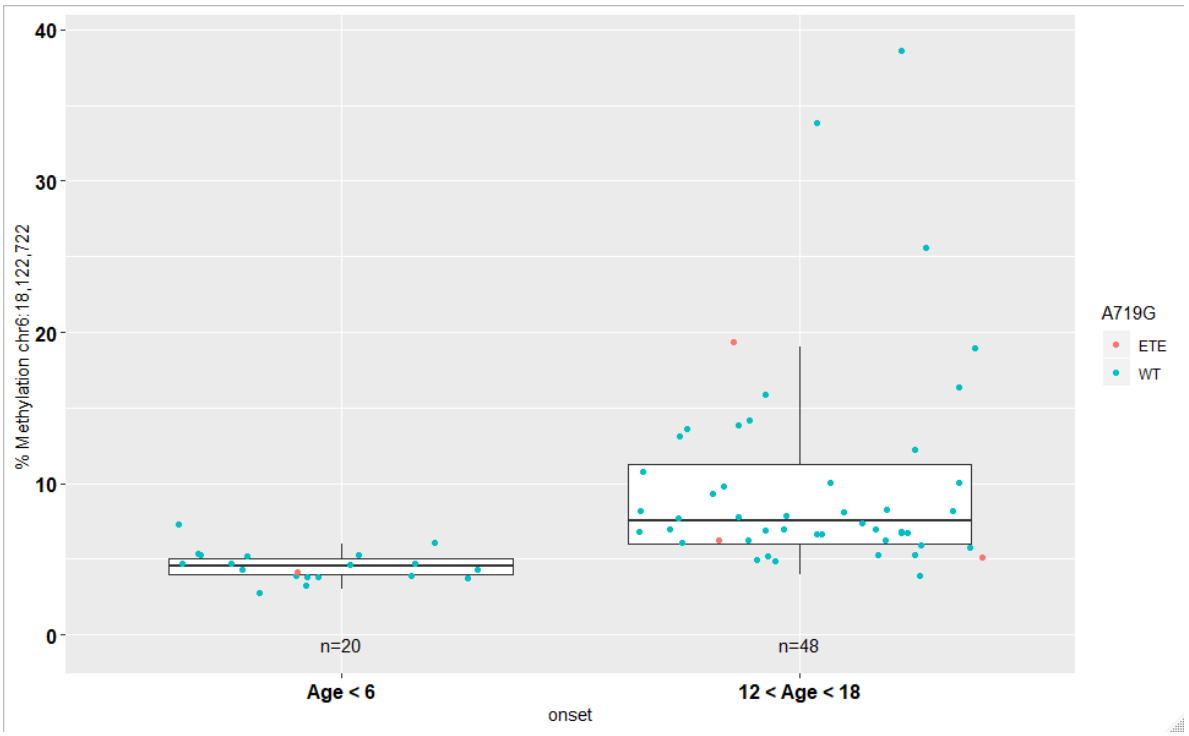

Figure 20. The 3 boxplots show chr6:18,122,713, chr6:18,122,715 and chr6:18,122,722 methylation (%) in patients with early-onset IBD (aged < 6 years) than in non-early–onset IBD (aged > 12 and <18 years); blue and red points display methylation values for patients with wild-type and variant TPMT for A719G respectively.

4.2.7.1 Correlation between pharmacological variables and cg22736354 methylation

The correlation between all the pharmacological phenotypes and the methylation of cg22736354 was assessed in the same 20 cases and 48 controls using Spearman correlation. From this analysis a statistically significant association emerged between cg22736354 methylation and both TGN concentration and TGN metabolites/azathioprine dose ratio (p-value Spearman: 0.01 and 0.01 respectively, figure 21) while no associations were present considering AZA dose, AZA duration, MMPN levels and TPMT activity (p-value Spearman: 0.47, 0.33, 0.93 and 0.91 respectively, data not shown). The correlations are influenced by the sparse data at higher TGN concentrations (data not evenly distributed across all concentrations). This combined with the outliers at >20% methylation could indicate some additional biological factors of influence.

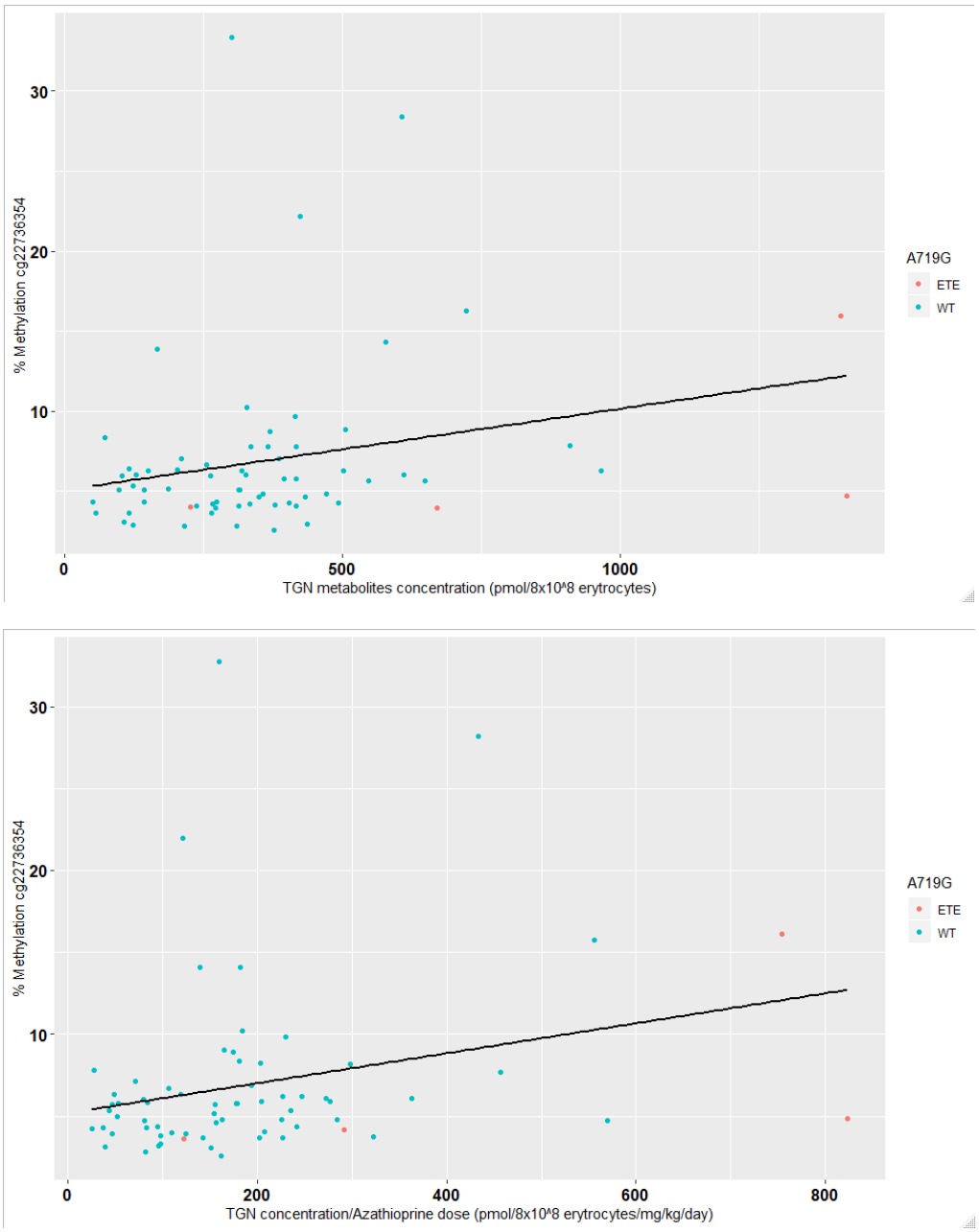

Figure 21. The 2 graphs show the correlation between cg22736354 methylation (%) and TGN concentration and TNG/Dose ratio respectively in patients with early-onset IBD (aged < 6 years) than in non-early–onset IBD (aged > 12 and <18 years); blue and red points display methylation values for patients with wild-type and variant TPMT for A719G respectively.

4.2.8 Analysis of the methylation of two CpG sites on TPMT promoter using pyrosequencing in a cohort composed of 20 early onset and 48 non-early onset pediatric IBD patients

The DNAs of the 20 EO and 48 non-EO patients described on the previous paragraphs were also available for the methylation analysis of 2 CpG sites located on TPMT promoter. In particular, the DNAs extracted from blood have been processed and analyzed by

pyrosequencing in order to quantify the methylation amount of the CpG sites located at chr6:18154813 and chr6:18154820 of the human genome 19 reference sequence. No statistically significant differences emerged between EO and non-EO patients regarding the methylation of both chr6:18154813 and chr6:18154820 as reported in table 11.

Position	Early onset (median - IQR)	Non early onset (median - IQR)	p-value Wilcoxon
chr6:18154813	3.00 (3.00 - 3.00)	3.00 (3.00 - 3.00)	0.9
chr6:18154820	3.00 (3.00 - 4.00)	4.00 (3.00 - 4.00)	0.1

Table 11. Methylation of chr6:18154813 and chr6:18154820 expressed as median and inter-quartile-range (IQR) in early onset and non-early onset patients

4.2.9 TPMT gene expression in a subset of patients with Early-onset IBD in Comparison with Nonearly–onset IBD Patients

TPMT gene expression could be measured in a subset of patients for which sufficient blood sample was available at the time of blood collection in patients. This population was representative of the whole group because no demographic variable was different between this subgroup of patients and the whole study population in terms of the demographic, clinical, and pharmacological variables, as reported in table 7. Therefore, the expression of TPMT have been assessed in 14 EO and 24 non-EO IBD patients enrolled after January 2018. The results showed comparable TPMT expression values between EO and non-EO patients, probably due to the small number of patients analyzed (p-value ANOVA = 0.47, figure 22). Moreover, no association between TPMT expression and TPMT genotype was present (p-value: 0.84.

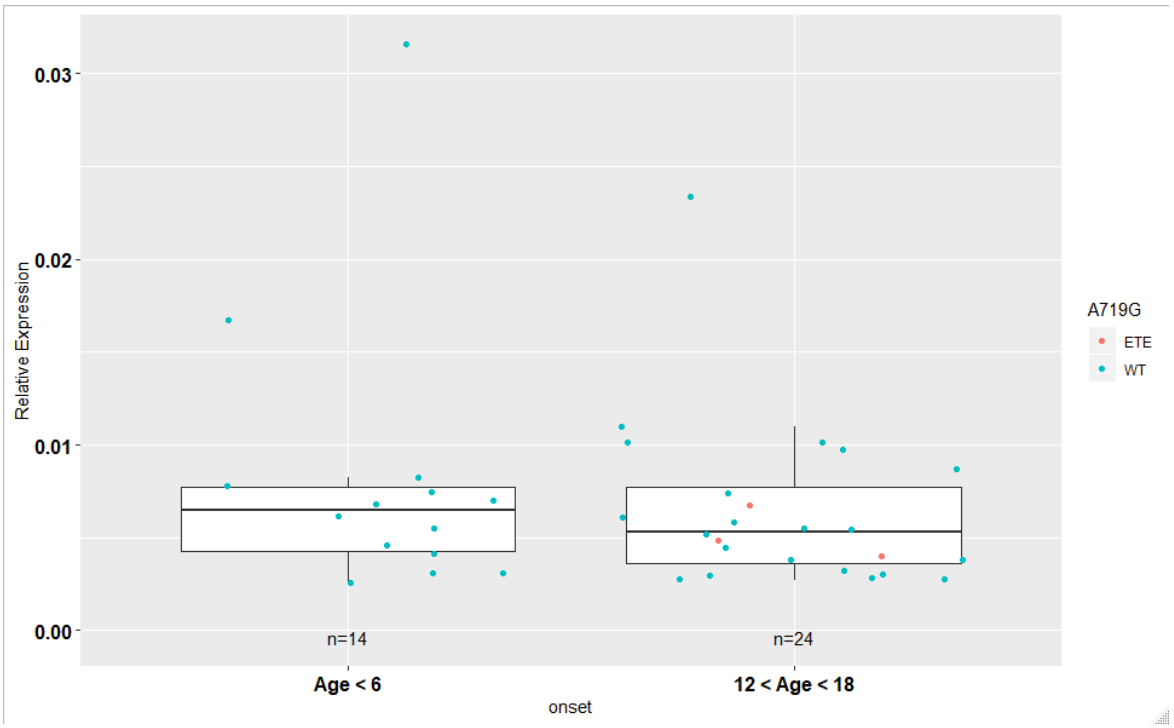

Figure 22. The boxplots show the ratio TPMT expression in patients with early-onset IBD (aged < 6 years) or nonearly–onset IBD (aged > 12 and <18 years); blue and red points display TPMT expression values for patients with wild-type and variant TPMT for A719G respectively.

4.3 CDH4 DNA METHYLATION AND METHOTREXATE RESPONSE IN PEDIATRIC PATIENTS WITH JUVENILE IDIOPATHIC ARTHRITIS

4.3.1 Patients

Seventy-six patients with JIA treated with methotrexate were enrolled at different centers. Both baseline sample and a follow up visit sample (collected after 3, 6 or 12 months of MTX therapy) were obtained from patients. We present, therefore, the results of 71 children whose full core set variable data and DNA sample were available. From the Italian cohort, DNA samples of 19 patients have been collected at 6 months after starting MTX therapy while for 5 patients DNA was collected after 12 months of MTX therapy; all patients from the Italian cohort were Caucasian. Regarding the Cincinnati Children Hospital Medical Center (CCHMC) cohort the DNA sample of 15 patients have been collected after 6 months of MTX therapy while of 4 patients after 3 months of MTX therapy. Finally, for the Children Mercy Hospital (CMH) cohort, DNA sample of 17 patients have been collected after 3 months of MTX therapy while of 11 patients after 6 months of MTX therapy. Response to MTX has been evaluated according to the ACR Ped index, measured at last follow-up visit. Demographic and clinical data are reported in table 12.

	Italian cohort	**CCHMC cohort**	**CMH cohort**
Patients number	24	19	28
Female number (%)	22 (91.6%)	15 (78.9%)	17 (60.7%)
Hispanic patients' number (%)	0 (0%)	1 (5.2%)	2 (7.1%)
African American patients' (%)	0 (0%)	0 (0%)	1 (3.5%)
NR (%)	3 (12.5%)	7 (36.9%)	11 (39.3%)
ACR30 (%)	2 (8.3%)	1 (5.2%)	3 (10.7%)
ACR50 (%)	0 (0%)	0 (0%)	7 (25.0%)
ACR70 (%)	19 (79.2%)	11 (57.9%)	7 (25.0%)
JIA subtype at the beginning of therapy with MTX			
Enthesitis related arthritis	0 (0%)	0 (0%)	4 (14.3%)
Oligoarticular extended	1 (4.2%)	1 (5.3%)	2 (7.1%)
Oligoarticular persistent	16 (66.6%)	1 (5.3%)	3 (10.7%)
Psoriatic	0 (0%)	0 (0%)	4 (14.3%)
Polyarticular RF−	7 (29.2%)	12 (63.2%)	10 (35.7%)

Polyarticular RF +	0 (0%)	4 (21.0%)	2 (7.1%)
Undifferentiated	0 (0%)	1 (5.3%)	3 (10.7%)

Table 12. Demographic and clinical characteristics of patients enrolled. Abbreviations: NR, non-responders; CCHMC, Cincinnati Children Hospital Medical Center; CMH, Children Mercy Hospital (Kansas City), RF, rheumatoid factor

4.3.2 Correlation between CDH4 DNA methylation and ACR Pedi in 71 pediatric patients with JIA

CDH4 methylation at baseline and at last follow up visit was measured using Infinium Methylation EPIC BeadChip Array in 71 patients with JIA. Five-hundred-thirteen (513) CpG sites, available on the EPIC array, on CDH4 gene including also its neighboring regions, 50kb upstream and downstream the gene itself (chr20: 59731711 - 60611444 according to human genome assembly 19), have been analyzed independently in each of the 3 cohorts and then data have been pooled together with a meta-analysis using the weighted inverse Z method, weighting by sample size and considering the direction of the effect. The methylation at baseline visit of 16 CpG sites, out of the 513 available on the array, correlates significantly with the ACR Ped index after meta-analysis (table 13). Interestingly, 7 CpG sites located on CDH4 neighboring regions resulted significant while the other 9 were all located within the CDH4 gene itself (p-value Fisher test = 0.08). Furthermore, CDH4 methylation at last follow-up visit of 86 CpG sites, out of the 513 available on the array, correlates significantly with the ACR Ped index after meta-analysis (table 14). Interestingly, only 10 CpG sites located on CDH4 neighboring regions resulted significant while the other 76 were all located within the CDH4 gene itself (p-value Fisher test = 0.003). Four CpG sites, and in particular cg00111102, cg06707970, cg06787089 and cg08903736, resulted significant in both the previous analyses performed, with methylation that decreases as the ACR Pedi index improves. Moreover, in order to evaluate changes in CDH4 methylation due to MTX therapy, the analysis between CDH4 methylation measured at baseline and at last follow-up visit was performed. Results showed 81 statistically significant CpG sites after meta-analysis (table 15). In particular, 21 CpG sites located on CDH4 neighboring regions resulted significant while the other 60 were all located within the CDH4 gene itself (p-value Fisher test = 0.67). After merging the results of alle the 3 analyses, cg00111102 was the only CpG in common.

ProbeID	*Genomic location*	Gene Name	*Gene location*	*Mean (NR)*	*SD (NR)*	*Mean (ACR30)*	*SD (ACR30)*	*Mean (ACR50)*	*SD (ACR50)*	*Mean (ACR70)*	*SD (ACR70)*	*p-value*	*FDR*
cg04277784	59731711			0.49	0.06	0.46	0.02	0.50	0.04	0.46	0.06	0.038	0.98
cg16748847	59761387			0.26	0.06	0.30	0.08	0.27	0.08	0.30	0.04	0.042	0.98
cg04792530	59768565			0.64	0.04	0.69	0.02	0.66	0.03	0.66	0.04	0.027	0.98
cg03349664	59826138	CDH4	TSS1500	0.67	0.06	0.69	0.03	0.64	0.04	0.65	0.04	0.036	0.98
cg17252482	59870663	CDH4	Body	0.73	0.05	0.77	0.02	0.72	0.04	0.72	0.05	0.047	0.98
cg23706586	59924510	CDH4	Body	0.65	0.04	0.66	0.03	0.64	0.03	0.63	0.04	0.019	0.98
cg06707970	59962861	CDH4	Body	0.09	0.01	0.09	0.01	0.08	0.01	0.10	0.02	0.030	0.98
cg08903736	60074300	CDH4	TSS200	0.80	0.03	0.80	0.02	0.79	0.03	0.79	0.04	0.008	0.98
cg06787089	60198369	CDH4	Body	0.37	0.05	0.38	0.03	0.37	0.03	0.37	0.03	0.029	0.98
cg05357864	60282100	CDH4	Body	0.75	0.04	0.74	0.02	0.73	0.03	0.74	0.06	0.013	0.98
cg02335185	60491905	CDH4	Body	0.68	0.03	0.69	0.03	0.69	0.03	0.67	0.03	0.019	0.98
cg00111102	60509975	CDH4	Body	0.71	0.04	0.72	0.02	0.68	0.03	0.68	0.07	0.009	0.98
cg13152974	60527023			0.32	0.05	0.44	0.10	0.36	0.06	0.37	0.07	0.033	0.98
cg24959147	60531577			0.60	0.05	0.65	0.05	0.63	0.08	0.62	0.05	0.047	0.98
cg15833447	60546782			0.84	0.03	0.86	0.02	0.84	0.01	0.86	0.02	0.006	0.98
cg00218415	60586720	TAF4	Body	0.71	0.07	0.76	0.05	0.71	0.08	0.76	0.04	0.043	0.98

Table 13. Statistically significant CpG sites after meta-analysis of the correlation between DNA methylation measured at baseline and ACR pedi calculated at last follow up visit. Abbreviations: NR, non-responders; SD, standard deviation; Meta, meta-analysis; FDR, false discovery rate; TSS1500, transcription starting site 1500; TSS200, transcription starting site 200.

ProbeID	*Genomic location*	*Gene Name*	*Gene Location*	*Mean (NR)*	*SD (NR)*	*Mean (ACR30)*	*SD (ACR30)*	*Mean (ACR50)*	*SD (ACR50)*	*Mean (ACR70)*	*SD (ACR70)*	*Meta p-value*	*FDR*
cg01212869	59760310			0.73	0.05	0.72	0.04	0.73	0.05	0.70	0.04	0.0104	0.184
cg03688854	59767609			0.72	0.04	0.73	0.02	0.72	0.04	0.69	0.04	0.0039	0.142
cg12975488	59803310			0.71	0.04	0.71	0.04	0.72	0.04	0.69	0.03	0.0130	0.203
cg22118299	59805388			0.75	0.04	0.76	0.04	0.73	0.03	0.74	0.04	0.0378	0.262
cg24968332	59808043			0.63	0.04	0.64	0.04	0.65	0.04	0.62	0.04	0.0305	0.252
cg09706324	59825485			0.77	0.04	0.77	0.04	0.73	0.04	0.74	0.03	0.0368	0.262
cg15534366	59826207	CDH4	TSS1500	0.67	0.05	0.67	0.06	0.62	0.04	0.64	0.05	0.0041	0.142
cg16379868	59826744	CDH4	TSS1500	0.38	0.03	0.37	0.03	0.36	0.03	0.37	0.04	0.0152	0.211
cg05363005	59835988	CDH4	Body	0.79	0.03	0.76	0.05	0.76	0.03	0.76	0.03	0.0039	0.142
cg24138605	59836416	CDH4	Body	0.80	0.03	0.81	0.02	0.79	0.02	0.78	0.03	0.0042	0.142
cg09505835	59857061	CDH4	Body	0.58	0.05	0.59	0.03	0.56	0.05	0.54	0.04	0.0035	0.142
cg11314019	59860325	CDH4	Body	0.72	0.05	0.74	0.04	0.69	0.03	0.70	0.03	0.0067	0.156
cg22198192	59863030	CDH4	Body	0.43	0.07	0.47	0.08	0.40	0.06	0.38	0.09	0.0099	0.184
cg00264578	59864534	CDH4	Body	0.72	0.19	0.78	0.02	0.70	0.14	0.71	0.14	0.0127	0.203
cg12243633	59866704	CDH4	Body	0.81	0.03	0.81	0.03	0.78	0.05	0.80	0.02	0.0358	0.26
cg17659852	59873551	CDH4	Body	0.55	0.05	0.57	0.04	0.54	0.03	0.54	0.05	0.0150	0.211
cg23508779	59895374	CDH4	Body	0.72	0.04	0.73	0.05	0.72	0.05	0.70	0.04	0.0248	0.222
cg13190849	59897273	CDH4	Body	0.55	0.06	0.56	0.06	0.53	0.06	0.53	0.05	0.0181	0.216
cg08098208	59898468	CDH4	Body	0.70	0.04	0.74	0.05	0.67	0.08	0.68	0.04	0.0209	0.216
cg03215161	59906962	CDH4	Body	0.72	0.04	0.73	0.03	0.69	0.03	0.70	0.05	0.0199	0.216
cg09922579	59937911	CDH4	Body	0.54	0.05	0.55	0.06	0.51	0.03	0.52	0.05	0.0253	0.222
cg21109279	59945887	CDH4	Body	0.77	0.03	0.78	0.01	0.75	0.04	0.76	0.04	0.0441	0.281
cg06707970	59962861	CDH4	Body	0.10	0.02	0.10	0.01	0.08	0.01	0.09	0.02	0.0054	0.155
cg02930348	59968939	CDH4	Body	0.69	0.05	0.69	0.04	0.70	0.04	0.67	0.04	0.0178	0.216
cg25213956	59987301	CDH4	Body	0.59	0.04	0.61	0.05	0.59	0.03	0.57	0.04	0.0333	0.255
cg08641142	59989628	CDH4	Body	0.75	0.04	0.74	0.04	0.73	0.03	0.74	0.04	0.0243	0.222
cg21538645	60005790	CDH4	Body	0.35	0.05	0.34	0.05	0.29	0.03	0.33	0.06	0.0024	0.142
cg26370130	60011450	CDH4	Body	0.49	0.05	0.51	0.08	0.43	0.07	0.47	0.07	0.0207	0.216
cg22038372	60034285	CDH4	Body	0.85	0.03	0.76	0.13	0.83	0.06	0.81	0.07	0.0204	0.216

cg23876123	60053469	CDH4	Body	0.74	0.05	0.56	0.28	0.68	0.13	0.65	0.16	0.0060	0.156
cg20387359	60060868	CDH4	Body	0.48	0.06	0.49	0.06	0.43	0.05	0.46	0.07	0.0194	0.216
cg07347959	60074240	CDH4		0.64	0.06	0.66	0.06	0.63	0.04	0.63	0.05	0.0401	0.271
cg08903736	60074300	CDH4		0.80	0.03	0.79	0.05	0.79	0.02	0.78	0.03	0.0230	0.222
cg15007972	60076206	CDH4		0.59	0.04	0.57	0.04	0.55	0.04	0.57	0.04	0.0444	0.281
cg12258763	60076907	CDH4		0.81	0.03	0.80	0.03	0.76	0.07	0.79	0.03	0.0264	0.226
cg09718955	60083755	CDH4		0.69	0.04	0.72	0.04	0.67	0.03	0.67	0.04	0.0075	0.168
cg00626837	60096228	CDH4		0.25	0.05	0.25	0.04	0.24	0.04	0.23	0.04	0.0255	0.222
cg22275543	60096549	CDH4		0.66	0.06	0.66	0.04	0.63	0.02	0.63	0.05	0.0053	0.155
cg02976561	60100552	CDH4		0.30	0.03	0.29	0.03	0.28	0.02	0.28	0.04	0.0123	0.203
cg05788049	60101313	CDH4		0.44	0.07	0.42	0.05	0.42	0.06	0.40	0.05	0.0027	0.142
cg22566085	60104822	CDH4		0.74	0.04	0.77	0.04	0.74	0.03	0.73	0.04	0.0497	0.292
cg25872678	60108457	CDH4		0.67	0.05	0.69	0.05	0.65	0.05	0.66	0.04	0.0149	0.211
cg19227053	60116795	CDH4	Body	0.85	0.03	0.84	0.01	0.84	0.02	0.84	0.02	0.0344	0.256
cg02255917	60135178	CDH4		0.78	0.04	0.79	0.02	0.76	0.04	0.76	0.03	0.0119	0.203
cg19948169	60141183	CDH4		0.48	0.04	0.50	0.05	0.49	0.04	0.47	0.04	0.0313	0.255
cg16755747	60156273	CDH4		0.64	0.06	0.63	0.04	0.58	0.04	0.62	0.04	0.0494	0.292
cg11478714	60174029	CDH4		0.52	0.04	0.53	0.04	0.47	0.02	0.50	0.04	0.0374	0.262
cg17036908	60174898	CDH4		0.38	0.04	0.41	0.05	0.35	0.02	0.37	0.05	0.0026	0.142
cg24711888	60189853	CDH4		0.69	0.04	0.70	0.05	0.67	0.03	0.66	0.04	0.0044	0.142
cg19931514	60191418	CDH4		0.60	0.05	0.59	0.04	0.54	0.03	0.57	0.04	0.0030	0.142
cg24166294	60194963	CDH4		0.76	0.04	0.78	0.02	0.73	0.03	0.76	0.03	0.0230	0.222
cg06787089	60198369	CDH4		0.37	0.05	0.37	0.04	0.34	0.03	0.36	0.04	0.0143	0.211
cg19417613	60203769	CDH4		0.64	0.04	0.66	0.04	0.63	0.04	0.62	0.06	0.0030	0.142
cg07756236	60254244	CDH4		0.71	0.05	0.71	0.05	0.69	0.02	0.69	0.05	0.0201	0.216
cg07130626	60288598	CDH4		0.74	0.03	0.74	0.02	0.71	0.03	0.73	0.04	0.0470	0.291
cg23436303	60297699	CDH4		0.82	0.07	0.82	0.02	0.80	0.02	0.79	0.08	0.0386	0.264
cg18519834	60303394	CDH4	Body	0.63	0.06	0.63	0.04	0.61	0.01	0.61	0.04	0.0275	0.231
cg25418743	60315187	CDH4		0.47	0.05	0.47	0.04	0.43	0.04	0.45	0.04	0.0087	0.174
cg13021439	60331453	CDH4		0.43	0.05	0.44	0.08	0.40	0.05	0.42	0.05	0.0458	0.286

cg10287611	60332244	CDH4		0.67	0.05	0.67	0.04	0.67	0.03	0.65	0.05	0.0251	0.222
cg05038287	60334931	CDH4		0.59	0.05	0.60	0.04	0.58	0.02	0.56	0.05	0.0197	0.216
cg25660529	60337213	CDH4		0.69	0.05	0.71	0.05	0.69	0.03	0.68	0.04	0.0324	0.255
cg20247326	60373402	CDH4	Body	0.55	0.03	0.57	0.03	0.54	0.05	0.53	0.04	0.0061	0.156
cg22871098	60373450	CDH4	Body	0.77	0.03	0.79	0.03	0.79	0.02	0.76	0.03	0.0224	0.222
cg12278216	60390950	CDH4		0.77	0.04	0.78	0.04	0.75	0.05	0.74	0.04	0.0016	0.142
cg20892657	60392957	CDH4		0.65	0.04	0.67	0.05	0.62	0.05	0.64	0.03	0.0330	0.255
cg04785786	60409787	CDH4		0.75	0.05	0.75	0.08	0.72	0.05	0.72	0.05	0.0103	0.184
cg22209466	60420773	CDH4		0.68	0.04	0.68	0.06	0.65	0.03	0.66	0.05	0.0169	0.216
cg09051966	60471657	CDH4	Body	0.28	0.03	0.30	0.02	0.25	0.03	0.27	0.04	0.0427	0.278
cg00966763	60472065	CDH4	Body	0.67	0.05	0.68	0.05	0.63	0.06	0.65	0.05	0.0017	0.142
cg09204484	60475464	CDH4		0.45	0.06	0.49	0.08	0.40	0.03	0.42	0.06	0.0040	0.142
cg03040028	60477110	CDH4		0.45	0.06	0.47	0.05	0.41	0.04	0.43	0.05	0.0324	0.255
cg01470395	60477187	CDH4		0.52	0.04	0.53	0.06	0.51	0.05	0.50	0.05	0.0066	0.156
cg05685185	60484360	CDH4		0.77	0.05	0.76	0.03	0.75	0.06	0.74	0.03	0.0425	0.278
cg01298884	60484469	CDH4		0.71	0.04	0.73	0.06	0.67	0.08	0.68	0.04	0.0004	0.142
cg03582787	60492176	CDH4	Body	0.81	0.03	0.82	0.02	0.81	0.02	0.80	0.03	0.0360	0.26
cg02685032	60498717	CDH4	Body	0.61	0.05	0.65	0.05	0.61	0.02	0.60	0.04	0.0249	0.222
cg12695754	60500069	CDH4		0.71	0.04	0.72	0.03	0.70	0.02	0.69	0.04	0.0339	0.256
cg20818253	60509306	CDH4	Body	0.64	0.05	0.64	0.03	0.63	0.03	0.63	0.04	0.0410	0.273
cg00111102	60509975	CDH4	Body	0.72	0.04	0.70	0.05	0.69	0.04	0.68	0.06	0.0018	0.142
cg11853697	60510235	CDH4	Body	0.32	0.06	0.32	0.05	0.27	0.05	0.30	0.06	0.0164	0.216
cg12411847	60512094	CDH4	3'UTR	0.70	0.04	0.71	0.04	0.68	0.05	0.69	0.05	0.0210	0.216
cg18761221	60518478			0.96	0.02	0.95	0.03	0.95	0.03	0.95	0.03	0.0088	0.174
cg23580287	60554468	TAF4	Body	0.78	0.03	0.78	0.05	0.77	0.02	0.76	0.03	0.0080	0.171
cg05378081	60579036	TAF4	Body	0.72	0.04	0.72	0.03	0.70	0.01	0.71	0.03	0.0197	0.216
cg21181318	60583095	TAF4	Body	0.83	0.03	0.82	0.02	0.82	0.03	0.82	0.03	0.0485	0.292

Table 14. Statistically significant CpG sites after meta-analysis of the correlation between DNA methylation measured at last follow up visit and ACR pedi calculated at last follow up visit. Abbreviations: NR, non-responders; SD, standard deviation; Meta, meta-analysis; FDR, false discovery rate; TSS1500, transcription starting site 1500; 3'UTR, 3' untranslated region.

ProbeID	*Gene Name*	*Genomic location*	*CpG location*	*Mean (baseline)*	*SD (baseline)*	*Mean (last follow up)*	*SD (last follow up)*	*Meta p-value*	*FDR*
cg04968625		59738174		0.50	0.06	0.53	0.04	0.00918	0.14925
cg02353175		59762914		0.64	0.05	0.66	0.05	0.00924	0.14925
cg14189988		59804332		0.08	0.02	0.09	0.02	0.03085	0.26079
cg24968332		59808043		0.63	0.04	0.65	0.03	0.01595	0.18601
cg09500995		59809165		0.81	0.04	0.82	0.04	0.03779	0.28557
cg01613195	CDH4	59832270	Body	0.65	0.05	0.63	0.06	0.00202	0.09870
cg19635562	CDH4	59851109	Body	0.83	0.03	0.82	0.03	0.00029	0.07497
cg00127528	CDH4	59853894	Body	0.59	0.04	0.61	0.04	0.00504	0.13403
cg19578541	CDH4	59856571	Body	0.70	0.04	0.72	0.04	0.00078	0.09870
cg19054096	CDH4	59868424	Body	0.59	0.04	0.61	0.04	0.04648	0.31312
cg21256764	CDH4	59871148	Body	0.62	0.04	0.64	0.04	0.01336	0.17570
cg11444661	CDH4	59873575	Body	0.65	0.16	0.68	0.13	0.02815	0.25791
cg14414759	CDH4	59883394	Body	0.78	0.05	0.80	0.03	0.03785	0.28557
cg00851543	CDH4	59887007	Body	0.53	0.04	0.55	0.04	0.00745	0.14154
cg08098208	CDH4	59898468	Body	0.68	0.05	0.70	0.04	0.04734	0.31312
cg23706586	CDH4	59924510	Body	0.64	0.04	0.66	0.04	0.01019	0.15375
cg18314193	CDH4	59927510	Body	0.07	0.03	0.08	0.02	0.02076	0.22981
cg02929169	CDH4	59928451	Body	0.54	0.16	0.48	0.09	0.01180	0.16269
cg13212668	CDH4	59928453	Body	0.64	0.10	0.61	0.08	0.00361	0.12020
cg00071702	CDH4	60019041	Body	0.60	0.04	0.63	0.04	0.00343	0.12020
cg11704352	CDH4	60033929	Body	0.81	0.03	0.80	0.03	0.00909	0.14925
cg03794124	CDH4	60076707	Body	0.64	0.06	0.67	0.04	0.00398	0.12020
cg09826217	CDH4	60089107	Body	0.49	0.05	0.51	0.04	0.00193	0.09870
cg03300039	CDH4	60098437	Body	0.82	0.03	0.81	0.03	0.03098	0.26079
cg15282999	CDH4	60124848	Body	0.85	0.03	0.84	0.03	0.00100	0.09870
cg05822299	CDH4	60131439	Body	0.77	0.04	0.79	0.03	0.00937	0.14925
cg07452415	CDH4	60133701	Body	0.78	0.04	0.76	0.04	0.01205	0.16269
cg02255917	CDH4	60135178	Body	0.78	0.03	0.76	0.04	0.00686	0.13535
cg02501498	CDH4	60145048	Body	0.88	0.03	0.89	0.02	0.03397	0.27369

cg17301773	CDH4	60145125	Body	0.83	0.03	0.82	0.03	0.00172	0.09870
cg21800599	CDH4	60148355	Body	0.70	0.04	0.71	0.04	0.04849	0.31312
cg06672474	CDH4	60165592	Body	0.74	0.04	0.76	0.04	0.00176	0.09870
cg21079157	CDH4	60169020	Body	0.77	0.05	0.79	0.04	0.03037	0.26079
cg12206539	CDH4	60174740	Body	0.52	0.05	0.54	0.06	0.01456	0.17786
cg20573205	CDH4	60187828	Body	0.59	0.05	0.61	0.04	0.00601	0.13403
cg09813632	CDH4	60192437	Body	0.76	0.04	0.75	0.04	0.04944	0.31312
cg17379088	CDH4	60201880	Body	0.68	0.03	0.66	0.03	0.00503	0.13403
cg15101902	CDH4	60214785	Body	0.83	0.03	0.82	0.03	0.00960	0.14925
cg11655827	CDH4	60242590	Body	0.71	0.03	0.70	0.03	0.02806	0.25791
cg18519834	CDH4	60303394	Body	0.62	0.04	0.64	0.04	0.00332	0.12020
cg13021439	CDH4	60331453	Body	0.42	0.05	0.44	0.05	0.04361	0.31312
cg02692214	CDH4	60343472	Body	0.77	0.06	0.79	0.04	0.00858	0.14925
cg18627496	CDH4	60349210	Body	0.71	0.03	0.72	0.03	0.02395	0.23627
cg09599986	CDH4	60352417	Body	0.60	0.05	0.62	0.06	0.03380	0.27369
cg11882888	CDH4	60364704	Body	0.67	0.05	0.65	0.04	0.03579	0.28249
cg02619941	CDH4	60370985	Body	0.69	0.04	0.70	0.04	0.03414	0.27369
cg02095226	CDH4	60388556	Body	0.42	0.04	0.43	0.05	0.04614	0.31312
cg03008286	CDH4	60394429	Body	0.78	0.04	0.76	0.03	0.00004	0.02132
cg16928869	CDH4	60397766	Body	0.64	0.05	0.66	0.05	0.04512	0.31312
cg23328777	CDH4	60433845	Body	0.80	0.03	0.81	0.02	0.04375	0.31312
cg09350944	CDH4	60439676	Body	0.66	0.04	0.67	0.03	0.00598	0.13403
cg23899424	CDH4	60456296	Body	0.62	0.04	0.64	0.05	0.03678	0.28557
cg24688309	CDH4	60456498	Body	0.81	0.03	0.83	0.04	0.02333	0.23627
cg00594944	CDH4	60466703	Body	0.67	0.04	0.69	0.04	0.02363	0.23627
cg02313492	CDH4	60467407	Body	0.42	0.04	0.44	0.04	0.00182	0.09870
cg22255095	CDH4	60472331	Body	0.70	0.05	0.72	0.03	0.00565	0.13403
cg13369471	CDH4	60472885	Body	0.76	0.03	0.78	0.04	0.01057	0.15490
cg02625694	CDH4	60473786	Body	0.66	0.04	0.68	0.04	0.00212	0.09870
cg06899776	CDH4	60482939	Body	0.83	0.02	0.83	0.03	0.02105	0.22981

cg01856511	CDH4	60486653	Body	0.74	0.03	0.72	0.03	0.01393	0.17630
cg02685032	CDH4	60498717	Body	0.60	0.05	0.62	0.04	0.00257	0.11002
cg15656087	CDH4	60502022	Body	0.91	0.02	0.91	0.02	0.04683	0.31312
cg00111102	CDH4	60509975	Body	0.69	0.06	0.72	0.04	0.01951	0.22244
cg11853697	CDH4	60510235	Body	0.30	0.04	0.32	0.04	0.01409	0.17630
cg12411847	CDH4	60512094	3'UTR	0.69	0.04	0.71	0.05	0.01192	0.16269
cg23711059		60513733		0.60	0.04	0.62	0.04	0.02631	0.24991
cg16491680		60528285		0.60	0.05	0.62	0.05	0.02395	0.23627
cg06048153	MIR1257	60528844	TSS200	0.55	0.04	0.57	0.05	0.00526	0.13403
cg01273384	MIR1257	60529758	TSS1500	0.54	0.06	0.56	0.04	0.03844	0.28577
cg15833447		60546782		0.85	0.03	0.86	0.02	0.02522	0.24413
cg00328497	TAF4	60551707	Body	0.73	0.03	0.74	0.03	0.00076	0.09870
cg13173722	TAF4	60553138	Body	0.62	0.05	0.64	0.03	0.00386	0.12020
cg03057951	TAF4	60553530	Body	0.62	0.04	0.63	0.03	0.00676	0.13535
cg00845415	TAF4	60553835	Body	0.82	0.05	0.84	0.04	0.02391	0.23627
cg23580287	TAF4	60554468	Body	0.78	0.03	0.76	0.04	0.00639	0.13535
cg01475704	TAF4	60560761	Body	0.75	0.05	0.73	0.05	0.04856	0.31312
cg20908267	TAF4	60582771	Body	0.83	0.03	0.81	0.02	0.03012	0.26079
cg00218415	TAF4	60586720	Body	0.74	0.06	0.76	0.04	0.03101	0.26079
cg09692950	TAF4	60598027	Body	0.81	0.05	0.83	0.03	0.04541	0.31312
cg14028166	TAF4	60599257	Body	0.83	0.03	0.84	0.03	0.01495	0.17835
cg04011567	TAF4	60611444	Body	0.83	0.03	0.83	0.03	0.04935	0.31312

Table 15. Statistically significant CpG sites after meta-analysis of the correlation between DNA methylation measured at baseline and at last follow up visit. Abbreviations: NR, non-responders; SD, standard deviation; Meta, meta-analysis; FDR, false discovery rate; TSS1500, transcription starting site 1500; 3'UTR, 3'untranslated region.

4.3.3 CDH4 gene expression in a cohort of JIA patients under MTX therapy and in controls available on GEO

In order to evaluate whether a different CDH4 expression between responder and non-responder was present, RNA-seq data available on GEO have been analyzed (GSE81259). In particular, CDH4 expression from RNA-seq data of 47 JIA patients (29 responders and 18 non responders to MTX) and 14 age-matched controls have been evaluated. Baseline demographic data of patients with JIA at MTX start and age-matched controls are reported in table 16.

Characteristic	JIA patients (all)	JIA R	JIA NR	Controls
Number of cases	47	29	18	14
Gender, female, n (%)	38 (81)	25 (86)	13 (72)	10 (71)
JIA subtype, n (%)				
Oligoarticular persistent	3 (6)	2 (7)	1 (6)	
Oligoarticular extended	3 (6)	3 (10)	0 (0)	
Polyarticular RF^{-}	32 (68)	17 (59)	15 (83)	
Polyarticular RF^{+}	9 (19)	7 (24)	2 (11)	
Clinical variables				
Disease duration, years	0.6 (0.3–1.6)	0.6 (0.3–1.2)	0.6 (0.3–1.6)	
Age at starting MTX, years	11.8 (7.2–15.4)	13.0 (8.8–15.3)	9.7 (5.7–14.7)	
Physician's VAS	5 (4–7)	5 (4–7)	5 (4–6.8)	
Active joints	9 (5–17.5)	9 (5–12)	13 (4.5–19.5)	
Restricted joints	6 (2–12)	4.5 (2–9.3)	7 (4.3–21.3)	
Parent's VAS	3 (1.5–6.7)	3 (1.4–6.3)	4 (1.5–7.9)	
CHAQ	0.4 (0–1.13)	0.4 (0.03–0.96)	0.7 (0.03–1.41)	
ESR, mm/h	25 (8–42)	12.5 (5.75–30)	33 (28–49)	
MTX dose, mg/m^2	11.4 (9.1–13.3)	10.6 (8.3–13.0)	12.3 (10.2–13.7)	

Table 16. Demographic and clinical characteristics of patients enrolled. Data are the median and interquartile range, unless otherwise indicated. Abbreviations: NR, non-responders; RF, rheumatoid factor; CHAQ childhood health assessment questionnaire; R, responder; VAS, visual analogue scale.

No statistically significant difference was present in CDH4 expression between responder and non-responder JIA patients (Wilcoxon p-value: 0.67, figure 23) while, interestingly, controls presented a higher CDH4 expression then patients (Wilcoxon p-value: 0.033, figure 24).

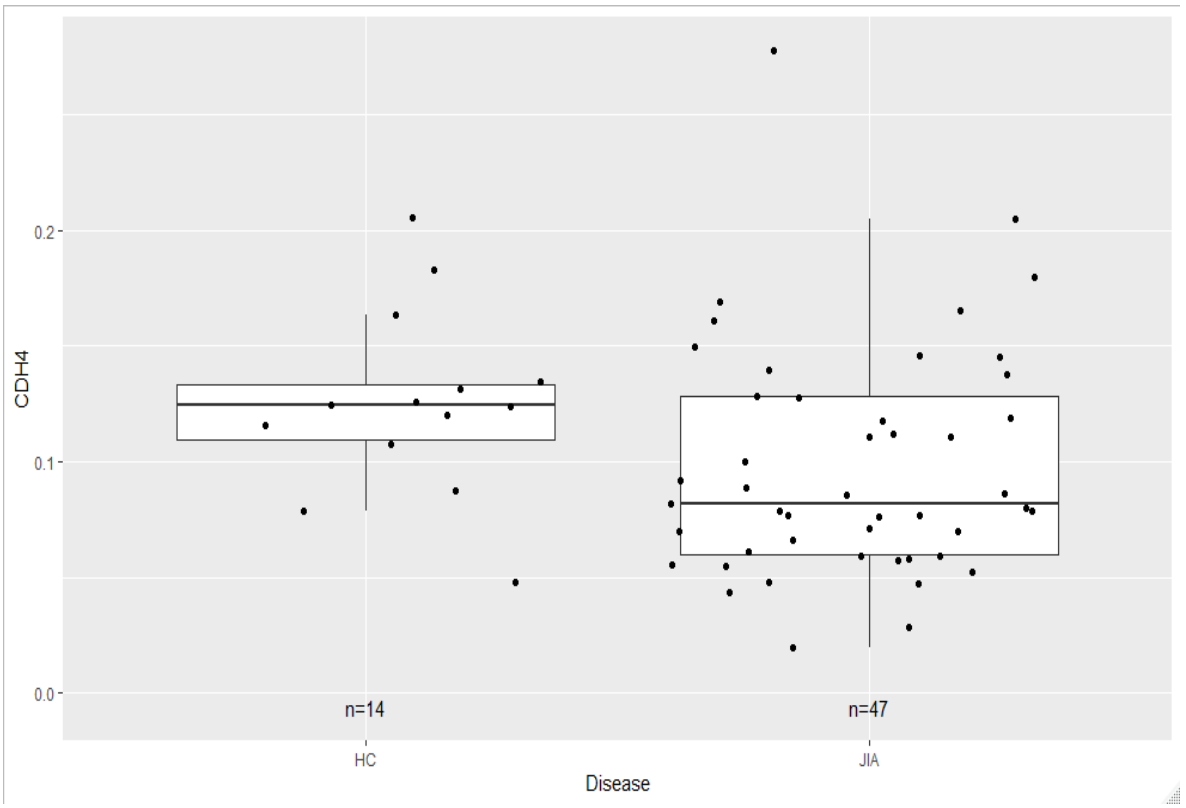

Figure 23. The boxplots show the expression of the CDH4 gene in healthy controls (HC) and in juvenile idiopathic arthritis (JIA) patients.

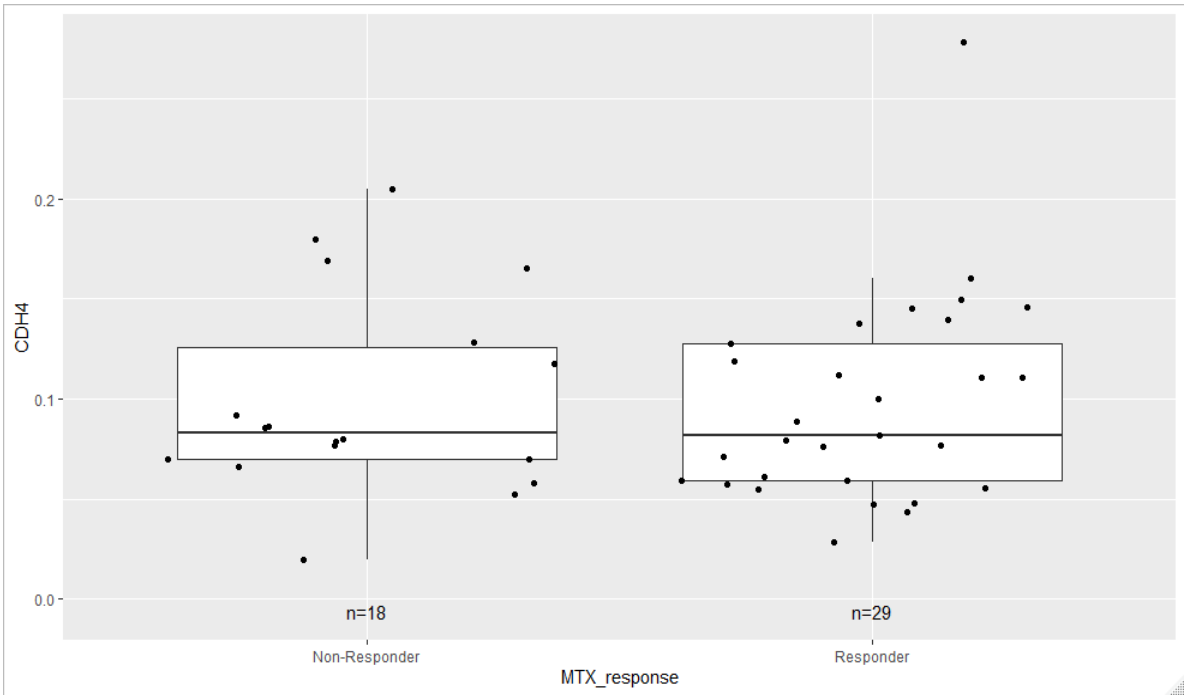

Figure 24. The boxplots show the expression of the CDH4 between Responder and Non-Responder JIA patients.

Even though a significant difference was detected, overall, the absolute CDH4 expression resulted extremely low in both patients and controls if compared with the expression of the GAPDH, a common housekeeping gene (figure 25).

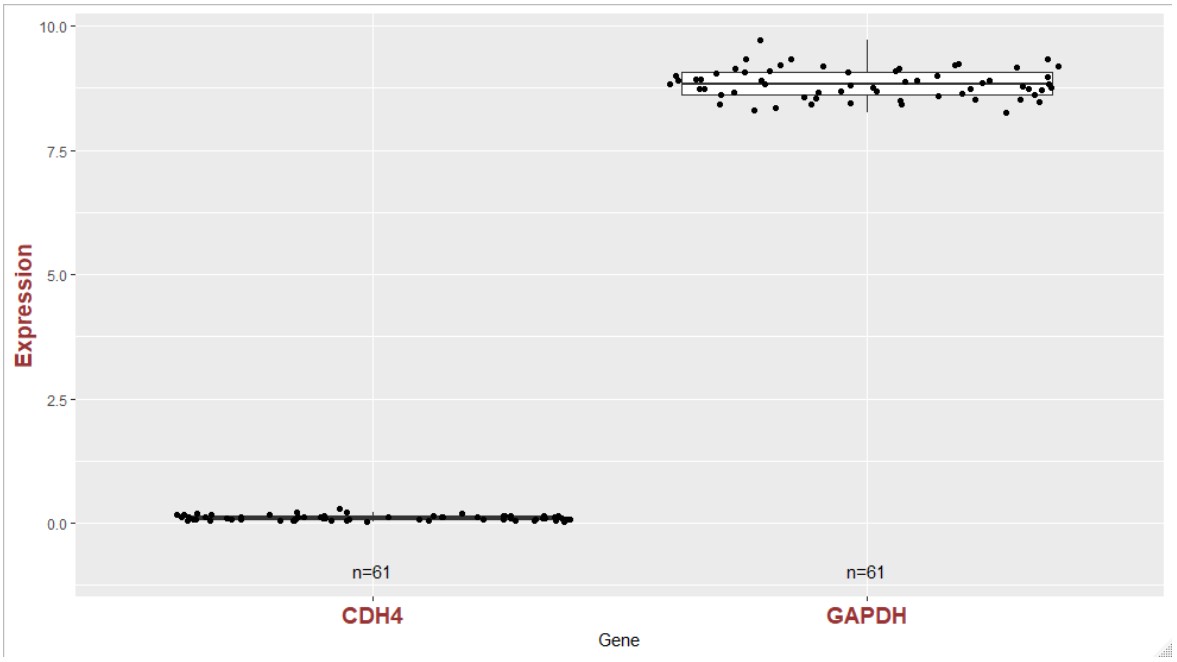

Figure 25. The boxplots show the absolute expression of the CDH4 gene compared to the glyceraldehyde 3-phosphate dehydrogenase (GAPDH), a common housekeeping gene.

4.3.4 CDH4 expression in JIA patients' whole blood and in immortalized cell lines

In order to validate the CDH4 gene expression results obtained on the RNA-seq GEO cohort described above, CDH4 expression from RNA obtained from whole blood of 20 JIA patients (16 females, 8 polyarticular JIA, 6 oligoarticular JIA and 6 undifferentiated JIA) has been analyzed using a TaqMan assay. The CDH4 gene resulted expressed only in 1 patient while it resulted extremely low in 10 patients and null in 9 patients as shown in figure 26.

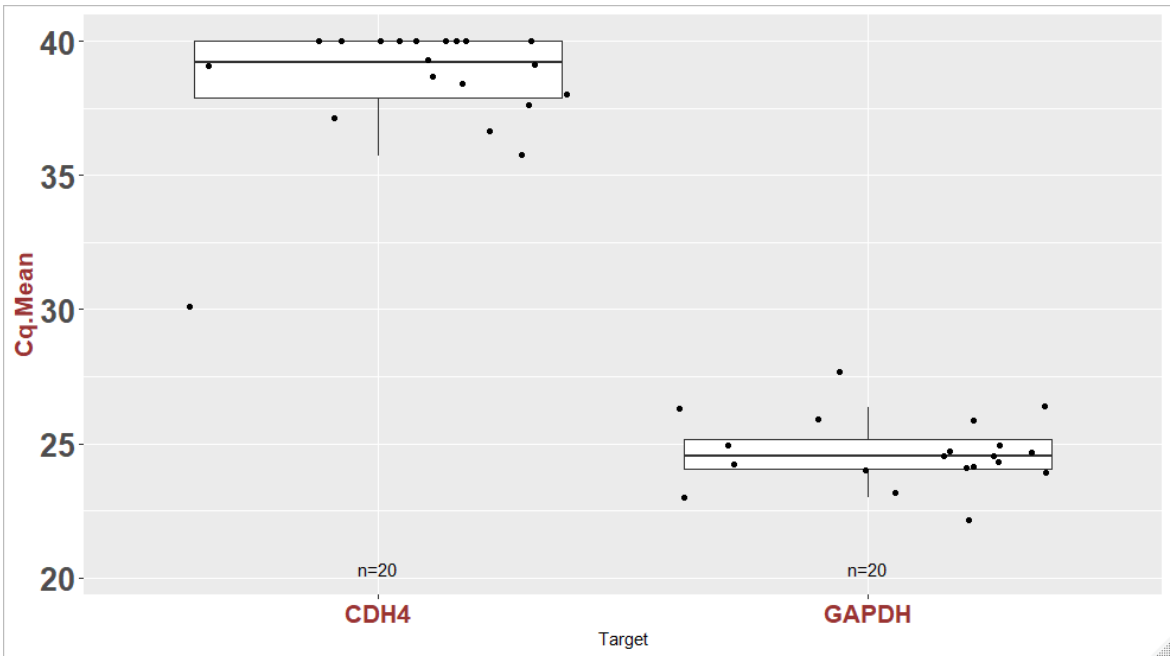

Figure 26. The boxplots show the Cq mean expression of the CDH4 gene compared to a common housekeeping gene (GAPDH). The higher the Cq mean value, the lower the expression of the gene (values of 40 represent null expression).

Moreover, the CDH4 cadherin expression was assessed in 5 immortalized cell lines. Four of the 5 cell lines (Jurkat, THP1, THP1-derived macrophages, NALM6) did not express the CDH4 gene at all (Cq mean > 40.0) while U937 monocytes presented a moderate CDH4 gene expression (Cq mean CDH4: 30.24 ± 0.13, Ct mean GAPDH: 20.50 ± 0.05).

5. DISCUSSION

Evidence has accumulated that epigenetic mechanisms such as DNA methylation can regulate pharmacological pathways and can be used in identifying differentially methylated genes or regions, potentially associated with pharmacological phenotypes such as drug response, pharmacokinetics, or drug toxicity (152). In this thesis the role of DNA methylation of 3 candidate genes as epigenetic biomarker for the personalization of therapy in 3 different autoinflammatory diseases was assessed. In particular, NLRP3 promoter methylation in relation to age and sex in patients with INS was analyzed, together with the role of NLRP3 in modulating steroid response in INS; TPMT methylation in relation to AZA pharmacokinetics in EO pediatric patients with IBD and CDH4 methylation in relation to MTX response in pediatric patients with JIA.

GCs, and in particular prednisone, are the first line therapy to treat both pediatric and adult INS and a high variability in response is often observed with almost 15% of patients presenting steroid resistance (73). Moreover, a recent study published by our group showed a lower NLRP3 promoter methylation in GC resistant INS patients (153). The hypothesis is that an epigenetic regulation, due to different DNA methylation, plays a pivotal role for the activation of NLRP3 inflammasome, a multiprotein complex that recruits pro-caspase-1 via ASC and then proceeds to cleave the cytokine precursors pro-IL-1β and pro-IL-18 into mature IL-1β and IL-18, that has previously been associated with GCs response in pediatric patients with acute lymphoblastic leukemia (ALL). In particular, the paper published by Paugh and collaborators reported a lower NLRP3 promoter methylation and a higher NLRP3 gene expression in steroid resistant pediatric patients with ALL (36) due to a higher activation of caspase-1 (CASP1) which was found able to cleave the GC receptor (GR), leading it into an inactive form. In the same paper the authors validated the role of the NLRP3 inflammasome pathway in modulating the sensitivity to GCs by an in vitro model using the immortalized B-lymphoblast cell line NALM6 in which the inflammasome pathway was activated by LPS/ATP with consequent increased CASP1 activation.

In the first part of the thesis the methylation of cg21991396 located on the NLRP3 gene was evaluated in 21 pediatric patients and 28 adult patients with INS and in 52 healthy subjects divided in 11 children and 41 adults. An inverse correlation between NLRP3 methylation and age was present in INS patients considering the pediatric and the adult cohort combined, while NLRP3 promoter methylation resulted comparable between males and females in both patients' cohorts. Interestingly, NLRP3 methylation was markedly reduced in adult INS patients compared to adult healthy controls, whereas pediatric patients

with INS did not differ from pediatric healthy controls, perhaps because of a different disease mechanism or less prolonged inflammation possibly caused by the presence, in adults, of additional comorbidities and treatments such as dialysis (154). Therefore, a major contribution of NLRP3 methylation in determining GC resistance in adult patients than in the pediatric ones, might be considered in further studies. On these bases, it will be important to include age, together with NLRP3 methylation in a prediction model for GC resistance in patients with INS. Further studies to investigate the association between age and NLRP3 methylation, considering age-stratified groups of pediatric patients, could give interesting insights on NRLP3 methylation changes in young patients. Furthermore, the absence in our dataset of GC-resistant adult patients with MCD and the absence of GC-sensitive children with FSGS may reveal a potential disease-correlation effect. In fact, it is already known in the literature that adult patients with MCD are less prone to develop steroid resistance while, on the other hand, pediatric FSGS is usually steroid-resistant and, if not controlled by more aggressive therapy, typically progresses to ESRD (155).

An in vitro model was also set up in this thesis in order to clarify the role of NLRP3 in regulating GC sensitivity in patients with INS. For this purpose, the U937 monocytes cell line was selected because of the relevant role of monocytes in INS pathology (156–158) and in GC response (159,160). A variety of stimuli, including danger-associated molecular patterns (DAMPs, such as silica and uric acid crystals) and pathogen-associated molecular patterns (PAMPs) such as lipopolysaccharide (LPS) can activate NLRP3 inflammasome. Our results showed a statistically significant reduction in GC sensitivity after inflammasome activation with LPS/ATP in U937 monocytes compared to not activated cells. Secondarily, a reduction of the GR was detected in the activated U937 monocytes through western blot analysis, confirming the hypothesis of an increased steroid resistance in cells where the NLRP3 inflammasome is overactivated, due to increased CASP1 activation, with consequent cleavage of the GR which will be less active. Finally, the mRNA expression of glucocorticoid-induced leucine zipper (GILZ), an anti-inflammatory protein expressed in all peripheral blood cells that is trans-activated by the GR, was also evaluated in U937 monocytes in presence or absence of NLRP3 inflammasome activation. Interestingly GILZ was downregulated in activated U937 cells, confirming a reduced GR activity where the NLRP3 pathway is over-activated.

Taken together, our results uncovered a new biological mechanism whereby patients with INS may develop resistance to GCs via leukocyte epigenetic differences in NLRP3 gene

methylation. In particular, differences in DNA methylation should be taken into account between steroid resistant and sensitive patients, considering also the impact of age in regulating NLRP3 methylation.

The second part of this work focused on the role of epigenetic regulation of TPMT gene by DNA methylation in AZA pharmacokinetics in EO pediatric patients with IBD. AZA is a pro-drug frequently used to maintain disease remission both in CD and UC even though a significant proportion of patients does not respond to therapy or develops important adverse events (100). As a pro-drug, AZA requires intracellular activation, catalyzed by multiple enzymes, into the active metabolites TGNs to exert cytotoxicity (104). The causes of the interindividual variability in response to AZA are not completely understood although a consistent amount of evidence supports an important role of several SNPs carried by the TPMT gene, with consequent reduced enzyme activity (100). TPMT is a key enzyme that catalyzes the S-methylation of thiopurine drugs, converting them into an inactive form and for this reason, its activity can interfere with the final plasma concentration of TGNs (161). Recently it has been demonstrated by our group that EO pediatric patients with IBD (age < 6 years) present an altered AZA pharmacokinetics compared to adolescent patients (12 < age < 18) and in particular they showed lower TGN plasma concentration normalized to AZA dose, likely because of an age-dependent increase in TPMT activity (91). Other publications showed elevated TPMT activity in newborns, in comparison with children (162) and in younger children in comparison with older ones and adults (163) while some other papers did not report a higher TPMT activity in young children (164).

However, the molecular mechanism underlying the age-related progressive reduction in TPMT activity in IBD patients described in the previous papers has not yet been identified. An epigenetic regulation of TPMT due to an age-dependent increase in its DNA methylation has been proposed as possible mechanism influencing AZA response (91) and has been analyzed in this thesis.

In the context of a multicentric case-control (1:3) study, 30 EO and 90 non-EO pediatric IBD patients were enrolled: lower TGN plasma levels were observed in early onset patients, even though they were given a higher dose of AZA then non-EO patients. This result differs from that observed in the previous published paper by our group (91), where comparable TGN levels were present between EO and non-EO. In the present cohort, the increased AZA dose given to EO patients may not be sufficient to compensate for the

pharmacokinetic differences between EO and non-EO pediatric IBD patients, even though the median TGN levels are in the therapeutic range also for EO patients. Moreover, the ratio of active TGN metabolites per unit of daily AZA dose resulted significantly reduced and TPMT activity increased in EO patients, confirming the observations of the abovementioned studies and further supporting the hypothesis that patients with EO IBD have increased inactivation of thiopurines and, therefore, may be less sensitive to the drug than non-EO patients.

In order to investigate the molecular mechanisms explaining the pharmacokinetics differences between EO and non-EO pediatric patients with IBD, and in particular the different TPMT activity, the DNA methylation of the TPMT gene, including also its neighboring regions, was analyzed. A pilot study was conducted in a subgroup of 10 EO and 8 non-EO patients using the genome wide Illumina DNA methylation EPIC BeadChip array. The results showed 5 differentially methylated CpG sites between EO and non-EO patients, 4 of which were located in the neighboring regions of TPMT while the remaining one was located on the TPMT gene body. The methylation of cg22736354 was the only one that increased with age, while for the other 4 CpGs a reduced methylation was observed in non-EO patients. The cohort analyzed in the pilot study did not present pharmacological differences between EO patients and non-EO patients except the duration of AZA therapy that might represent a relevant bias, considering the potential role of thiopurines in influencing DNA methylation (165,166). Therefore, in order to achieve more statistical power and reduce the impact of the biases of our cohort, in particular the different AZA duration between cases and controls and the reduced number of patients analyzed, we performed a meta-analysis between our cohort and 3 other cohorts available on the GEO platform. Results showed 4 differentially methylated CpG sites after FDR adjustment. The CpG site cg22736354, the only one whose methylation increased with age in all the cohorts, resulted statistically significant both in our pilot study cohort and in the meta-analysis and, for this reason, was selected as candidate CpG site for further validation by pyrosequencing in a larger cohort of pediatric patients with IBD. Due to pyrosequencing assay design, a total of 4 CpG sites, including cg22736354, have been analyzed. In particular, 2 CpG sites upstream and 1 CpG site downstream cg22736354 were included. The methylation of all the 4 CpG sites resulted markedly lower in early onset patients, indicating an age-dependent regulation of all the region that includes cg22736354. Moreover, the methylation of cg22736354 resulted significantly associated with TGN and TGN/dose ratio in the subgroup analyzed while no statistically significant association

emerged between the other pharmacological variables and cg22736354 methylation. The age-dependent changes in DNA methylation of cg22736354 have been previously reported by several studies. In particular, this specific CpG site was found to overlap both in Hannum (47) and Horvath (48) epigenetic clocks. Hannum and collaborators used DNA methylation profiles from whole blood to identify 71 CpG sites that correlate with chronological age, while Horvath used data from 51 different tissue types from multiple studies to identify 353 CpG sites whose methylation levels can be combined to form an age predictor. Moreover, the cytosine cg22736354 emerged as the only CpG site in cis-acting methylation quantitative trait loci with rs76244256 and rs7744541 that intersects with both the Hannum and Horvath clocks that emerged in a meta-analysis published in 2019 (49).

In order to exclude a potential effect of TPMT promoter methylation in regulating TPMT activity and AZA pharmacokinetics, 2 CpG sites located on TPMT promoter have also been analyzed by pyrosequencing in this thesis, also because of a lack of coverage of TPMT promoter on the Illumina methylation array. The methylation of both CpG sites resulted very low and almost identical between early onset and non-early onset pediatric patients with IBD supporting the hypothesis of a stronger impact of cg22736354 methylation in regulating AZA pharmacokinetics in young patients with IBD. However, we were not able to identify statistically significant differences in whole blood TPMT gene expression, in a subgroup composed of 14 early onset and 24 non early onset patients probably because of the small number of patients analyzed.

It has previously been reported that the methylation of the neighboring regions of a gene can alter the expression of the gene itself (167) due to an altered recruitment and binding capacity of methylation sensitive transcription factor such as sp1 (168), known to be an important transcription factor also for TPMT (169). However, further studies are needed in order to better investigate on the molecular mechanism by which the methylation of the neighboring region of TPMT, that includes cg22736354, influences TPMT expression. In particular, modulating the methylation of cg22736354 in vitro, with a CRISPR-Cas9 system for targeted DNA methylation, as reported by Aleksandar Vojta and collaborators (170), should be considered.

This is the first study demonstrating that patients with EO IBD present an increased inactivating azathioprine metabolism, possibly because of elevated activity of the enzyme TPMT that could be explained, at least in part, by a lower cg22736354 DNA methylation in young IBD patients. Other pharmacokinetic factors influenced by age such as changes in

absorption and bioavailability (171,172), may also contribute to defining AZA pharmacokinetics differences and should be evaluated in further studies.

The last part of this work focused on the potential role of CDH4 methylation in relation to MTX response in pediatric patients with JIA. MTX is the first choice disease-modifying anti-rheumatic drug in JIA, however, 35-45% of patients fail to respond (128,129), and the delay in identifying the optimal treatment at an early stage of disease can influence the disease-related long-term joint damage. The CDH4 gene encodes for R-cadherin, an important glycoprotein that was found to be related to MTX effects in 2 different papers. In particular, Haupl and collaborators reported an overexpression of the CDH4 gene in synovial cells of rheumatoid arthritis patients compared to healthy donors that became comparable after MTX treatment (143). Moreover, a genome wide study from Cobb and colleagues identified 10 intronic SNPs on the CDH4 gene that correlate with the visual analog scale (VAS), the ACR ped index and limited joints count (144), measures currently used in JIA patients to determine disease activity status. In addition, several studies have been published describing the impact of the methylation of the CpG island located on the first exon of the CDH4 gene in regulating the expression of the gene itself (140–142).

Considering the previously described evidence, whole blood DNA methylation of the CDH4 gene and its neighboring regions in 3 different cohorts of JIA patients under MTX therapy was analyzed, in order to identify differentially methylated CpG sites useful as biomarker of MTX response. For this analysis, the ACR ped index, considered after a median of 6 months of therapy, was used as measure of disease improvement after MTX treatment. The meta-analysis performed on p-values obtained independently for each cohort, from the correlation analysis between DNA methylation at baseline and ACR ped at last follow up visit showed 16 differentially methylated CpG sites. Furthermore, the meta-analysis performed on p-values obtained independently for each cohort, from the correlation analysis between DNA methylation and ACR ped both considered at last follow up visit showed 86 differentially methylated CpG sites. Finally, in order to detect the CpG sites, the methylation of which changes because of MTX treatment, we performed a meta-analysis on p-values obtained independently for each cohort, between DNA methylation at baseline and DNA methylation at last follow up visit. Results showed 81 differentially methylated CpG sites. Interestingly, the methylation of several CpG sites resulted influenced by MTX treatment as previously demonstrated also for other genes

(136), indicating the strong impact of MTX in modulating DNA methylation. Moreover, the highest number of statistically significant CpG sites emerged in the analysis between DNA methylation and ACR Pedi considered both at last follow up.

After merging the results of the correlation between methylation measured at baseline and ACR Pedi at last follow up visit and of the correlation between methylation measured at last follow up visit and ACR Pedi at last follow up visit, 4 CpG sites resulted in common (cg00111102, cg06707970, cg06787089 and cg08903736). In order to exclude all the CpG sites that could be influenced more on MTX treatment than ACR Pedi response, one CpG (cg00111102), the methylation of which resulted significantly different between baseline and last follow up visit, was excluded. Therefore, 3 CpG sites (cg06707970, cg06787089 and cg08903736) considered both at baseline and at last follow up visit, associated with ACR Pedi response and not influenced by MTX therapy, have been identified. All 3 CpG sites are located within the gene body but none of them is located on the first exon, known to be important to regulate the CDH4 expression, so the mechanism by which the methylation of these positions influences MTX response remains to be elucidated.

In order to assess whether CDH4 gene was differentially expressed between MTX responder and non-responder JIA patients, RNA seq data on JIA patients available on GEO have been analyzed. No differences emerged between MTX responder and non-responder patients while a statistically significant difference emerged between JIA patients and healthy subjects. Even though a difference was present between patients and controls, the expression of the CDH4 gene resulted extremely low in all patients and healthy subjects. Moreover, CDH4 gene expression in blood of 20 JIA patients and 5 immortalized cellular lines was evaluated and, surprisingly, the expression was almost null in all patients and immortalized cellular lines except in the U937 line. The principal reason why DNA methylation can be considered an ideal biomarker for clinical or pharmacological purposes is its physical stability across time if compared to RNA expression (173,174). In fact, while RNA expression can vary consistently also within different hours of the same day (175), DNA methylation was demonstrated to be particularly stable during time (2). For this reason, it is likely that a different CDH4 methylation in MTX non responder patients reflects an epigenetic signature that may not be associated with differences in its mRNA expression in circulating lymphocytes or, at least, not so easily detectable. Interestingly, CDH4 seems to be expressed in the spleen. Further studies should consider a potential role of spleen cells in modulating MTX response in JIA.

This work suggests the use of CDH4 DNA methylation as biomarker of MTX response in JIA patients even though further studies performed on larger cohort of JIA patients will be extremely useful in order to make the DNA methylation of the CDH4 gene a predictive biomarker of MTX response potentially usable in the clinical practice.

To date, a biomarker able to predict MTX response in JIA is not available, even if several pharmacogenetics studies have been conducted (130). To our knowledge there is only one paper available that investigates the role of DNA methylation in relation to MTX response in JIA (176). In particular the authors identified 145 differentially methylated CpG sites between JIA patients and healthy controls. Moreover, the removal of four samples exposed to MTX from the analysis reduced the number of statistically significant CpG sites to 11, indicating an important role of MTX in modulating DNA methylation.

To our knowledge this is the first study that identified 3 CpG sites on the CDH4 gene that can be used as predictive biomarkers of MTX response in JIA patients. For the future, great expectations rely on the role of epigenetics and in particular DNA methylation as potential biomarker of MTX response in pediatric patients with JIA.

6. CONCLUSIONS

In conclusion, this study reported the potential role of DNA methylation as epigenetic biomarker for therapy personalization in three pediatric chronic autoimmune diseases.

The pivotal role of NLRP3 promoter methylation in INS as potential biomarker of steroid response was demonstrated thanks to the in vitro model established using U937 monocytes that demonstrated an increased steroid resistance after NLRP3 inflammasome activation. Moreover, a reduced NLRP3 methylation in INS patients and a correlation between NLRP3 methylation and age was also identified.

In pediatric patients with IBD, a significant reduction in the methylation of cg22736354 located on TPMT downstream neighboring region was observed in children with early onset IBD, that may be related to the increased biotransformation and reduced bioavailability of AZA confirmed in this group of patients.

Finally, in pediatric patients with JIA the methylation of 3 CpG sites on the CDH4 gene resulted associated with the ACR Pedi, independently from the MTX treatment. Moreover, the CDH4 gene expression resulted extremely low in all the models evaluated.

This thesis has brought new information to the field of DNA methylation and drug response in different pediatric chronic autoimmune diseases, even though this is still an emerging area and further studies should be performed to extend the DNA methylation analysis to other drugs and pathologies with the aim of therapy personalization.

7. REFERENCES

1. Waddington CH. The epigenotype. 1942. Int J Epidemiol. 2012 Feb;41(1):10–3.

2. Moore LD, Le T, Fan G. DNA methylation and its basic function. Neuropsychopharmacol Off Publ Am Coll Neuropsychopharmacol. 2013 Jan;38(1):23–38.

3. Martincorena I, Campbell PJ. Somatic mutation in cancer and normal cells. Science. 2015 Sep 25;349(6255):1483–9.

4. Mohn F, Schübeler D. Genetics and epigenetics: stability and plasticity during cellular differentiation. Trends Genet TIG. 2009 Mar;25(3):129–36.

5. Wang X. Stem cells in tissues, organoids, and cancers. Cell Mol Life Sci CMLS. 2019 Oct;76(20):4043–70.

6. Fan G, Martinowich K, Chin MH, He F, Fouse SD, Hutnick L, et al. DNA methylation controls the timing of astrogliogenesis through regulation of JAK-STAT signaling. Dev Camb Engl. 2005 Aug;132(15):3345–56.

7. Lister R, Mukamel EA, Nery JR, Urich M, Puddifoot CA, Johnson ND, et al. Global epigenomic reconfiguration during mammalian brain development. Science. 2013 Aug 9;341(6146):1237905.

8. Srinageshwar B, Maiti P, Dunbar GL, Rossignol J. Role of Epigenetics in Stem Cell Proliferation and Differentiation: Implications for Treating Neurodegenerative Diseases. Int J Mol Sci. 2016 Feb 2;17(2):E199.

9. Atlasi Y, Stunnenberg HG. The interplay of epigenetic marks during stem cell differentiation and development. Nat Rev Genet. 2017 Nov;18(11):643–58.

10. Arnsdorf EJ, Tummala P, Castillo AB, Zhang F, Jacobs CR. The epigenetic mechanism of mechanically induced osteogenic differentiation. J Biomech. 2010 Nov 16;43(15):2881–6.

11. Wu H, Deng Y, Feng Y, Long D, Ma K, Wang X, et al. Epigenetic regulation in B-cell maturation and its dysregulation in autoimmunity. Cell Mol Immunol. 2018 Jul;15(7):676–84.

12. Nandakumar V, Chou Y, Zang L, Huang XF, Chen S-Y. Epigenetic control of natural killer cell maturation by histone H2A deubiquitinase, MYSM1. Proc Natl Acad Sci U S A. 2013 Oct 8;110(41):E3927-3936.

13. Tammen SA, Friso S, Choi S-W. Epigenetics: the link between nature and nurture. Mol Aspects Med. 2013 Aug;34(4):753–64.

14. Wawrzyniak M, Scharl M. Genetics and epigenetics of inflammatory bowel disease. Swiss Med Wkly. 2018 Sep 10;148:w14671.

15. Cai SF, Levine RL. Genetic and epigenetic determinants of AML pathogenesis. Semin Hematol. 2019 Apr;56(2):84–9.

16. Stoccoro A, Coppedè F. Role of epigenetics in Alzheimer's disease pathogenesis. Neurodegener Dis Manag. 2018 Jun;8(3):181–93.

17. Hotchkiss RD. The quantitative separation of purines, pyrimidines, and nucleosides by paper chromatography. J Biol Chem. 1948 Aug;175(1):315–32.

18. Holliday R, Pugh JE. DNA modification mechanisms and gene activity during development. Science. 1975 Jan 24;187(4173):226–32.

19. Bird AP. CpG-rich islands and the function of DNA methylation. Nature. 1986 May 15;321(6067):209–13.

20. Shen L, Kondo Y, Guo Y, Zhang J, Zhang L, Ahmed S, et al. Genome-wide profiling of DNA methylation reveals a class of normally methylated CpG island promoters. PLoS Genet. 2007 Oct;3(10):2023–36.

21. Jang HS, Shin WJ, Lee JE, Do JT. CpG and Non-CpG Methylation in Epigenetic Gene Regulation and Brain Function. Genes. 2017 May 23;8(6).

22. Mariuswalter. English: DNA methylation landscape in mammals [Internet]. 2016 [cited 2021 Jun 22]. Available from: https://commons.wikimedia.org/wiki/File:DNAme_landscape.png

23. Li E, Zhang Y. DNA methylation in mammals. Cold Spring Harb Perspect Biol. 2014 May 1;6(5):a019133.

24. Smith ZD, Meissner A. The simplest explanation: passive DNA demethylation in PGCs. EMBO J. 2013 Feb 6;32(3):318–21.

25. Wu SC, Zhang Y. Active DNA demethylation: many roads lead to Rome. Nat Rev Mol Cell Biol. 2010 Sep;11(9):607–20.

26. DNA Demethylation | EpiGentek [Internet]. [cited 2021 Jun 22]. Available from: https://www.epigentek.com/catalog/dna-demethylation.php

27. Song C-X, Szulwach KE, Fu Y, Dai Q, Yi C, Li X, et al. Selective chemical labeling reveals the genome-wide distribution of 5-hydroxymethylcytosine. Nat Biotechnol. 2011 Jan;29(1):68–72.

28. Zhou Q, Li K, Yu K-K, Li N, Shi L, Chen H, et al. Aqueous Wittig reaction-mediated fast fluorogenic identification and single-base resolution analysis of 5-formylcytosine in DNA. Chem Commun Camb Engl. 2020 Oct 13;56(81):12158–61.

29. Jin L, Wang W, Hu D, Lü J. A new insight into the 5-carboxycytosine and 5-formylcytosine under typical bisulfite conditions: a deamination mechanism study. Phys Chem Chem Phys PCCP. 2014 Feb 28;16(8):3573–85.

30. Levenson VV. DNA methylation as a universal biomarker. Expert Rev Mol Diagn. 2010 May;10(4):481–8.

31. Cheung H-H, Lee T-L, Rennert OM, Chan W-Y. DNA methylation of cancer genome. Birth Defects Res Part C Embryo Today Rev. 2009 Dec;87(4):335–50.

32. Wong EM, Southey MC, Terry MB. Integrating DNA methylation measures to improve clinical risk assessment: are we there yet? The case of BRCA1 methylation marks to

improve clinical risk assessment of breast cancer. Br J Cancer. 2020 Apr;122(8):1133–40.

33. Ye L, Lin C, Wang X, Li Q, Li Y, Wang M, et al. Epigenetic silencing of SALL2 confers tamoxifen resistance in breast cancer. EMBO Mol Med. 2019 Dec;11(12):e10638.

34. Palomeras S, Diaz-Lagares Á, Viñas G, Setien F, Ferreira HJ, Oliveras G, et al. Epigenetic silencing of TGFBI confers resistance to trastuzumab in human breast cancer. Breast Cancer Res BCR. 2019 Jul 5;21(1):79.

35. García-Calzón S, Perfilyev A, Martinell M, Ustinova M, Kalamajski S, Franks PW, et al. Epigenetic markers associated with metformin response and intolerance in drug-naïve patients with type 2 diabetes. Sci Transl Med. 2020 Sep 16;12(561).

36. Paugh SW, Bonten EJ, Savic D, Ramsey LB, Thierfelder WE, Gurung P, et al. NALP3 inflammasome upregulation and CASP1 cleavage of the glucocorticoid receptor cause glucocorticoid resistance in leukemia cells. Nat Genet. 2015 Jun;47(6):607–14.

37. Schwartz JB. The current state of knowledge on age, sex, and their interactions on clinical pharmacology. Clin Pharmacol Ther. 2007 Jul;82(1):87–96.

38. Loebstein R, Koren G. Clinical pharmacology and therapeutic drug monitoring in neonates and children. Pediatr Rev. 1998 Dec;19(12):423–8.

39. Bergsma T, Rogaeva E. DNA Methylation Clocks and Their Predictive Capacity for Aging Phenotypes and Healthspan. Neurosci Insights. 2020;15:2633105520942221.

40. Horvath S, Raj K. DNA methylation-based biomarkers and the epigenetic clock theory of ageing. Nat Rev Genet. 2018 Jun;19(6):371–84.

41. Rakyan VK, Down TA, Maslau S, Andrew T, Yang T-P, Beyan H, et al. Human aging-associated DNA hypermethylation occurs preferentially at bivalent chromatin domains. Genome Res. 2010 Apr;20(4):434–9.

42. Hernandez DG, Nalls MA, Gibbs JR, Arepalli S, van der Brug M, Chong S, et al. Distinct DNA methylation changes highly correlated with chronological age in the human brain. Hum Mol Genet. 2011 Mar 15;20(6):1164–72.

43. Bell JT, Tsai P-C, Yang T-P, Pidsley R, Nisbet J, Glass D, et al. Epigenome-wide scans identify differentially methylated regions for age and age-related phenotypes in a healthy ageing population. PLoS Genet. 2012;8(4):e1002629.

44. Jung M, Pfeifer GP. Aging and DNA methylation. BMC Biol. 2015 Jan 31;13:7.

45. Lander ES, Linton LM, Birren B, Nusbaum C, Zody MC, Baldwin J, et al. Initial sequencing and analysis of the human genome. Nature. 2001 Feb 15;409(6822):860–921.

46. Rodríguez-Rodero S, Fernández-Morera JL, Fernandez AF, Menéndez-Torre E, Fraga MF. Epigenetic regulation of aging. Discov Med. 2010 Sep;10(52):225–33.

47. Hannum G, Guinney J, Zhao L, Zhang L, Hughes G, Sadda S, et al. Genome-wide methylation profiles reveal quantitative views of human aging rates. Mol Cell. 2013 Jan 24;49(2):359–67.

48. Horvath S. DNA methylation age of human tissues and cell types. Genome Biol. 2013;14(10):R115.

49. Gibson J, Russ TC, Clarke T-K, Howard DM, Hillary RF, Evans KL, et al. A meta-analysis of genome-wide association studies of epigenetic age acceleration. PLoS Genet. 2019 Nov;15(11):e1008104.

50. Nephrotic syndrome in children: prediction of histopathology from clinical and laboratory characteristics at time of diagnosis. A report of the International Study of Kidney Disease in Children. Kidney Int. 1978 Feb;13(2):159–65.

51. Banh THM, Hussain-Shamsy N, Patel V, Vasilevska-Ristovska J, Borges K, Sibbald C, et al. Ethnic Differences in Incidence and Outcomes of Childhood Nephrotic Syndrome. Clin J Am Soc Nephrol CJASN. 2016 Oct 7;11(10):1760–8.

52. Deschênes G, Leclerc A. [Epidemiology of the idiopathic nephrotic syndrome]. Arch Pediatr Organe Off Soc Francaise Pediatr. 2010 Jun;17(6):622–3.

53. Vivarelli M, Massella L, Ruggiero B, Emma F. Minimal Change Disease. Clin J Am Soc Nephrol CJASN. 2017 Feb 7;12(2):332–45.

54. minimal-change-capillary.png (immagine PNG, 650 × 352 pixel) [Internet]. [cited 2021 Jun 22]. Available from: https://unckidneycenter.org/wp-content/uploads/sites/413/2017/10/minimal-change-capillary.png

55. Klein M, Henschkowski J, Yu Z, Vogt B. [Edema and the nephrotic syndrome]. Ther Umsch Rev Ther. 2004 Nov;61(11):655–60.

56. Eddy AA, Symons JM. Nephrotic syndrome in childhood. Lancet Lond Engl. 2003 Aug 23;362(9384):629–39.

57. Kaneko K, Tsuji S, Kimata T, Kitao T, Yamanouchi S, Kato S. Pathogenesis of childhood idiopathic nephrotic syndrome: a paradigm shift from T-cells to podocytes. World J Pediatr WJP. 2015 Feb;11(1):21–8.

58. Rosenberg AZ, Kopp JB. Focal Segmental Glomerulosclerosis. Clin J Am Soc Nephrol CJASN. 2017 Mar 7;12(3):502–17.

59. Maas RJ, Deegens JK, Smeets B, Moeller MJ, Wetzels JF. Minimal change disease and idiopathic FSGS: manifestations of the same disease. Nat Rev Nephrol. 2016 Dec;12(12):768–76.

60. special issue: “Focus on pediatric nephrology,” Colavita L, Salpietro C, Cuppari C, Sallemi A, Di Benedetto V, et al. Nephrotic syndrome: immunological mechanisms. J Biol Regul Homeost Agents. 2019 Oct;33(5 Suppl. 1):13–8.

61. Noone DG, Iijima K, Parekh R. Idiopathic nephrotic syndrome in children. Lancet Lond Engl. 2018 Jul 7;392(10141):61–74.

62. Kobayashi Y, Aizawa A, Takizawa T, Igarashi K, Hatada I, Arakawa H. Changes in DNA methylation in naïve T helper cells regulate the pathophysiological state in minimal-change nephrotic syndrome. BMC Res Notes. 2017 Sep 15;10(1):480.

63. McCaffrey J, Lennon R, Webb NJA. The non-immunosuppressive management of childhood nephrotic syndrome. Pediatr Nephrol Berl Ger. 2016 Sep;31(9):1383–402.

64. Siligato R, Cernaro V, Nardi C, De Gregorio F, Gembillo G, Costantino G, et al. Emerging therapeutic strategies for minimal change disease and focal and segmental glomerulosclerosis. Expert Opin Investig Drugs. 2018 Nov;27(11):839–79.

65. Bereshchenko O, Bruscoli S, Riccardi C. Glucocorticoids, Sex Hormones, and Immunity. Front Immunol. 2018;9:1332.

66. Oakley RH, Cidlowski JA. The biology of the glucocorticoid receptor: new signaling mechanisms in health and disease. J Allergy Clin Immunol. 2013 Nov;132(5):1033–44.

67. Kirschke E, Goswami D, Southworth D, Griffin PR, Agard DA. Glucocorticoid receptor function regulated by coordinated action of the Hsp90 and Hsp70 chaperone cycles. Cell. 2014 Jun 19;157(7):1685–97.

68. Pratt WB, Morishima Y, Murphy M, Harrell M. Chaperoning of glucocorticoid receptors. Handb Exp Pharmacol. 2006;(172):111–38.

69. Xavier AM, Anunciato AKO, Rosenstock TR, Glezer I. Gene Expression Control by Glucocorticoid Receptors during Innate Immune Responses. Front Endocrinol. 2016;7:31.

70. Ronchetti S, Migliorati G, Riccardi C. GILZ as a Mediator of the Anti-Inflammatory Effects of Glucocorticoids. Front Endocrinol. 2015;6:170.

71. Lucafo M, De Iudicibus S, Di Silvestre A, Pelin M, Candussio L, Martelossi S, et al. Long noncoding RNA GAS5: a novel marker involved in glucocorticoid response. Curr Mol Med. 2015;15(1):94–9.

72. Liberman AC, Budziñski ML, Sokn C, Gobbini RP, Steininger A, Arzt E. Regulatory and Mechanistic Actions of Glucocorticoids on T and Inflammatory Cells. Front Endocrinol. 2018;9:235.

73. Tullus K, Webb H, Bagga A. Management of steroid-resistant nephrotic syndrome in children and adolescents. Lancet Child Adolesc Health. 2018 Dec;2(12):880–90.

74. Warejko JK, Tan W, Daga A, Schapiro D, Lawson JA, Shril S, et al. Whole Exome Sequencing of Patients with Steroid-Resistant Nephrotic Syndrome. Clin J Am Soc Nephrol CJASN. 2018 Jan 6;13(1):53–62.

75. Cuzzoni E, De Iudicibus S, Stocco G, Favretto D, Pelin M, Messina G, et al. In vitro sensitivity to methyl-prednisolone is associated with clinical response in pediatric idiopathic nephrotic syndrome. Clin Pharmacol Ther. 2016 Sep;100(3):268–74.

76. Kelley N, Jeltema D, Duan Y, He Y. The NLRP3 Inflammasome: An Overview of Mechanisms of Activation and Regulation. Int J Mol Sci. 2019 Jul 6;20(13):E3328.

77. Jo E-K, Kim JK, Shin D-M, Sasakawa C. Molecular mechanisms regulating NLRP3 inflammasome activation. Cell Mol Immunol. 2016 Mar;13(2):148–59.

78. Yang Y, Wang H, Kouadir M, Song H, Shi F. Recent advances in the mechanisms of NLRP3 inflammasome activation and its inhibitors. Cell Death Dis. 2019 Feb 12;10(2):128.

79. Mihai S, Codrici E, Popescu ID, Enciu A-M, Albulescu L, Necula LG, et al. Inflammation-Related Mechanisms in Chronic Kidney Disease Prediction, Progression, and Outcome. J Immunol Res. 2018;2018:2180373.

80. Xiang H, Zhu F, Xu Z, Xiong J. Role of Inflammasomes in Kidney Diseases via Both Canonical and Non-canonical Pathways. Front Cell Dev Biol. 2020;8:106.

81. Fan J, Xie K, Wang L, Zheng N, Yu X. Roles of Inflammasomes in Inflammatory Kidney Diseases. Mediators Inflamm. 2019;2019:2923072.

82. Li L, Tang W, Yi F. Role of Inflammasome in Chronic Kidney Disease. In: Liu B-C, Lan H-Y, Lv L-L, editors. Renal Fibrosis: Mechanisms and Therapies [Internet]. Singapore: Springer; 2019 [cited 2021 Jun 27]. p. 407–21. (Advances in Experimental Medicine and Biology). Available from: https://doi.org/10.1007/978-981-13-8871-2_19

83. Granata S, Masola V, Zoratti E, Scupoli MT, Baruzzi A, Messa M, et al. NLRP3 inflammasome activation in dialyzed chronic kidney disease patients. PloS One. 2015;10(3):e0122272.

84. Zhu Y, Zhu C, Yang H, Deng J, Fan D. Protective effect of ginsenoside Rg5 against kidney injury via inhibition of NLRP3 inflammasome activation and the MAPK signaling pathway in high-fat diet/streptozotocin-induced diabetic mice. Pharmacol Res. 2020 May;155:104746.

85. Niu X, Yao Q, Li W, Zang L, Li W, Zhao J, et al. Harmine mitigates LPS-induced acute kidney injury through inhibition of the TLR4-NF-κB/NLRP3 inflammasome signalling pathway in mice. Eur J Pharmacol. 2019 Apr 15;849:160–9.

86. Zhou Z, Wang L, Wen Z, Zheng S, Ye X, Liu D, et al. Association Analysis of NLRP3 Inflammation-Related Gene Promotor Methylation as Well as Mediating Effects on T2DM and Vascular Complications in a Southern Han Chinese Population. Front Endocrinol. 2018;9:709.

87. Wei M, Wang L, Wu T, Xi J, Han Y, Yang X, et al. NLRP3 Activation Was Regulated by DNA Methylation Modification during Mycobacterium tuberculosis Infection. BioMed Res Int. 2016;2016:4323281.

88. Yu YR, Rodriguez JR. Clinical presentation of Crohn's, ulcerative colitis, and indeterminate colitis: Symptoms, extraintestinal manifestations, and disease phenotypes. Semin Pediatr Surg. 2017 Dec;26(6):349–55.

89. Vavricka SR, Schoepfer A, Scharl M, Lakatos PL, Navarini A, Rogler G. Extraintestinal Manifestations of Inflammatory Bowel Disease. Inflamm Bowel Dis. 2015 Aug;21(8):1982–92.

90. GBD 2017 Inflammatory Bowel Disease Collaborators. The global, regional, and national burden of inflammatory bowel disease in 195 countries and territories, 1990-2017: a systematic analysis for the Global Burden of Disease Study 2017. Lancet Gastroenterol Hepatol. 2020 Jan;5(1):17–30.

91. Stocco G, Martelossi S, Arrigo S, Barabino A, Aloi M, Martinelli M, et al. Multicentric Case-Control Study on Azathioprine Dose and Pharmacokinetics in Early-onset Pediatric Inflammatory Bowel Disease. Inflamm Bowel Dis. 2017 Apr;23(4):628–34.

92. Sairenji T, Collins KL, Evans DV. An Update on Inflammatory Bowel Disease. Prim Care. 2017 Dec;44(4):673–92.

93. Moran CJ. Very early onset inflammatory bowel disease. Semin Pediatr Surg. 2017 Dec;26(6):356–9.

94. Ottman M, Lahtinen A, Apiainen S, Hasari S, Koivukoski ML, Similä AL, et al. [How the delivery is experienced by mothers and by fathers attending the delivery]. Katilolehti. 1988 Aug;93(5):19–21.

95. Shim JO. Recent Advance in Very Early Onset Inflammatory Bowel Disease. Pediatr Gastroenterol Hepatol Nutr. 2019 Jan;22(1):41–9.

96. Kuhbacher T, Fölsch UR. Practical guidelines for the treatment of inflammatory bowel disease. World J Gastroenterol. 2007 Feb 28;13(8):1149–55.

97. Hanauer SB, Meyers S. Management of Crohn's disease in adults. Am J Gastroenterol. 1997 Apr;92(4):559–66.

98. Sanderson IR. Growth problems in children with IBD. Nat Rev Gastroenterol Hepatol. 2014 Oct;11(10):601–10.

99. Ruemmele FM, Veres G, Kolho KL, Griffiths A, Levine A, Escher JC, et al. Consensus guidelines of ECCO/ESPGHAN on the medical management of pediatric Crohn's disease. J Crohns Colitis. 2014 Oct;8(10):1179–207.

100. Lucafò M, Franca R, Selvestrel D, Curci D, Pugnetti L, Decorti G, et al. Pharmacogenetics of treatments for inflammatory bowel disease. Expert Opin Drug Metab Toxicol. 2018 Dec;14(12):1209–23.

101. Williams C, Panaccione R, Ghosh S, Rioux K. Optimizing clinical use of mesalazine (5-aminosalicylic acid) in inflammatory bowel disease. Ther Adv Gastroenterol. 2011 Jul;4(4):237–48.

102. Corica D, Romano C. Biological Therapy in Pediatric Inflammatory Bowel Disease: A Systematic Review. J Clin Gastroenterol. 2017 Feb;51(2):100–10.

103. Miller T, Suskind DL. Exclusive enteral nutrition in pediatric inflammatory bowel disease. Curr Opin Pediatr. 2018 Oct;30(5):671–6.

104. Thiopurine Pathway, Pharmacokinetics/Pharmacodynamics [Internet]. PharmGKB. [cited 2021 Jun 27]. Available from: https://www.pharmgkb.org/pathway/PA2040

105. Bökkerink JP, Stet EH, De Abreu RA, Damen FJ, Hulscher TW, Bakker MA, et al. 6-Mercaptopurine: cytotoxicity and biochemical pharmacology in human malignant T-lymphoblasts. Biochem Pharmacol. 1993 Apr 6;45(7):1455–63.

106. Inamochi H, Higashigawa M, Shimono Y, Nagata T, Cao DC, Mao XY, et al. Delayed cytotoxicity of 6-mercaptopurine is compatible with mitotic death caused by DNA damage due to incorporation of 6-thioguanine into DNA as 6-thioguanine nucleotide. J Exp Clin Cancer Res CR. 1999 Sep;18(3):417–24.

107. Karim H, Ghalali A, Lafolie P, Vitols S, Fotoohi AK. Differential role of thiopurine methyltransferase in the cytotoxic effects of 6-mercaptopurine and 6-thioguanine on human leukemia cells. Biochem Biophys Res Commun. 2013 Jul 26;437(2):280–6.

108. Poppe D, Tiede I, Fritz G, Becker C, Bartsch B, Wirtz S, et al. Azathioprine suppresses ezrin-radixin-moesin-dependent T cell-APC conjugation through inhibition of Vav guanosine exchange activity on Rac proteins. J Immunol Baltim Md 1950. 2006 Jan 1;176(1):640–51.

109. Stocco G, Pelin M, Franca R, De Iudicibus S, Cuzzoni E, Favretto D, et al. Pharmacogenetics of azathioprine in inflammatory bowel disease: a role for glutathione-S-transferase? World J Gastroenterol. 2014 Apr 7;20(13):3534–41.

110. Ujiie S, Sasaki T, Mizugaki M, Ishikawa M, Hiratsuka M. Functional characterization of 23 allelic variants of thiopurine S-methyltransferase gene (TPMT*2 - *24). Pharmacogenet Genomics. 2008 Oct;18(10):887–93.

111. Relling MV, Schwab M, Whirl-Carrillo M, Suarez-Kurtz G, Pui C-H, Stein CM, et al. Clinical Pharmacogenetics Implementation Consortium Guideline for Thiopurine Dosing Based on TPMT and NUDT15 Genotypes: 2018 Update. Clin Pharmacol Ther. 2019 May;105(5):1095–105.

112. Nguyen CM, Mendes MAS, Ma JD. Thiopurine methyltransferase (TPMT) genotyping to predict myelosuppression risk. PLoS Curr. 2011 May 15;3:RRN1236.

113. Barut K, Adrovic A, Şahin S, Kasapçopur Ö. Juvenile Idiopathic Arthritis. Balk Med J. 2017 Mar;34(2):90–101.

114. Palman J, Shoop-Worrall S, Hyrich K, McDonagh JE. Update on the epidemiology, risk factors and disease outcomes of Juvenile idiopathic arthritis. Best Pract Res Clin Rheumatol. 2018 Apr;32(2):206–22.

115. Thierry S, Fautrel B, Lemelle I, Guillemin F. Prevalence and incidence of juvenile idiopathic arthritis: a systematic review. Joint Bone Spine. 2014 Mar;81(2):112–7.

116. Petty RE, Southwood TR, Manners P, Baum J, Glass DN, Goldenberg J, et al. International League of Associations for Rheumatology classification of juvenile idiopathic arthritis: second revision, Edmonton, 2001. J Rheumatol. 2004 Feb;31(2):390–2.

117. Nigrovic PA, Raychaudhuri S, Thompson SD. Review: Genetics and the Classification of Arthritis in Adults and Children. Arthritis Rheumatol Hoboken NJ. 2018 Jan;70(1):7–17.

118. Horton DB, Shenoi S. Review of environmental factors and juvenile idiopathic arthritis. Open Access Rheumatol Res Rev. 2019;11:253–67.

119. Cobb JE, Hinks A, Thomson W. The genetics of juvenile idiopathic arthritis: current understanding and future prospects. Rheumatol Oxf Engl. 2014 Apr;53(4):592–9.

120. Hersh AO, Prahalad S. Immunogenetics of juvenile idiopathic arthritis: A comprehensive review. J Autoimmun. 2015 Nov;64:113–24.

121. Chua-Aguilera CJ, Möller B, Yawalkar N. Skin Manifestations of Rheumatoid Arthritis, Juvenile Idiopathic Arthritis, and Spondyloarthritides. Clin Rev Allergy Immunol. 2017 Dec;53(3):371–93.

122. Sen ES, Ramanan AV. Juvenile idiopathic arthritis-associated uveitis. Best Pract Res Clin Rheumatol. 2017 Aug;31(4):517–34.

123. Giancane G, Consolaro A, Lanni S, Davì S, Schiappapietra B, Ravelli A. Juvenile Idiopathic Arthritis: Diagnosis and Treatment. Rheumatol Ther. 2016 Dec;3(2):187–207.

124. Cimaz R. Systemic-onset juvenile idiopathic arthritis. Autoimmun Rev. 2016 Sep;15(9):931–4.

125. Thatayatikom A, Modica R, De Leucio A. Juvenile Idiopathic Arthritis. In: StatPearls [Internet]. Treasure Island (FL): StatPearls Publishing; 2021 [cited 2021 Jun 27]. Available from: http://www.ncbi.nlm.nih.gov/books/NBK554605/

126. Vanoni F, Minoia F, Malattia C. Biologics in juvenile idiopathic arthritis: a narrative review. Eur J Pediatr. 2017 Sep;176(9):1147–53.

127. Dent PB, Walker N. Intra-articular corticosteroids in the treatment of juvenile rheumatoid arthritis. Curr Opin Rheumatol. 1998 Sep;10(5):475–80.

128. Foell D, Wulffraat N, Wedderburn LR, Wittkowski H, Frosch M, Gerss J, et al. Methotrexate withdrawal at 6 vs 12 months in juvenile idiopathic arthritis in remission: a randomized clinical trial. JAMA. 2010 Apr 7;303(13):1266–73.

129. Giannini EH, Brewer EJ, Kuzmina N, Shaikov A, Maximov A, Vorontsov I, et al. Methotrexate in resistant juvenile rheumatoid arthritis. Results of the U.S.A.-U.S.S.R. double-blind, placebo-controlled trial. The Pediatric Rheumatology Collaborative Study Group and The Cooperative Children's Study Group. N Engl J Med. 1992 Apr 16;326(16):1043–9.

130. Pastore S, Stocco G, Favretto D, De Iudicibus S, Taddio A, d'Adamo P, et al. Genetic determinants for methotrexate response in juvenile idiopathic arthritis. Front Pharmacol. 2015;6:52.

131. Gorlick R, Goker E, Trippett T, Waltham M, Banerjee D, Bertino JR. Intrinsic and acquired resistance to methotrexate in acute leukemia. N Engl J Med. 1996 Oct 3;335(14):1041–8.

132. Barredo JC, Synold TW, Laver J, Relling MV, Pui CH, Priest DG, et al. Differences in constitutive and post-methotrexate folylpolyglutamate synthetase activity in B-lineage and T-lineage leukemia. Blood. 1994 Jul 15;84(2):564–9.

133. Becker ML, Gaedigk R, van Haandel L, Thomas B, Lasky A, Hoeltzel M, et al. The effect of genotype on methotrexate polyglutamate variability in juvenile idiopathic arthritis and association with drug response. Arthritis Rheum. 2011 Jan;63(1):276–85.

134. Pastore S, Stocco G, Moressa V, Zandonà L, Favretto D, Malusà N, et al. 5-Aminoimidazole-4-carboxamide ribonucleotide-transformylase and inosine-triphosphate-pyrophosphatase genes variants predict remission rate during methotrexate therapy in patients with juvenile idiopathic arthritis. Rheumatol Int. 2015 Apr;35(4):619–27.

135. Ramsey LB, Moncrieffe H, Smith CN, Sudman M, Marion MC, Langefeld CD, et al. Association of SLCO1B1 *14 Allele with Poor Response to Methotrexate in Juvenile Idiopathic Arthritis Patients. ACR Open Rheumatol. 2019 Mar;1(1):58–62.

136. Nair N, Plant D, Verstappen SM, Isaacs JD, Morgan AW, Hyrich KL, et al. Differential DNA methylation correlates with response to methotrexate in rheumatoid arthritis. Rheumatol Oxf Engl. 2020 Jun 1;59(6):1364–71.

137. Guderud K, Sunde LH, Flåm ST, Mæhlen MT, Mjaavatten MD, Lillegraven S, et al. Rheumatoid Arthritis Patients, Both Newly Diagnosed and Methotrexate Treated, Show More DNA Methylation Differences in CD4+ Memory Than in CD4+ Naïve T Cells. Front Immunol. 2020;11:194.

138. Chavez-Valencia RA, Chiaroni-Clarke RC, Martino DJ, Munro JE, Allen RC, Akikusa JD, et al. The DNA methylation landscape of CD4+ T cells in oligoarticular juvenile idiopathic arthritis. J Autoimmun. 2018 Jan;86:29–38.

139. Li Z, Su D, Ying L, Yu G, Mao W. Study on expression of CDH4 in lung cancer. World J Surg Oncol. 2017 Jan 17;15(1):26.

140. Miotto E, Sabbioni S, Veronese A, Calin GA, Gullini S, Liboni A, et al. Frequent aberrant methylation of the CDH4 gene promoter in human colorectal and gastric cancer. Cancer Res. 2004 Nov 15;64(22):8156–9.

141. Du C, Huang T, Sun D, Mo Y, Feng H, Zhou X, et al. CDH4 as a novel putative tumor suppressor gene epigenetically silenced by promoter hypermethylation in nasopharyngeal carcinoma. Cancer Lett. 2011 Oct 1;309(1):54–61.

142. Sato S, Tsueda M, Kanezaki Y, Takenaka S. Detection of an aberrant methylation of CDH4 gene in PCR product by ferrocenylnaphthalene diimide-based electrochemical hybridization assay. Anal Chim Acta. 2012 Feb 17;715:42–8.

143. Häupl T, Yahyawi M, Lübke C, Ringe J, Rohrlach T, Burmester GR, et al. Gene expression profiling of rheumatoid arthritis synovial cells treated with antirheumatic drugs. J Biomol Screen. 2007 Apr;12(3):328–40.

144. Cobb J, Cule E, Moncrieffe H, Hinks A, Ursu S, Patrick F, et al. Genome-wide data reveal novel genes for methotrexate response in a large cohort of juvenile idiopathic arthritis cases. Pharmacogenomics J. 2014 Aug;14(4):356–64.

145. Stevens PE, Levin A, Kidney Disease: Improving Global Outcomes Chronic Kidney Disease Guideline Development Work Group Members. Evaluation and management of chronic kidney disease: synopsis of the kidney disease: improving global outcomes 2012 clinical practice guideline. Ann Intern Med. 2013 Jun 4;158(11):825–30.

146. Livak KJ, Schmittgen TD. Analysis of relative gene expression data using real-time quantitative PCR and the 2(-Delta Delta C(T)) Method. Methods San Diego Calif. 2001 Dec;25(4):402–8.

147. Tian Y, Morris TJ, Webster AP, Yang Z, Beck S, Feber A, et al. ChAMP: updated methylation analysis pipeline for Illumina BeadChips. Bioinforma Oxf Engl. 2017 Dec 15;33(24):3982–4.

148. Dervieux T, Boulieu R. Simultaneous determination of 6-thioguanine and methyl 6-mercaptopurine nucleotides of azathioprine in red blood cells by HPLC. Clin Chem. 1998 Mar;44(3):551–5.

149. Anglicheau D, Sanquer S, Loriot MA, Beaune P, Thervet E. Thiopurine methyltransferase activity: new conditions for reversed-phase high-performance liquid chromatographic assay without extraction and genotypic-phenotypic correlation. J Chromatogr B Analyt Technol Biomed Life Sci. 2002 Jun 25;773(2):119–27.

150. Willer CJ, Li Y, Abecasis GR. METAL: fast and efficient meta-analysis of genomewide association scans. Bioinforma Oxf Engl. 2010 Sep 1;26(17):2190–1.

151. Consolaro A, Ruperto N, Bazso A, Pistorio A, Magni-Manzoni S, Filocamo G, et al. Development and validation of a composite disease activity score for juvenile idiopathic arthritis. Arthritis Rheum. 2009 May 15;61(5):658–66.

152. Cascorbi I, Schwab M. Epigenetics in Drug Response. Clin Pharmacol Ther. 2016 May;99(5):468–70.

153. Lucafò M, Granata S, Bonten EJ, McCorkle R, Stocco G, Caletti C, et al. Hypomethylation of NLRP3 gene promoter discriminates glucocorticoid-resistant from glucocorticoid-sensitive idiopathic nephrotic syndrome patients. Clin Transl Sci. 2020 Dec 31;

154. Zaza G, Pontrelli P, Pertosa G, Granata S, Rossini M, Porreca S, et al. Dialysis-related systemic microinflammation is associated with specific genomic patterns. Nephrol Dial Transplant Off Publ Eur Dial Transpl Assoc - Eur Ren Assoc. 2008 May;23(5):1673–81.

155. Tune BM, Mendoza SA. Treatment of the idiopathic nephrotic syndrome: regimens and outcomes in children and adults. J Am Soc Nephrol JASN. 1997 May;8(5):824–32.

156. Nagata K, Takahashi Y, Waga S, Fujita M, Kuronuma T, Aoyama R. Monocyte function in idiopathic nephrotic syndrome in childhood. Tohoku J Exp Med. 1981 Dec;135(4):413–7.

157. Matsumoto K, Kanmatsuse K. Increased IL-12 release by monocytes in nephrotic patients. Clin Exp Immunol. 1999 Aug;117(2):361–7.

158. Hammad A, Yahia S, Gouida MS, Bakr A, El-farahaty RM. Low expression of glucocorticoid receptors in children with steroid-resistant nephrotic syndrome. Pediatr Nephrol Berl Ger. 2013 May;28(5):759–63.

159. Ehrchen JM, Roth J, Barczyk-Kahlert K. More Than Suppression: Glucocorticoid Action on Monocytes and Macrophages. Front Immunol. 2019;10:2028.

160. Wang C, Nanni L, Novakovic B, Megchelenbrink W, Kuznetsova T, Stunnenberg HG, et al. Extensive epigenomic integration of the glucocorticoid response in primary human monocytes and in vitro derived macrophages. Sci Rep. 2019 Feb 26;9(1):2772.

161. Lennard L. Clinical implications of thiopurine methyltransferase--optimization of drug dosage and potential drug interactions. Ther Drug Monit. 1998 Oct;20(5):527–31.

162. McLeod HL, Krynetski EY, Wilimas JA, Evans WE. Higher activity of polymorphic thiopurine S-methyltransferase in erythrocytes from neonates compared to adults. Pharmacogenetics. 1995 Oct;5(5):281–6.

163. Serpe L, Calvo PL, Muntoni E, D'Antico S, Giaccone M, Avagnina A, et al. Thiopurine S-methyltransferase pharmacogenetics in a large-scale healthy Italian-Caucasian population: differences in enzyme activity. Pharmacogenomics. 2009 Nov;10(11):1753–65.

164. Chouchana L, Narjoz C, Beaune P, Loriot M-A, Roblin X. Review article: the benefits of pharmacogenetics for improving thiopurine therapy in inflammatory bowel disease. Aliment Pharmacol Ther. 2012 Jan;35(1):15–36.

165. Yuan B, Zhang J, Wang H, Xiong L, Cai Q, Wang T, et al. 6-Thioguanine reactivates epigenetically silenced genes in acute lymphoblastic leukemia cells by facilitating proteasome-mediated degradation of DNMT1. Cancer Res. 2011 Mar 1;71(5):1904–11.

166. Hogarth LA, Redfern CPF, Teodoridis JM, Hall AG, Anderson H, Case MC, et al. The effect of thiopurine drugs on DNA methylation in relation to TPMT expression. Biochem Pharmacol. 2008 Oct 15;76(8):1024–35.

167. Kim BJ, Kim Y, Hong EP, Jeon JP, Yang JS, Choi HJ, et al. Correlation Between Altered DNA Methylation of Intergenic Regions of ITPR3 and Development of Delayed Cerebral Ischemia in Patients with Subarachnoid Hemorrhage. World Neurosurg. 2019 Oct;130:e449–56.

168. Sun Z, Yu S, Chen S, Liu H, Chen Z. SP1 regulates KLF4 via SP1 binding motif governed by DNA methylation during odontoblastic differentiation of human dental pulp cells. J Cell Biochem. 2019 Sep;120(9):14688–99.

169. Zukic B, Radmilovic M, Stojiljkovic M, Tosic N, Pourfarzad F, Dokmanovic L, et al. Functional analysis of the role of the TPMT gene promoter VNTR polymorphism in TPMT gene transcription. Pharmacogenomics. 2010 Apr;11(4):547–57.

170. Vojta A, Dobrinić P, Tadić V, Bočkor L, Korać P, Julg B, et al. Repurposing the CRISPR-Cas9 system for targeted DNA methylation. Nucleic Acids Res. 2016 Jul 8;44(12):5615–28.

171. Grossman AB, Noble AJ, Mamula P, Baldassano RN. Increased dosing requirements for 6-mercaptopurine and azathioprine in inflammatory bowel disease patients six years and younger. Inflamm Bowel Dis. 2008 Jun;14(6):750–5.

172. Ogungbenro K, Aarons L, CRESim & Epi-CRESim Project Groups. Physiologically based pharmacokinetic model for 6-mercpatopurine: exploring the role of genetic polymorphism in TPMT enzyme activity. Br J Clin Pharmacol. 2015 Jul;80(1):86–100.

173. Ballestar E, Sawalha AH, Lu Q. Clinical value of DNA methylation markers in autoimmune rheumatic diseases. Nat Rev Rheumatol. 2020 Sep;16(9):514–24.

174. Houseley J, Tollervey D. The many pathways of RNA degradation. Cell. 2009 Feb 20;136(4):763–76.

175. Benegiamo G, Brown SA, Panda S. RNA Dynamics in the Control of Circadian Rhythm. Adv Exp Med Biol. 2016;907:107–22.

176. Ellis JA, Munro JE, Chavez RA, Gordon L, Joo JE, Akikusa JD, et al. Genome-scale case-control analysis of CD4+ T-cell DNA methylation in juvenile idiopathic arthritis reveals potential targets involved in disease. Clin Epigenetics. 2012 Nov 13;4(1):20.